



---

# **AAPM Recommendations on Dose Prescription and Reporting Methods for Permanent Interstitial Brachytherapy for Prostate Cancer**

---

**Report of AAPM Task Group 137**

**December 2009**

**DISCLAIMER:** This publication is based on sources and information believed to be reliable, but the AAPM, the authors, and the editors disclaim any warranty or liability based on or relating to the contents of this publication.

---

The AAPM does not endorse any products, manufacturers, or suppliers. Nothing in this publication should be interpreted as implying such endorsement.

DISCLAIMER: This publication is based on sources and information believed to be reliable, but the AAPM, the authors, and the publisher disclaim any warranty or liability based on or relating to the contents of this publication.

The AAPM does not endorse any products, manufacturers, or suppliers. Nothing in this publication should be interpreted as implying such endorsement.

ISBN: 978-1-888340-91-4  
ISSN: 0271-7344

© 2009 by American Association of Physicists in Medicine

All rights reserved.

Published by  
American Association of Physicists in Medicine  
One Physics Ellipse  
College Park, MD 20740-3846

## **Task Group 137 Members**

**Ravinder Nath**

*Department of Therapeutic Radiology, Yale University School of Medicine, New Haven, CT*

**William S. Bice**

*International Medical Physics, San Antonio, TX*

**Wayne M. Butler**

*Schiffler Cancer Center, Wheeling Hospital, Wheeling, WV*

**Zhe Chen**

*Department of Therapeutic Radiology, Yale University School of Medicine, New Haven, CT*

**Ali S. Meigooni**

*University of Kentucky, Lexington, KY*

**Vrinda Narayana**

*Department of Radiation Oncology, Providence Cancer Center, Southfield, MI*

**Mark J. Rivard**

*Department of Radiation Oncology, Tufts University School of Medicine, Boston, MA*

**Yan Yu**

*Department of Radiation Oncology, Thomas Jefferson University Hospital, Philadelphia, PA*

## **Acknowledgments**

The authors wish to acknowledge the thoughtful criticisms and the generous assistance of our European colleagues, members of the BRAPHYQS and PROBATE working groups within GEC-ESTRO, for reviewing this document. We have adopted many of the recommendations from their recent report. Some of this work (ZC and RN) was supported in part by a grant from the National Institutes of Health R01-CA134627.

## Contents

Abstract.....	1
<b>I. INTRODUCTION.....</b>	<b>1</b>
<b>II. CLINICAL BACKGROUND ON DOSE RESPONSE AND REPORTING.....</b>	<b>2</b>
II.1. Selected Cure Rate Studies of Prostate Implants.....	4
II.2. Selected Complication Rates Studies of Prostate Implants .....	6
II.2.a. Urinary Complications.....	8
II.2.b. Rectal Complications .....	8
II.2.c. Erectile Complications.....	9
II.C Historical Perspective on Dose Reporting.....	10
<b>III. IMPACT OF IMAGING MODALITY ON DOSE REPORTING.....</b>	<b>11</b>
III.1. Ultrasound Imaging .....	11
III.2. CT Imaging .....	12
III.3. MR Imaging .....	14
III.4. Recommendations on Imaging of Prostate Implants .....	17
<b>IV. EFFECT OF IMAGING TIMING ON DOSE REPORTING.....</b>	<b>19</b>
IV.1. General Characteristics of Post-Implant Prostate Edema .....	20
IV.2. Quantitative Characterization of Prostate Edema .....	20
IV.2.a. Edema Magnitude.....	21
IV.2.b. The 1st Half-life of Edema Resolution.....	23
IV.3. Effect of Prostate Edema on Brachytherapy Dosimetry .....	24
IV.3.a. Theoretical Expectations.....	24
IV.3.b. “Optimal” Timing of Post-Implant Dosimetry.....	24
IV.3.c. Relationships between Dosimetry Performed at Different Post-Implant Times .....	25
IV.4. Recommendations on Timing of Imaging.....	26
<b>V. COMMON TREATMENT PLANNING APPROACHES FOR PROSTATE IMPLANTS.....</b>	<b>27</b>
V.1. Modified Uniform and Modified Peripheral Loading.....	28
V.2. Target and Critical Structure Dose Indices .....	28

V.3.	Target Volume Definition and the Necessity for Margins .....	30
V.4.	Choice of Radionuclide .....	30
V.5.	Appropriate Seed Strengths.....	30
V.6.	Calculation Algorithm and its Effect on Target Dose Indices .....	31
V.7.	Recommendations for Planning and Dose Reporting of Prostate Implants.....	32
<b>VI.</b>	<b>INTRAOPERATIVE PROSTATE PLANNING AND ITS IMPACT ON DOSE REPORTING .....</b>	<b>35</b>
VI.1.	Intraoperative Preplanning .....	36
VI.2.	Interactive Planning .....	36
VI.3.	Dynamic Dose Calculation .....	37
VI.4.	Recommendations on Intraoperative Planning and Evaluation.....	38
<b>VII.</b>	<b>SECTOR ANALYSIS OF POST-IMPLANT DOSIMETRY .....</b>	<b>38</b>
VII.1.	Sector Analysis .....	38
VII.2.	Recommendations on Sector Analysis for Prostate Implants.....	40
<b>VIII.</b>	<b>BIOPHYSICAL MODELS USED FOR PROSTATE IMPLANTS .....</b>	<b>40</b>
VIII.1.	BED for Spatially Uniform Dose Irradiations.....	43
VIII.1.a.	BED for Acute Irradiations .....	44
VIII.1.b.	BED for Fractionated Irradiations.....	44
VIII.1.c.	BED for Prostate Implants Using a Single Type of Radionuclide ....	44
VIII.1.d.	BED for Implants Containing a Mixture of Radionuclides with Different Decay Half-lives .....	46
VIII.1.e.	BED for Permanent Implants in Presence of Prostate Edema .....	46
VIII.2.	BED and Equivalent Uniform Dose (EUD) for Inhomogeneous Dose Distributions .....	48
VIII.2.a.	BED for Inhomogeneous Dose Distribution .....	48
VIII.2.b.	EUD for Inhomogeneous Dose Distribution.....	48
VIII.3.	Tumor Control Probability (TCP).....	50
VIII.4.	Model Parameters for Prostate Cancer .....	51
VIII.5.	Recommendations for Reporting Relative Radiobiological Response .....	52
<b>IX.</b>	<b>DISCUSSION .....</b>	<b>53</b>
<b>X.</b>	<b>REFERENCES .....</b>	<b>54</b>

## ABSTRACT

During the past decade, permanent radioactive source implantation of the prostate has become the standard of care for selected prostate cancer patients, and the techniques for implantation have evolved in many different forms. Although most implants use  $^{125}\text{I}$  or  $^{103}\text{Pd}$  sources, clinical use of  $^{131}\text{Cs}$  sources has also recently been introduced. These sources produce different dose distributions and irradiate the tumors at different dose rates. Ultrasound was used originally to guide the planning and implantation of sources in the tumor. More recently, CT and/or MR are used routinely in many clinics for dose evaluation and planning. Several investigators reported that the tumor volumes and target volumes delineated from ultrasound, CT, and MR can vary substantially because of the inherent differences in these imaging modalities. It has also been reported that these volumes depend critically on the time of imaging after the implant. Many clinics, in particular those using intraoperative implantation, perform imaging only on the day of the implant. Because the effects of edema caused by surgical trauma can vary from one patient to another and resolve at different rates, the timing of imaging for dosimetry evaluation can have a profound effect on the dose reported (to have been delivered), i.e., for the same implant (same dose delivered), CT at different timing can yield different doses reported. Also, many different loading patterns and margins around the tumor volumes have been used, and these may lead to variations in the dose delivered. In this report, the current literature on these issues is reviewed, and the impact of these issues on the radiobiological response is estimated. The radiobiological models for the biological equivalent dose (BED) are reviewed. Starting with the BED model for acute single doses, the models for fractionated doses, continuous low-dose-rate irradiation, and both homogeneous and inhomogeneous dose distributions, as well as tumor cure probability models, are reviewed. Based on these developments in literature, the AAPM recommends guidelines for dose prescription from a physics perspective for routine patient treatment, clinical trials, and for treatment planning software developers. The authors continue to follow the current recommendations on using  $D_{90}$  and  $V_{100}$  as the primary quantities, with more specific guidelines on the use of the imaging modalities and the timing of the imaging. The AAPM recommends that the postimplant evaluation should be performed at the optimum time for specific radionuclides. In addition, they encourage the use of a radiobiological model with a specific set of parameters to facilitate relative comparisons of treatment plans reported by different institutions using different loading patterns or radionuclides.

## I. INTRODUCTION

Permanent interstitial brachytherapy using low-energy photon emitters, such as  $^{125}\text{I}$  and  $^{103}\text{Pd}$ , has become the method of choice for treatment of early-stage organ-localized prostate cancer. Since its introduction about 50 years ago, a number of methods have been used for describing the dosimetry of these implants. In the early clinical implementation of this method before soft-issue imaging was available, it was common to report the prescription parameters that described the dose distribution in relation to the implanted seeds rather than to the underlying anatomy. These methods included concepts such as the “natural dose-volume histogram,” “matched peripheral dose,” etc. One common approach was to use the highest dose rate with a continuous

isodose surface that encloses the implanted volume.<sup>1</sup> Recently, it has become common practice to image soft tissues of interest using ultrasound, CT, and/or MRI to define the various clinical volumes such as GTV (gross target volume), CTV (clinical target volume), and PTV (planning target volume).<sup>2</sup> However, these volumes can be considerably different depending upon the imaging modality, the time of imaging, and the margins used. Different margins are chosen in different directions, and their sizes are also different in various clinics; sometimes there are differences among the physicians in the same clinic. With the widespread use of image-guided dosimetry, there is now a need for developing a consensus methodology for dose prescription and reporting for prostate implants. In 2006, the AAPM formed a task group to develop consensus guidelines on this issue. The Task Group charge was:

- a. To review various methods currently in use for dose prescription and reporting for permanent interstitial prostate brachytherapy such as minimum tumor dose, peripheral dose, average tumor dose, implanted activity,  $D_{90}$ ,  $D_{100}$ ,  $V_{100}$ ,  $V_{90}$ , DVH (dose-volume histogram) (along with definitions of CTV, PTV, etc., which depend on the imaging methodology and the timing of the imaging).
- b. To carry out a critical review of radiobiological issues and models available in order to select a radiobiology model for the comparison of different dose prescription and reporting methods. (Absolute values of radiobiological parameters or model assumptions may not be critical for this application because we use the same model and values for a relative comparison of the choices at hand. Also, a range of these values can be tested to investigate the sensitivity of the conclusions to the choice of radiobiological parameters.)
- c. To develop consensus on the minimum required methodology for dose prescription and reporting pre- and post-procedure dose distributions for permanent interstitial brachytherapy for prostate cancer.
- d. To recommend the optimum methodology for dose prescription and reporting pre- and post-procedure dose distributions for permanent interstitial brachytherapy for prostate cancer; (e.g.,  $D_{90}$ , harmonic mean, and  $D_{99}$ , as suggested by Butler et al. 2009)<sup>3</sup>.

This report from the AAPM Task Group 137 (TG-137) has been reviewed and approved by the AAPM Low Energy Brachytherapy Source Dosimetry subcommittee and the AAPM Therapy Physics Committee, and now represents the official recommendations of the AAPM on this issue. An Executive Summary has been published in *Medical Physics*\*.<sup>4</sup>

## II. CLINICAL BACKGROUND ON DOSE RESPONSE AND REPORTING

Prostate cancer is the most common cancer (other than skin cancers) in American men over 50 years old and it is the second leading cause of cancer death behind lung cancer. The American

---

\**Medical Physics*, vol. 36, issue 11, pp. 5310–5322 (2009). The Executive Summary is available at [www.aapm.org/pubs/reports/](http://www.aapm.org/pubs/reports/).

Cancer Society (ACS) estimates that during 2008 about 186,320 new cases of prostate cancer will be diagnosed in the United States. Clinical diagnosis of this disease is rare in men younger than 45, with the majority of cases in the United States occurring in men older than 65. About 1 man in 4 will be diagnosed with prostate cancer during his lifetime, but only 1 man in about 30 will die of it. About 2 million men in the United States are prostate cancer survivors.<sup>5</sup>

Improvements in diagnosis, particularly the widespread introduction of prostate specific antigen (PSA) screening, have facilitated detection of the disease. Approximately 91% of prostate cancers are discovered early enough to be treated with local rather than systemic therapies. Concurrently, improvements in patient selection, source placement, and implant dosimetry have dramatically enhanced the effectiveness of brachytherapy as a treatment option. In 1995, only about 2% of new cases were treated with brachytherapy; today that number is about 30%. In contrast to the methods practiced by early brachytherapists, who performed retropubic laparotomies in order to place the sources, almost all prostate brachytherapy is currently performed under transrectal ultrasound (TRUS) guidance using techniques pioneered by Holm in Denmark and advanced and promulgated by a group of investigators based in Seattle.<sup>6,7,8-10</sup> In this procedure, <sup>125</sup>I, <sup>103</sup>Pd, or <sup>131</sup>Cs brachytherapy sources are implanted through needles placed through the perineum and guided by a template. Needle placement and source deposition are visible under TRUS, allowing the brachytherapist to consistently deliver tumoricidal doses of radiation while sparing critical structures.

Prostate cancer is graded according to the Tumor-Node-Metastasis (TNM) staging system, although there are arguments for including PSA and Gleason Sum Score (GSS) in the staging system.<sup>11,12</sup> Early stage disease, T1 or T2, is largely organ-confined with a low probability of nodal involvement or metastasis. Because the disease is local, treatment with brachytherapy radiation is appropriate. However, even within local stage groupings the risk of extracapsular spread must be addressed and a suitable therapy chosen.<sup>13</sup> Unfavorable prognostic indicators for early stage prostate cancer include a T2c stage, a GSS of 7 or greater, and a PSA level greater than 10. Consequently early stage prostate cancer is classified into three risk groups, depending on the PSA level, GSS, and clinical T-stage. A common classification scheme used by the National Comprehensive Cancer Network (NCCN)<sup>14</sup> is as follows:

- Low-risk: T-stage  $\leq 2b$ , GSS  $\leq 6$ , and PSA  $\leq 10$ .
- Intermediate-risk: T-stage  $\leq 2b$  and a) GSS = 7 or b) PSA > 10 but  $\leq 20$ .
- High-risk: T-stage = 2c or GSS  $\geq 8$  or PSA > 20.

There are many other risk classification schemes in use, but almost all specify the same criteria for low risk patients. The NCCN scheme leaves it to physician discretion whether to move a patient with multiple adverse factors into a higher risk group. The pre-NCCN schemes simply classified all patients with a single violation of the low-risk criteria as intermediate risk while patients with two or more adverse factors are classified as high risk. Percentage positive biopsies also appear to have important, independent prognostic implications, but there is no consensus on the proper cut points.

Many brachytherapists treat low-risk disease with brachytherapy alone. Brachytherapy may be used in high-risk disease as a boost for external beam radiotherapy (EBRT). The choice

of monotherapy versus combination therapy (brachytherapy plus external beam) in intermediate-risk prostate cancer is controversial and is the subject of study by the Radiotherapy Oncology Group (RTOG 0232, 2003). Preliminary results of another randomized trial on intermediate-risk patients that compared 44 Gy pre-implant external beam radiation combined with 90 Gy  $^{103}\text{Pd}$  brachytherapy versus 20 Gy external beam combined with 115 Gy  $^{103}\text{Pd}$  shows no significant difference in biochemical outcomes between the groups.<sup>15</sup>

In addition to radical prostatectomy, external beam radiation, and brachytherapy, there are several alternative treatment options for the patient diagnosed with early stage prostate cancer. These include cryoablation, hyperthermia, and radiofrequency ablation with no one option clearly superior to the others with regard to long-term cure of the disease.<sup>16</sup> Hormonal manipulation to reduce or eliminate testosterone necessary for prostate cancer growth has been used in disease management, and watchful waiting, also known as active surveillance, may be appropriate, especially for elderly or infirm patients. Treatment decisions are made based not only on the likelihood of cure, but also on the patient's continued quality of life. Brachytherapy dosimetry guidelines then should follow this same principle.

## II.1. SELECTED CURE RATE STUDIES OF PROSTATE IMPLANTS

Cure rates in prostate brachytherapy are measured as overall survival, disease-specific survival, and biochemical control. Because prostate cancer grows slowly, survival studies are difficult to perform, with most investigators presenting outcomes, even long-term outcomes, as biochemical disease free survival (BDFS). There is some evidence that the use of PSA control as a surrogate for disease-specific survival is appropriate.<sup>17</sup> A multi-institutional analysis of long-term BDFS in 2693 hormone naïve patients treated with brachytherapy alone found that risk group was the strongest predictor of outcome as shown in Fig. 1.<sup>18</sup> These are undeniably good results, but dosimetric data were available for less than one-fourth of the patients analyzed from the 11 contributing institutions. Although the analysis was not broken down by institutions, it is clear that not all institutions had equal success. With reference to the low-risk patients whose 9-year freedom from biochemical failure is about 80%, there were single institution reports of 8- and 9-year biochemical survival in the range of 95% to 97%. Based on the updated Partin tables low-risk patients in the worst-case scenario (clinical stage T2b, PSA between 6.1 and 10.0 and Gleason sum 5 – 6) had a probability of seminal vesicle involvement of <5% and lymph node involvement of <2%.<sup>13</sup> The typical low-risk patient had stage T1c, PSA 4 – 6 and GSS 5 – 6. For such patients, the probability of seminal vesicle involvement was 1% and lymph node involvement was 0%. Approximately one-fifth of low risk patients had extracapsular extension and only 10% of these had extension greater than 5 mm, beyond the reach of an implant planned with 5 mm margins.<sup>19</sup> Based on the pathological characteristics of low-risk patients, long-term biochemical survival should exceed 90%.

Several studies have shown that clinical outcomes in prostate brachytherapy, both for the retropubic approach and the TRUS-guided technique, correlate with dose coverage parameters. The extensive clinical experience of Memorial Sloan-Kettering Institute (1078 patients with retropubic approach surgery) from 1970–1987 was presented by Zelefsky and Whitmore.<sup>19</sup> Multivariate-analysis revealed that an achieved matched peripheral dose (MPD) of 140 Gy was an independent predictor of recurrence-free local control at 5, 10, and 15 years ( $p=0.001$ ).

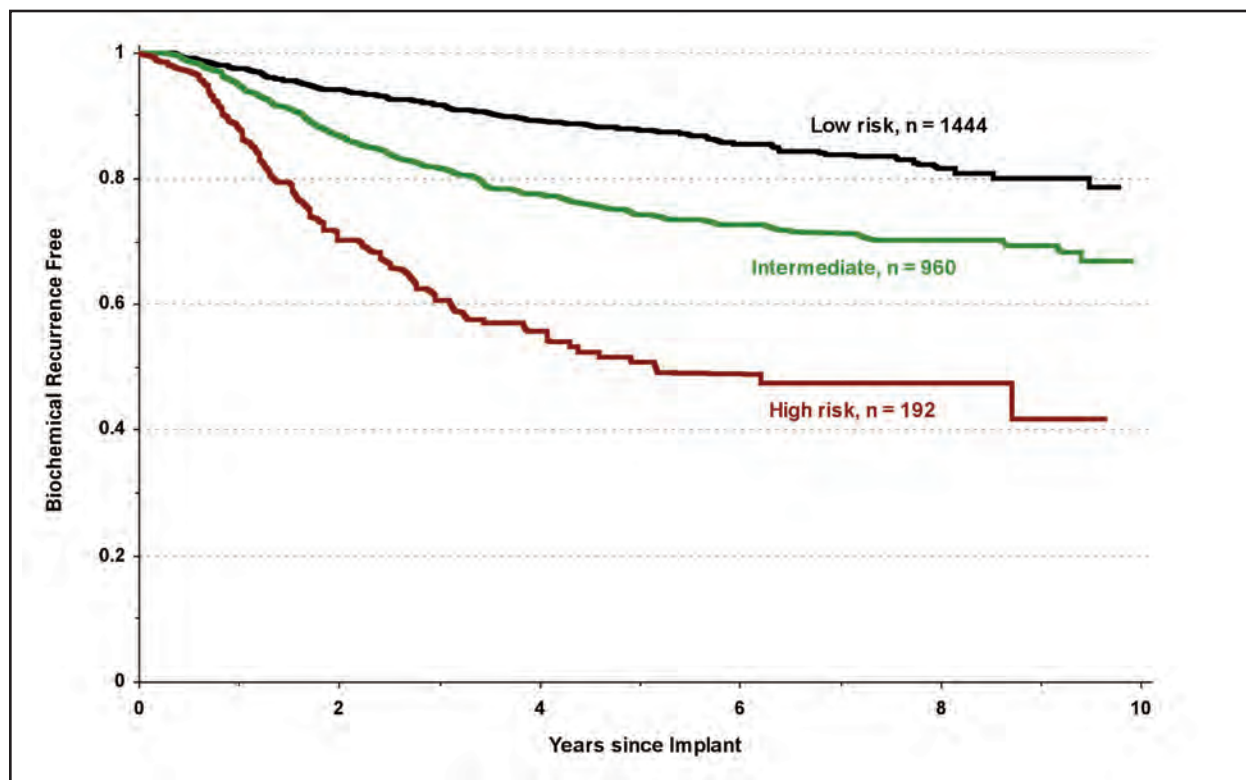


**Fig. 1.** Biochemical disease-free survival in 2693 hormone naïve patients treated with brachytherapy as monotherapy and stratified by NCCN risk group status. The number of patients in each risk group does not reflect prevalence—intermediate risk is the most prevalent diagnosis in patients with localized prostate cancer—but rather the reluctance among brachytherapists to treat higher risk patients with monotherapy. (Adapted from reference 18, *International Journal of Radiation Oncology, Biology, Physics*, vol 67, issue 2, M. J. Zelefsky, D. A. Kuban, L. B. Levy, L. Potters, D. C. Beyer, J. C. Blasko, B. J. Moran, J. P. Ciezki, A. L. Zietman, T. M. Pisansky, M. Elshaikh, and E. M. Horwitz. “Multi-institutional analysis of long-term outcome for stages T1-T2 prostate cancer treated with permanent seed implantation,” pp. 327–333, © 2007, with permission from Elsevier. <http://www.sciencedirect.com/science/journal/03603016>.)

MPD was defined as the dose delivered to a volume equal to the prostate volume. In this study the prostate volume was determined clinically prior to the implant. Similarly, a review of 110 implants at Yale University using the retropubic implant approach from 1976 to 1986 reported a correlation ( $p=0.02$ ) of clinically evaluated, recurrence-free local control after 10 years with  $V_{100}$ .<sup>21</sup> In contrast to the anatomic structure definition of  $V_{100}$  currently used, in this article  $V_{100}$  referred to the volume encompassed by the isodose surface described by 100% of the prescription dose of 160 Gy (using pre-TG-43 parameters). In this study the prostate volume was defined as the “minimum elliptical volume that would enclose most if not all of the seeds.” From this, the authors were able to calculate a coverage index (CI) that normalizes  $V_{100}$  with the target volume,  $CI = 100 (V_{100} - V_T)/V_T$  where  $V_T$  is the target volume. They were able to correlate the CI with cures in the 68-patient early stage subgroup.

Two recent retrospective studies of the TRUS technique also demonstrate that the clinical outcome depends on dose delivered and prostate volume coverage. Both studies were based on post-implant dosimetry taken from CT scans. Stock et al.<sup>22</sup> reported on an experience of 134 prostate cancer patients implanted with <sup>125</sup>I as the sole treatment modality (not treated with external beam therapy (EBRT) or hormonal therapy). They assessed rates of freedom from biochemical failure as a function of the  $D_{90}$  dose.  $D_{90}$  was defined as the minimum dose in the hottest 90% of the target volume. A significant increase in freedom from biochemical failure (92% vs. 68% after 4 years) was observed ( $p=0.02$ ) for patients ( $n=69$ ) where  $D_{90} \geq 140$  Gy.<sup>22</sup> In a later study, Potters et al.<sup>23</sup> recently reviewed the impact of various dosimetry parameters on biochemical control for their experience of 719 patients treated with permanent prostate brachytherapy. Many of these patients also received EBRT (28%) or hormone therapy (35%). Furthermore, 84% of the implants used <sup>103</sup>Pd with the remainder using <sup>125</sup>I. Their results indicated that patient age, radionuclide selection, and use of EBRT did not significantly affect biochemical relapse-free survival (PSA-RFS). The only dose-specification index that was predictive of PSA-RFS was  $D_{90}$ .<sup>23</sup> The close correlation between  $D_{90}$  and PSA-RFS and a dose response in the clinical dose range of 100 to 160 Gy are strong justifications for improved information and accuracy in the dosimetry for interstitial brachytherapy, the focus of this work.

It should be noted that  $D_{90}$  cut points for biochemical survival, like all prognostic cut points based on a continuous variable, are somewhat arbitrarily selected for statistical significance along a continuum of doses and outcomes. Determining that a patient lies in either the high-dose or the low-dose group does not ordain his outcome but merely assigns him an outcome probability based on the subgroup mean. The multi-institutional analysis of Zelefsky et al., of brachytherapy as monotherapy stratified patients into high and low  $D_{90}$  for <sup>125</sup>I and <sup>103</sup>Pd using cut points of 130 and 115 Gy, respectively, as illustrated in Fig. 2.<sup>18</sup> For both radionuclides, the long-term biochemical survival across all risk groups exceeds 90% in patients with good dosimetry, defined as  $D_{90}$  greater than 90% of the median prescribed dose.

## II.2. SELECTED COMPLICATION RATES STUDIES OF PROSTATE IMPLANTS

Tables 1 to 3 summarize those studies that correlate complications with post-implant dosimetry. There is very little consensus, not only with regard to doses, but also which organs should be considered at risk for causing complications. Multiple well-performed studies show conflicting results. Several investigators have looked at dose to the prostate gland as a portent of complications. The thinking is that, given a reproducible implant technique, high doses to the gland point to high doses to the critical structures, which lead to complications. This hypothesis obviates the need for drawing the critical structures or what dose limits they might require. For example, urinary frequency and increase in International Prostate Symptom Score (IPSS)<sup>24</sup> have been shown to correlate with  $D_{90} > 180$  Gy, while increased  $V_{150}$ ,  $V_{200}$ , and  $D_{90}$  seem to correlate with urethral stricture.<sup>25,26,27</sup>  $D_{90}$  values greater than 160 Gy tend to correlate with a decrease in potency.<sup>28</sup> Just as importantly there is also evidence that high-dose regions within the gland, which  $D_{90}$  and  $V_{150}$  convey, do not portend complications.<sup>29-31</sup>

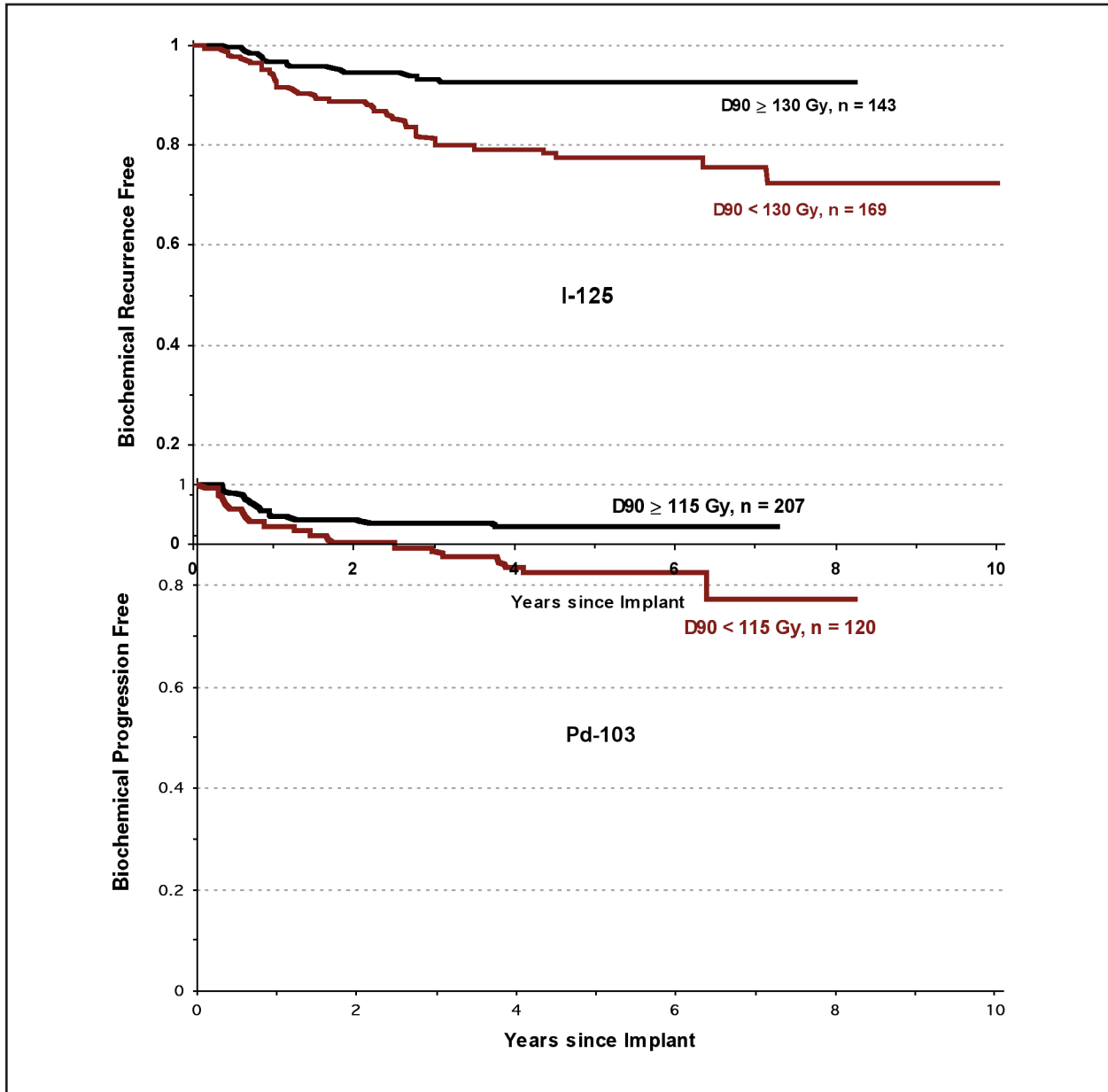


**Fig. 2.** Biochemical disease-free survival in hormone naïve patients treated with brachytherapy as monotherapy as a function of  $D_{90}$  group. The most statistically significant dosimetric cut point was 130 Gy for  $^{125}\text{I}$  (top graph) and 115 Gy for  $^{103}\text{Pd}$  (bottom graph). Patients from all risk groups are included, but the  $^{103}\text{Pd}$  population includes a higher proportion of intermediate and high risk. (Adapted from reference 18, *International Journal of Radiation Oncology, Biology, Physics*, vol 67, issue 2, M. J. Zelefsky, D. A. Kuban, L. B. Levy, L. Potters, D. C. Beyer, J. C. Blasko, B. J. Moran, J. P. Ciezki, A. L. Zietman, T. M. Pisansky, M. Elshaikh, and E. M. Horwitz. “Multi-institutional analysis of long-term outcome for stages T1-T2 prostate cancer treated with permanent seed implantation,” pp. 327–333, © 2007, with permission from Elsevier. <http://www.sciencedirect.com/science/journal/03603016>.)

**Table 1.** Post-implant dosimetry targets for avoiding urethral complications.

Structure	Goal	Refs
Prostatic Urethra	<360 (post-TG-43) Gy to significant lengths (10 mm) of the urethra	32
Prostate Gland	Urination Frequency, $D_{90} < 180$ Gy (200 Gy)	25,26
Prostate Gland	Dysuria, Dosimetry not predictive of dysuria	31
Membranous Urethra	Stricture, Dose to the membranous urethra < reference dose, no seeds >5 mm inferior to apical slice	27
Prostate Gland	Stricture, $V_{150} < 60\%$	27
Prostate Gland	No correlation between dose and complications, length of urethra is important	29
Prostate Gland	High-dose regions weakly correlate with IPSS score increases but only at 1 month	30

### II.2.a. Urinary Complications

A brachytherapy dose to more than 10 mm of the urethra exceeding 250% of the prescribed dose is likely to lead to RTOG Grade 2 or 3 morbidity according to Wallner et al., but with only modest urethral sparing techniques, such high doses are virtually unseen in the modern era.<sup>32</sup> Most short-term, acute urinary complications such as urinary obstruction or an increase in IPSS may be attributed more to needle trauma and to a lesser extent to dose and dose rate. In a study of 976 patients whose IPSS was determined at frequent intervals, the median time to return to pre-implant urinary baseline was <2 months.<sup>33</sup> It should be noted that all these patients were prescribed prophylactic  $\alpha$ -blockers such as Flomax™ beginning one week prior to implant and continuing, at the patient's discretion, as long as urinary dysfunction persisted. With regard to urinary complications, only excessive dose to the membranous urethra appears to be a sensible dose restriction to prevent urethral stricture.<sup>27</sup> A summary is presented in Table 1.

### II.2.b. Rectal Complications

Several investigators have shown that dose to the rectum correlates with rectal complications. Unfortunately, no two investigators seem to perform rectal dosimetry in quite the same fashion. Variants range from dose to the anterior rectal wall to dose to the surface of the outer rectal wall to dose to the annular volume between the outer and inner rectal walls. Table 2 depicts the success noted by these investigators.<sup>28,32,34–36</sup> The most useful of the resultant dosimetry guidelines was promulgated by Snyder et al.,<sup>28</sup> which based rectal dose constraints on an annular dose-volume histogram of the rectum, targeting to achieve less than 1.3 cm<sup>3</sup> to receive 160 Gy for iodine monotherapy. This rule is often modified by practitioners who prescribe 145 Gy minimum peripheral dose (mPD) to read less than 2.0 cm<sup>3</sup> to receive 145 Gy as this is also evident from the publication.<sup>28</sup> The mPD was defined by Rao et al. as the lowest dose at the intersection of the periphery of each seed array and a plane halfway between the planes carrying the seeds.<sup>37</sup>

**Table 2.** Post-implant dosimetry targets for avoiding rectal complications.

Structure	Goal	Refs
Rectum	Dose to >1 cm length of anterior mucosal wall < reference dose Dose to >5 mm length of anterior mucosal wall < 1.2 × reference dose Max dose to anterior mucosal wall <120% of reference dose	34
Rectum	Annular DVH of rectum <1.3 cm <sup>3</sup> to 160 Gy or <2.0 cm <sup>3</sup> to 145 Gy (I-125)	28
Rectum	Surface area of outer rectal wall <5 cm <sup>2</sup> to reference dose	35
Prostate	High dose regions, no correlation to rectal complications	30
Rectum	Surface area of outer rectal wall 30% < 100 Gy, 20% < 150 Gy, 10% < 300 Gy (I-125)	242

Crook et al., confirmed and recommended this technique.<sup>38</sup> As an aside, many practitioners, out of conservatism, limit the volume of the rectum receiving more than the prescription dose to less than 1 cm<sup>3</sup>. This conservatism is fueled by the fact that the overwhelming majority of malpractice claims involving prostate brachytherapy arise from the rare occurrence of rectal fistulas.<sup>39</sup>

### II.2c. Erectile Complications

Erectile dysfunction critical structure dosimetry is perplexing, probably because the etiology of erectile dysfunction is a multifactorial phenomenon.<sup>40</sup> A look at Table 3 reveals antithetical debate over the critical structures. Neurovascular bundles (NVB) and proximal penile structures

**Table 3.** Post-implant dosimetry targets for avoiding erectile dysfunction.

Structure	Goal	Refs
Neurovascular Bundles	Possible correlation between NVB dose and early impotence	243
Neurovascular Bundles	No correlation between NVB dose and erectile dysfunction	244
Prostate Gland	$D_{90} < 160$ Gy (I-125), $D_{90} < 100$ Gy (Pd-103)	28,35
Penile Bulb Dose	$PBD_{50} < 50$ Gy; $PBD_{50} < 40\%$ mPD, $PBD_{25} < 60\%$ mPD	36,122
Prostate Gland	Avoid external beam radiotherapy; reduces 6 year actuarial potency preservation from 50%–60% to 25%–30%	245,246
Penile Bulb	Radiation dose to the penile bulb does not correlate to erectile dysfunction	247
Penile Bulb	$PBD_{90} < 10\%$ mPD	248
Neurovascular Bundles	No correlation between dose and retention of potency	248
Penile Bulb	No correlation between dose to the penile bulb and retention of potency	249

are possible candidates, but there is neither consensus on these targets, nor any agreement on desirable dose limits. Dose to the penile bulb (PB) has been implicated in erectile dysfunction in a randomized external beam trial, and a brachytherapy cohort treated with penile bulb sparing techniques improved in potency retention to 51% compared with an earlier cohort at 39% potency retention treated without any potency sparing considerations.<sup>41,42</sup>

### II.3. HISTORICAL PERSPECTIVE ON DOSE REPORTING

Consistency in dose specification, prescription, and reporting is an important step towards establishing a uniform standard of practice in prostatic brachytherapy. Early efforts in this area were exclusively limited to idealized representations of the target using cubic, cylindrical, spherical or ellipsoidal volumes.<sup>43,44–46</sup> However, these investigations marked the departure from built-in target-size dependence in nomograph-based planning and prescription toward specification or prescription of a desired dose. The early experience with CT-based planning and evaluation for <sup>125</sup>I prostate implants at the Memorial Sloan-Kettering Cancer Center (MSKCC) was reported by Roy et al.<sup>47</sup> In their study, the peripheral dose was defined as the isodose surface that encompassed 99% of the target volume, or  $D_{99}$ . By analyzing 10 implant cases, they showed that the actual coverage of the target volume by the peripheral dose ranged from 78% to 96%, with an average coverage of 89%. In 1997, Willins and Wallner published a follow-up study presenting the analysis of 20 unselected implant cases performed by an experienced clinical team.<sup>48</sup> In this study, dose was prescribed to the planned minimum peripheral dose (mPD); post-implant dosimetry was carried out using CT taken on the day of implantation. The actual coverage of the target volume by the prescribed mPD ranged from 73% to 92%, with an average of 83%. The actual  $D_{100}$  delivered to the target volume was  $43\% \pm 8\%$  ( $\pm 1SD$ ) of the prescribed mPD. The authors identified subjectivity in interpreting post-implant CT scans and prostatic swelling as extraneous uncertainties, which would compound with any seed placement errors to result in apparently poor coverage by the mPD. The reliance on the mPD for dose prescription and reporting was discussed by Yu et al.<sup>49</sup> Based on simulated distributions of common seed placement errors, they concluded that generally 90% of the original PTV could be covered by the prescribed mPD when the average dimension of the PTV was greater than 3 cm. No consistent pattern was found for the magnitude of underdosage between the planned mPD and the realized  $D_{100}$ ; however, underdosage from the planned mPD to the realized  $D_{100}$  could easily exceed 20% due to common seed displacement.

Although the mPD as a dose specification parameter displays excessive sensitivity, it is the most direct measure of dosimetric coverage under 3D image-based treatment planning. Less-sensitive dosimetric parameters have been proposed for prescription and/or reporting, including the net minimum dose, the average peripheral dose, the harmonic mean dose, and the widely cited matched peripheral dose.<sup>1,44,45,49</sup> However, these parameters by definition do not provide the essential information on isodose coverage of the PTV. The practice of prescribing the treatment dose to the mPD is also consistent with modern external beam radiation therapy. The problem of achieving consistency between dose specification for prescription and dose reporting is closely related to the uncertainties in defining the PTV, which are discussed in more detail in the next section.

It must be concluded at this time that the present techniques for permanent seed implantation do not yet allow the planned mPD to be reproduced with any consistency; however, the percent coverage of the PTV by the planned mPD isodose surface is a reasonably consistent indicator of implant quality. Furthermore, the mPD required for clinical control of disease and avoidance of morbidity is currently unknown. Therefore, it is customary to use the percent coverage of the PTV, using  $V_{100}$  and  $D_{90}$  as the recommended method for dose prescription. We explore these issues further in this report.

### **III. IMPACT OF IMAGING MODALITY ON DOSE REPORTING**

Use of multiple imaging modalities and different margins in various directions and use of various dosimetry descriptors have led to a rich variety of new clinical information in the past decade. A brief overview of different methods used for this purpose is described in the following paragraphs.

The AAPM TG-64 and the American Brachytherapy Society (ABS) as well as European groups recommend the use of CT to evaluate the implant. Dosimetric parameters  $D_i$  and  $V_i$  that are used to score an implant are dependent on accurate identification of source position, dose calculation, and target delineation. Most inconsistencies in dose reporting are a result of disparity in target delineation. Various imaging modalities can be used to evaluate an implant. Plane films provide source positions but lack soft-tissue contrast. The ultrasound images provide prostate definition but cannot offer unambiguous seed positions. The use of CT to evaluate the implant is currently the standard of care. CT images of the pelvis provide excellent source definition within the limits of axial slice spacing and partial-volume artifact, and exhibit reasonable soft-tissue contrast. However they are not as reliable as MR images for prostate or normal tissue delineation. MR imaging requires multiple scans for optimal viewing of the soft tissue and sources. The effect of various imaging modalities on delineating target volumes and their impact on dose reporting is addressed below.

#### **III.1. ULTRASOUND IMAGING**

Both ABS and ESTRO (European Society of Therapeutic Radiology and Oncology) recommend the use of ultrasound for implantation but not for evaluation.<sup>50,51</sup> The PTV is the prostate as visualized using a transrectal ultrasound probe. In addition to the prostate, the rectal wall and urethra are clearly visible on ultrasound. Prostate volume definition on ultrasound is superior to the CT definition of the prostate. Despite the clarity of the prostate image on ultrasound there is a tendency to contour the lower sphincter on the ultrasound as prostate, and care should be taken to avoid this common oversight (Fig. 3). Studies have shown that inter- and intraobserver prostate volume definition can be minimized using 3D ultrasound scans.<sup>52,53</sup> The superior prostate definition on ultrasound would make this imaging modality the choice for implant evaluation over CT if the sources could also be visualized. Source identification on ultrasound is challenging and ambiguous. Sources that are not oriented perpendicular to the ultrasound beam are not clearly visualized.<sup>54</sup> Therefore, ultrasound images should be used with other imaging modalities like CT or fluoroscopic images to provide better source identification.

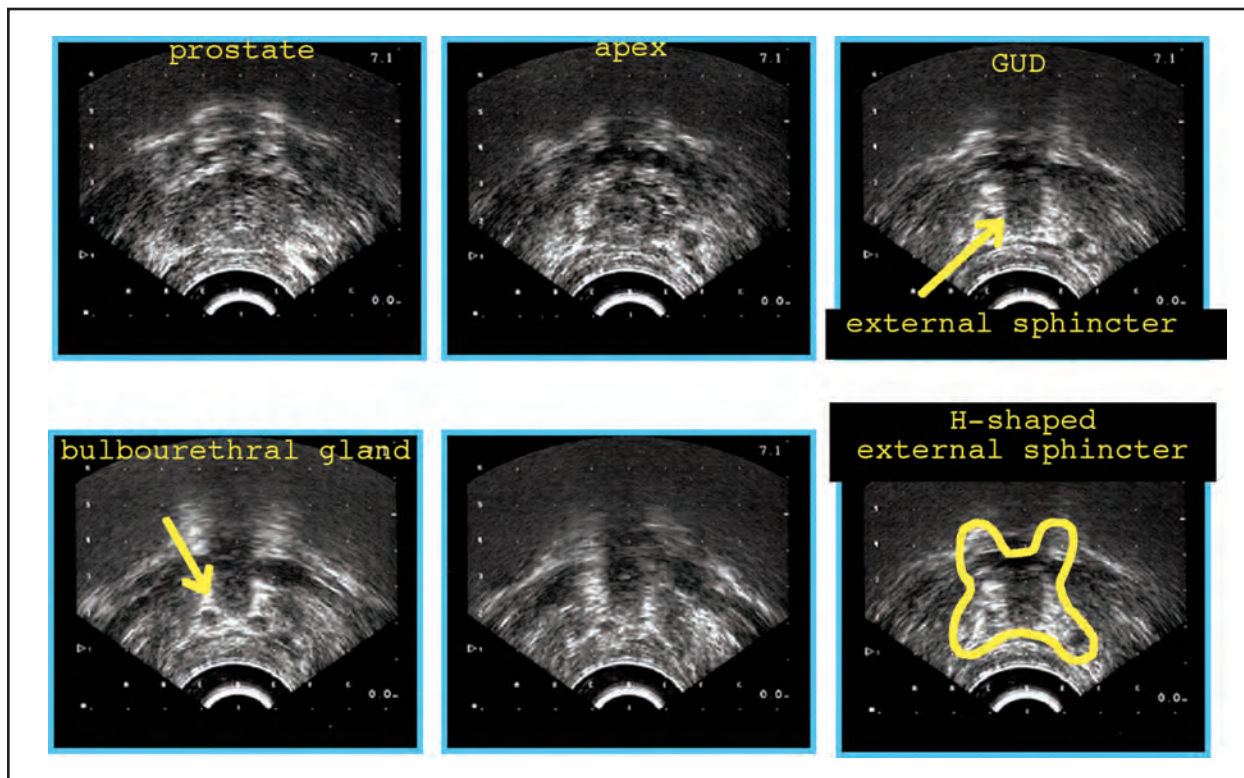


**Fig. 3.** A series of axial ultrasound images of the prostate showing the clear apex/genitourinary diaphragm (GUD) transition on ultrasound. In a less clear example the external sphincter may be contoured as prostate resulting in unnecessarily implanting normal tissue. Recognition of the light H-shaped GUD or bulbourethral gland indicates GUD.

Attempts made to register the ultrasound prostate images to the CT images are prone to problems arising from the ultrasound prostate distortion due to the presence of the probe in the rectum and the movement of the probe as it steps through the entire length of the prostate.<sup>55</sup> Techniques to register fluoroscopic seed positions to the ultrasound prostate images can provide a means of real-time dosimetry with accurate prostate volume delineation and source position definition.<sup>56,57</sup> Such a fusion, if accurately performed in conjunction with newer ultrasound equipment that does not distort the prostate during imaging, would reduce the variability in dose reporting.

The ultrasound imaging equipment used for brachytherapy should be checked for geometric accuracy following the recommendations in AAPM TG-1 report.<sup>58</sup> It should be noted that there is an AAPM task group (TG-128) charged with the development of quality control (QC) test procedures for endorectal ultrasound imaging.<sup>59</sup>

### III.2. CT IMAGING

Dose indices routinely reported in the literature, such as  $D_{90}$ , are CT based, and quality of the implant based on  $D_{90}$  is a standard. While CT is used to establish source positions, the clarity of CT images is inadequate to contour the prostate accurately. This is the primary cause of reported

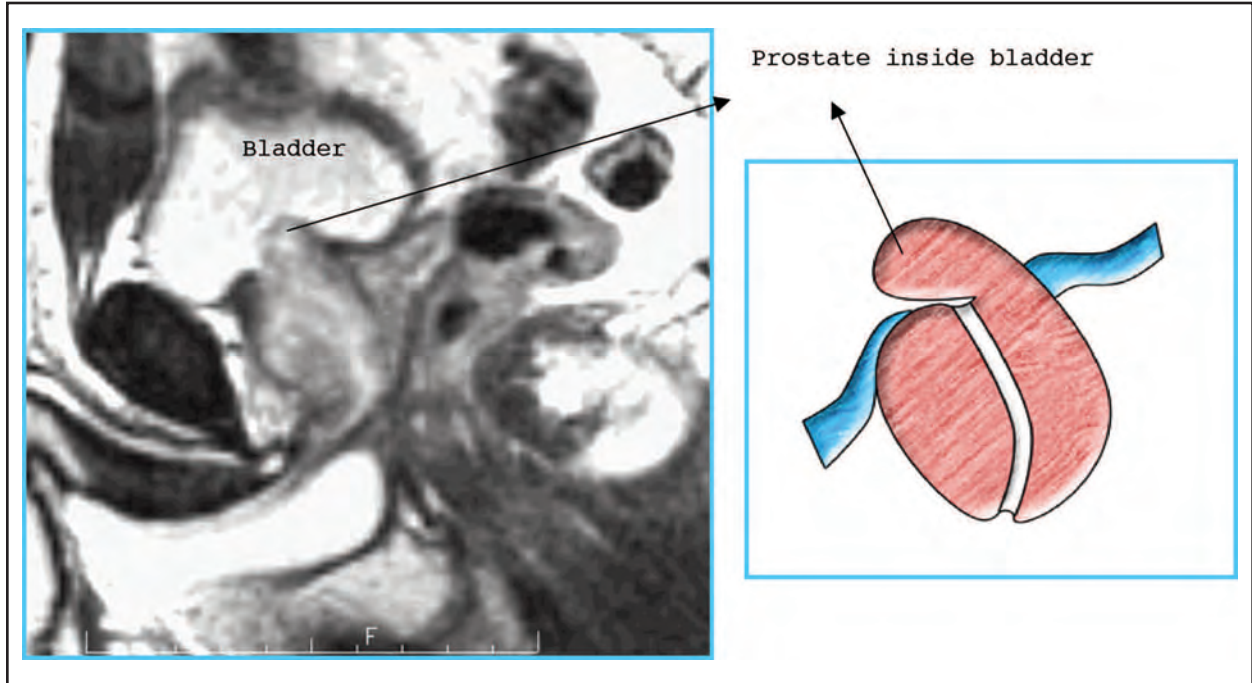


**Fig. 4a.** Sagittal view of a large prostate gland on MR infiltrating the bladder. On an axial CT, the prostate in the bladder neck will commonly be contoured as bladder.

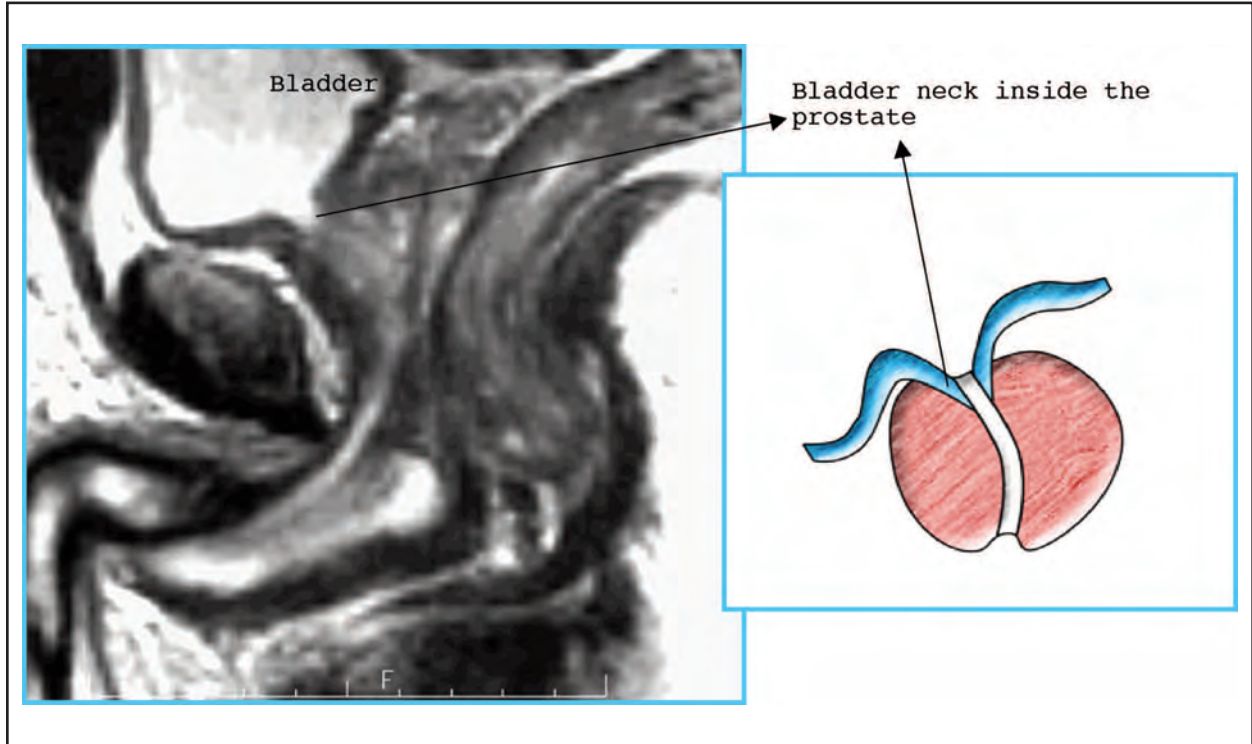


**Fig. 4b.** Sagittal view of a small prostate on MR with the bladder neck in the prostate. On an axial CT the bladder neck is commonly contoured as prostate.

large variations of inter- and intraobserver values of  $D_{90}$  and  $V_{100}$ .<sup>59,60,61,62</sup> In general, it is more difficult to identify accurately normal structures adjacent to the prostate in CT images than on MR because of lower soft-tissue contrast with CT compared to MR images. Also, it is difficult to distinguish the inferior part of the prostate, the apex, on CT, and the prostate volume tends to be overestimated by the observer.<sup>64</sup> The superior part of the prostate, the base, can also be particularly challenging to contour.<sup>65</sup> Large glands obliterate the bladder neck (Fig. 4a) and may not be contoured as prostate on CT. And the intact bladder neck for small glands is difficult to distinguish from the prostate and may be contoured as prostate (Fig. 4b). (A prominent median lobe penetrating the bladder as in Fig. 4a is easily identified on ultrasound. Because such median lobes are almost impossible to implant adequately, they are usually resected by the urologist prior to implant.) Furthermore, post-implant scans are distorted due to the presence of seeds and edema from the implant procedure. Despite accurate determination of seed position and dose calculation, the wide variation in doses reported is testimony to the difficulties in contouring the prostate on CT.

Inaccurate delineation of the prostate after implantation can potentially lead to incorrect conclusions. Overestimation of the prostate apex due to inadequate soft-tissue contrast can falsely result in a change in  $D_{90}$  and  $V_{100}$ . Underestimating the base on large glands and overestimating the base on small glands can also potentially lead to incorrect conclusions regarding base coverage. In addition, Han et al., have shown that the variation of the dose indices are based on the implant style with wide margin implants being insensitive to contouring differences.<sup>66</sup> Generally, most CT-based dose and volume indices reported in literature are limited due to the lack of consensus in contouring. Increased awareness of prostate anatomy and training in CT contouring can increase the agreement in dose reporting.<sup>67,68,69</sup>

Contouring normal structures responsible for urinary, rectal, and erectile function and determining the dose to these structures is crucial to delivering and evaluating optimal therapy. Outlining normal structures adjacent to the prostate responsible for these functions are also equally challenging on CT. The urethra cannot be distinguished on CT unless a Foley catheter with a contrast material is used. Seeds placed in the posterior region of the prostate obliterate the prostate-rectum interface and make contouring the outer rectum difficult. The inner rectum or the rectal mucosa, which is the radiation sensitive component of the rectum, cannot be unambiguously delineated on CT. The neurovascular bundle and structures associated with erectile function cannot be identified unambiguously on CT. Because of the difficulty in outlining normal structures while using CT-based evaluation, attempts have been made to correlate dose to the prostate and normal tissue complication. Other groups have reported dose to the normal structure by outlining the structures as viewed on CT or use surrogates. The geometric center of the prostate has been used as a dose point for the urethra. It is common to use the penile bulb dose as a surrogate for erectile function.

### III.3. MR IMAGING

In comparison to CT, MR imaging provides improved soft-tissue contrast such as base and apex definition and determination of the prostate rectal interface (Fig. 5). As shown in Figs. 6 and 7, T2-weighted images provide identification of the prostate and critical normal tissue adjacent to

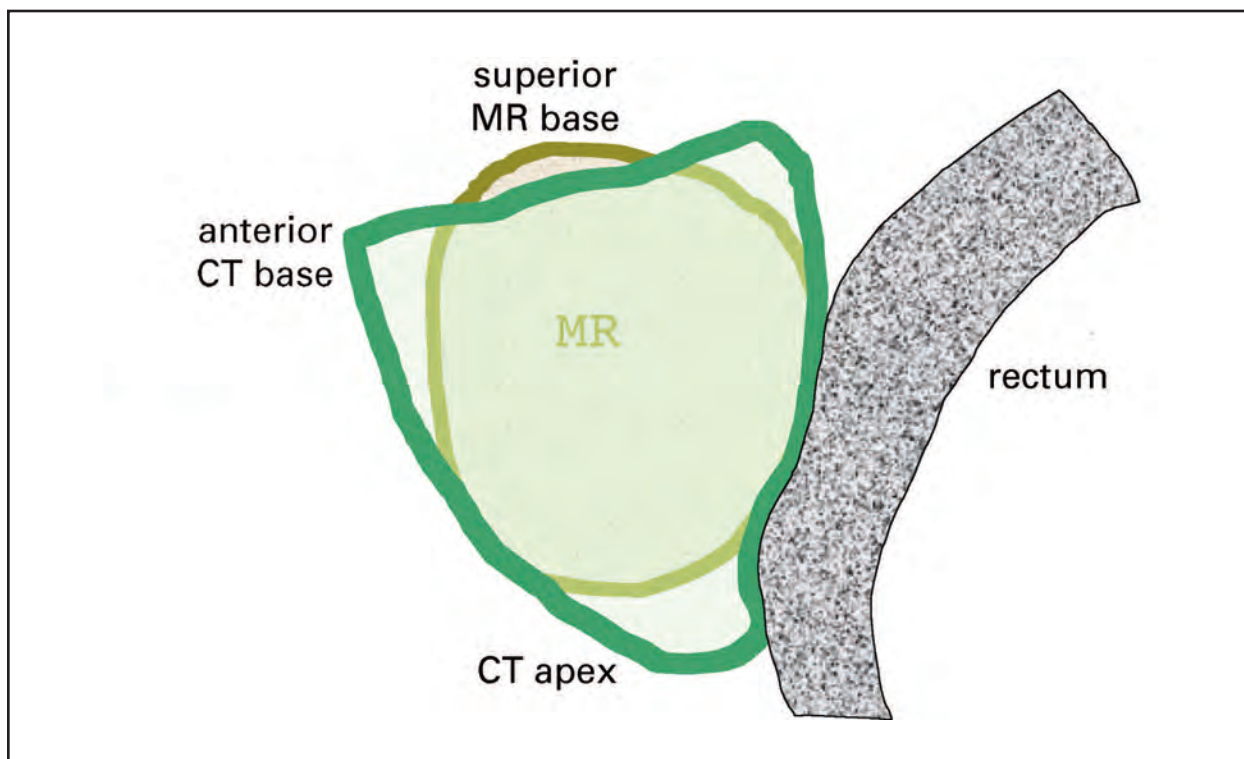


**Fig. 5.** A coronal view of the pitfalls commonly encountered with CT prostate contouring. The prostate on MR is shown as solid structure. The anterior CT base tends to be overestimated as a result of contouring the bladder muscle. The superior base tends to be underestimated if there are no seeds implanted in the superior base. The CT apex tends to be overestimated as a result of contouring the seeds and following the rectal surface.

the prostate.<sup>70</sup> The rectal wall comprising of the outer rectal muscle and the inner rectal mucosa can be distinguished on T2-weighted axial MR. McLaughlin et al., reported that the average rectal wall thickness in 10 patients adjacent to the prostate was 4.7 mm with a range of 3.2 mm to 6.8 mm.<sup>71</sup> The dose to the bladder, urethra, rectum, upper and lower sphincter, corpus cavernosum, penile bulb, neurovascular bundle, and pudendal arteries can further be determined using MR imaging and correlated to dose-toxicity and quality of life studies.

The variability in volume definition is reduced with MR images due to the clarity of the images. A pulse sequence that improves volume definition, however, does not allow the unambiguous determination of seed position. Seed localization is performed either on CT or planar images and fused with MR images.<sup>72,73–75</sup> Image registration involving two or more modalities introduces uncertainties depending on the timing of the scans. Difference in bladder and rectal filling can be significant even when CT and MR scans are obtained one immediately following the other with similar patient positioning. In addition, ideal anatomical registration can only be achieved over a certain region of interest and not over the entire volume of the patient.

Endorectal MR imaging has been used to determine both the seed position and to delineate anatomy.<sup>76</sup> While the use of endorectal coil increases patient discomfort and reduces the

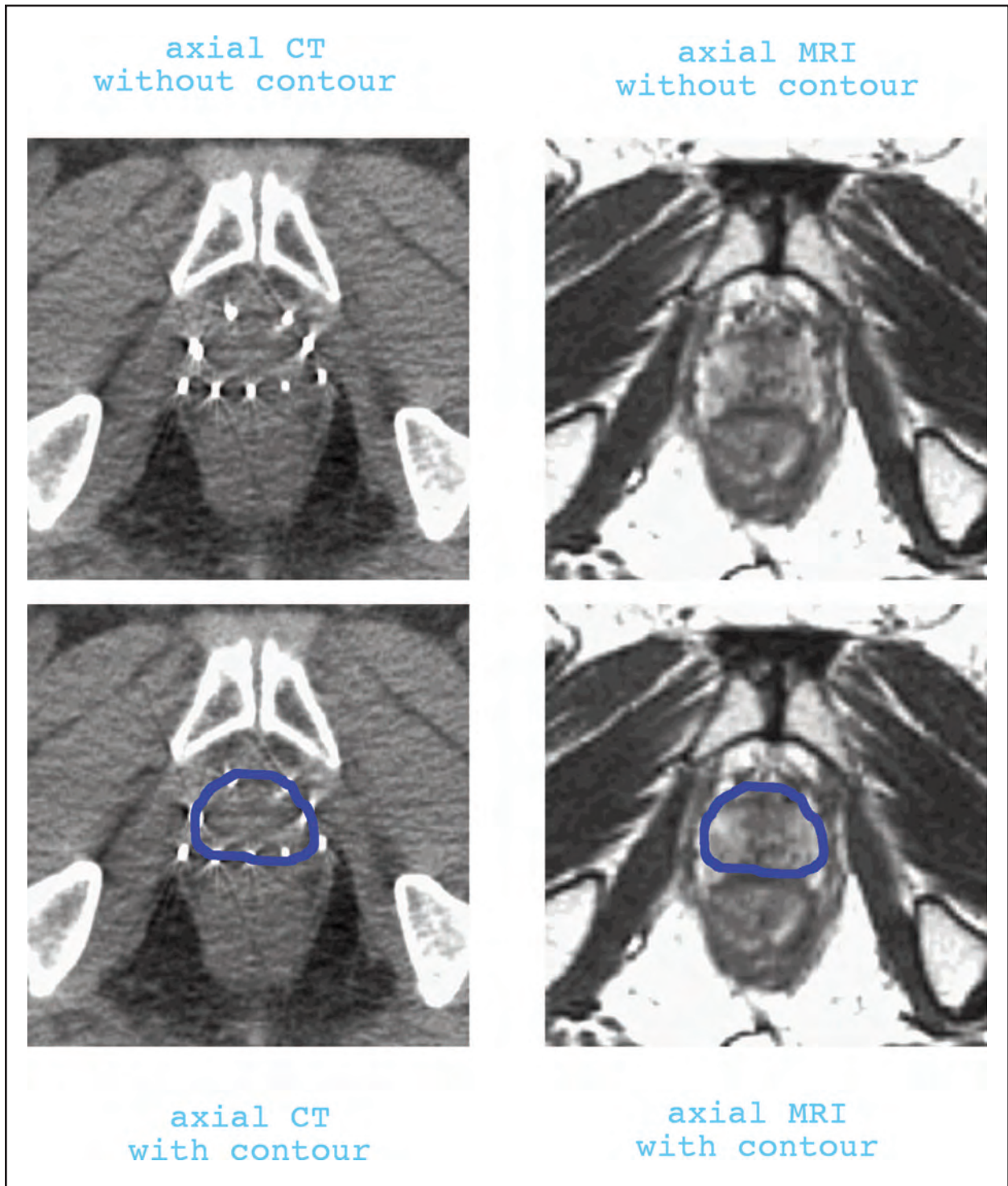


**Fig. 6.** Axial CT showing the degradation of the prostate-rectal boundary due to the presence of seeds. The corresponding axial MR view showing a clear prostate-rectal boundary with and without the prostate contour.

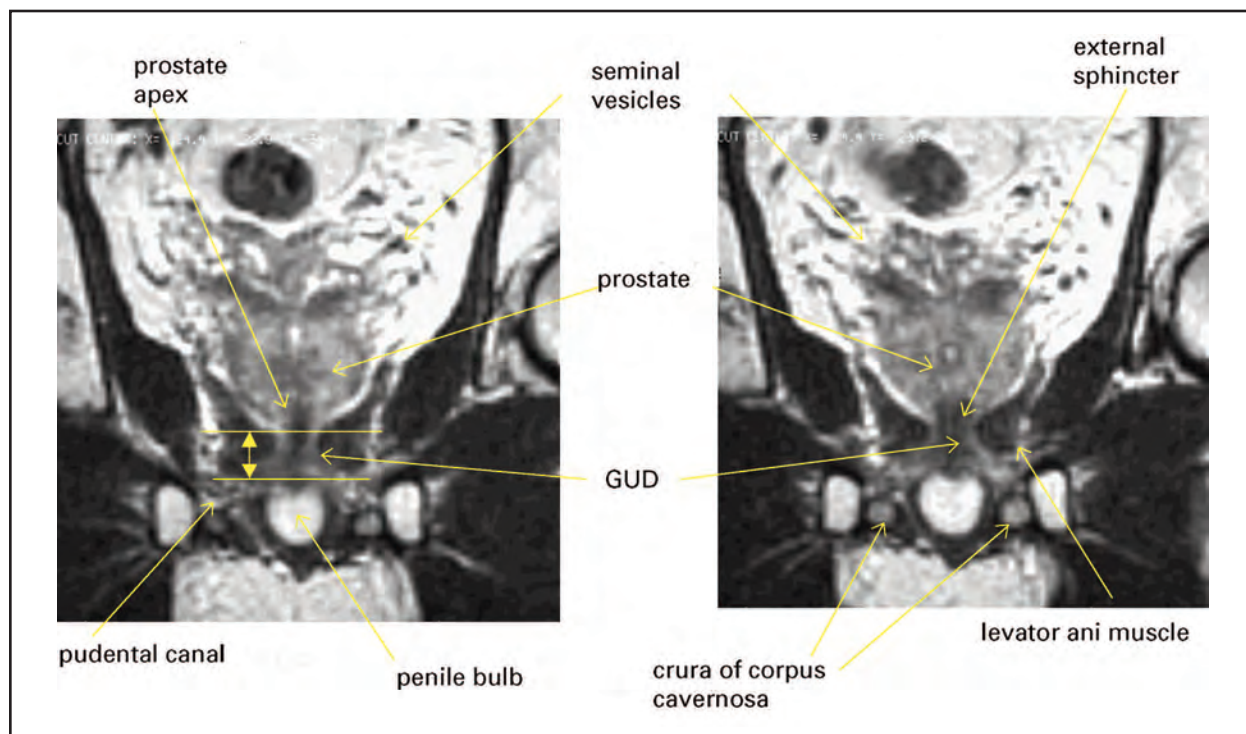


**Fig. 7.** Anatomical structures around the prostate on coronal MR.

reliability of dose determination to the rectum, it removes the need for fusion between different imaging modalities and associated uncertainties. MR images provide better anatomical definition but increase the cost of imaging. It should therefore be used only when a clear medical benefit has been identified. With improved instruction and education in contouring most structures can either be outlined or surrogates determined on CT. Training guidelines to contour the CT base and the apex reproducibly will improve consistency in reporting the existing dose parameters as shown in Fig. 8.<sup>77</sup>

#### III.4. RECOMMENDATIONS ON IMAGING OF PROSTATE IMPLANTS

Imaging plays a crucial role in dose reporting for prostate implant. The dose indices used for evaluating an implant are dependent on target and normal structure delineation, which is highly variable. With the intent of providing consistent and reproducible dosimetric information without increasing healthcare costs the following guidelines are suggested.

1. Axial CT (2–3 mm) contiguous images should be used for post-implant evaluation. Although drawing the prostate is easier with 5 mm slices because of better contrast, the seed locations are more precisely located using smaller slice thicknesses as demonstrated by the European group Brachytherapy Physics Quality Assurance System (BRAPHYQS) in a study using the Kiel phantom.<sup>78–80</sup>
2. The prostate should be contoured being mindful of the difficulties that are encountered at the prostate base and apex.

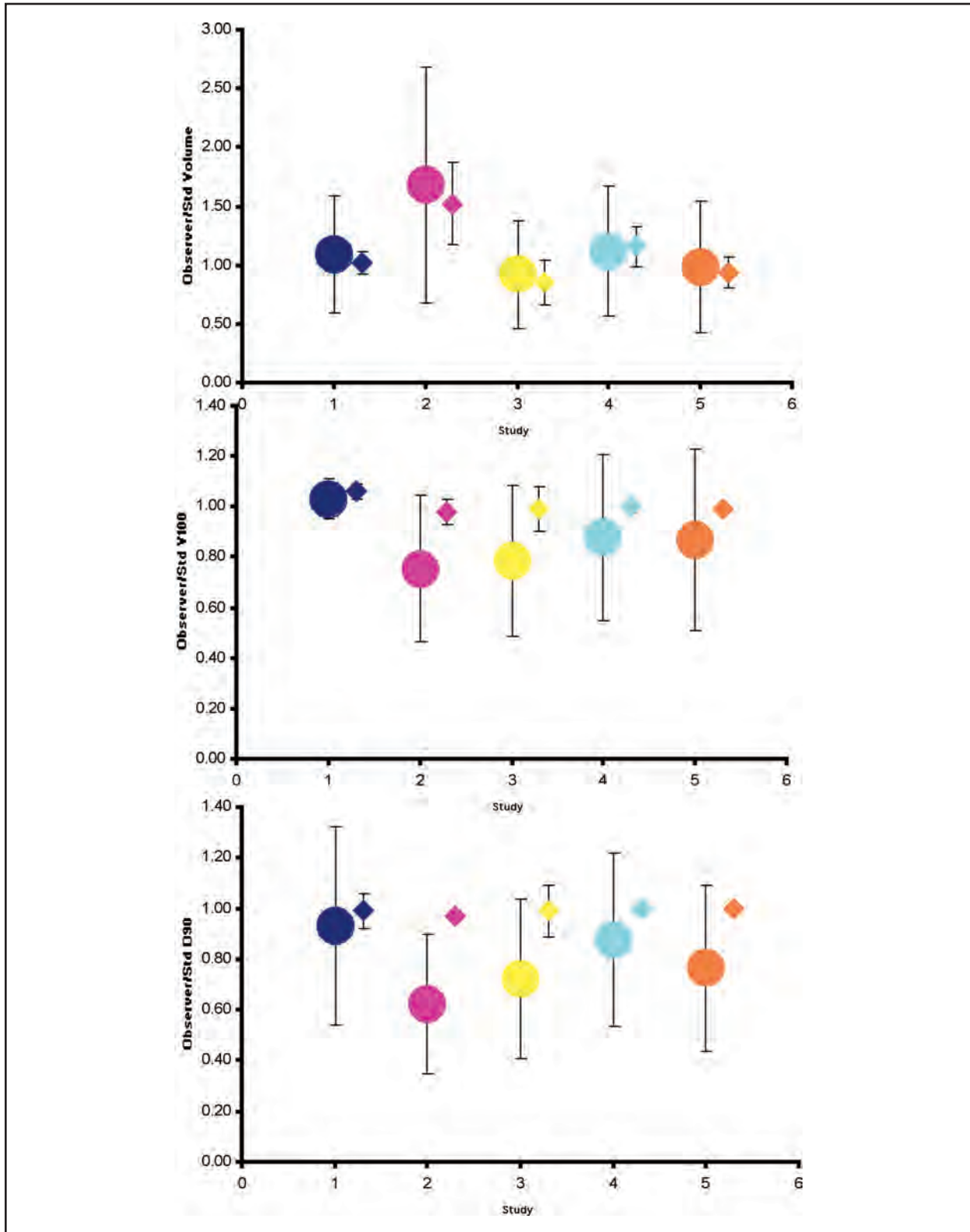


**Fig. 8.** Prostate volume,  $V_{100}$  and  $D_{90}$  for five post-implant CT datasets contoured by 6 radiation oncologists with training (diamonds) and 59 observers (circles) without training shows that the average prostate volume is similar. The standard deviation with training is smaller indicating that training can reduce variability in prostate contouring between individuals.

3. The outer rectum should be contoured 1 cm superior and inferior to the prostate on CT. Volume of the rectum receiving greater than 100% of the prescription dose should be recorded. The rectum should not be distended when scanned.
4. The rectal wall on CT can be approximated by a 0.5 cm contraction of the outer rectal surface.
5. A Foley catheter should be used during day 0 imaging, and the urethra should be contoured on all slices within the prostate. For post-implant dose evaluation, a Foley catheter is optional.
6. The penile-bulb dose (PBD) can be used as a surrogate for dose to erectile tissues.

It is recommended that the guidelines below be followed when MR imaging is available. Generally speaking, contours of the normal structures and tumor volumes are better identified with MR, whereas seed locations are more precisely located by CT. It is ideal that the CT and MR images be obtained on the same day and be fused using appropriate software.

1. Axial, coronal, and sagittal, T2-weighted images (3 mm) contiguous images should be obtained immediately before or immediately after the CT. The prostate should be contoured on MR using the information from axial, coronal, and sagittal scans.
2. Axial CT (2–3 mm) contiguous images should be used to determine the source positions for post-implant evaluation.
3. The outer and inner rectum should be contoured on axial MR 1 cm above and below the prostate. Volume of the rectum receiving greater than 100% of the prescription dose should be recorded. The rectum should not be distended when scanned (i.e., do not use a rectal coil).
4. The bladder should be contoured on the axial MR.
5. The axial and sagittal MR should be used to contour the urethra.
6. Other normal tissues responsible for erectile function should be contoured on MR.
7. MR and CT datasets should be registered only in the area immediately surrounding the prostate and not the entire pelvic region.
8. The dose distribution for the CT-determined seed positions should be displayed on an axial MR dataset.

#### **IV. EFFECT OF IMAGING TIMING ON DOSE REPORTING**

A number of studies have shown that the post-surgical edema and its resolution can alter the dose delivered by an implant.<sup>81–84</sup> The dynamics of edema resolution and the decay of radioactivity can lead to large changes in the dose delivered if this effect is not taken into account. The magnitude of this effect further depends upon the timing of imaging after the implant for the purpose of dose evaluation and dose reporting.

#### IV.1. GENERAL CHARACTERISTICS OF POST-IMPLANT PROSTATE EDEMA

For a typical implant, between 50 and 150 sources are placed into the prostate through transperineum guiding needles (usually 18 gauge, about 1.25 mm outer diameter). At least 15 and sometimes more than 30 guiding needles or needle-insertions are needed to place the sources to various spatial locations in the gland. The mechanical trauma caused by the needle insertion, the intraprostatic bleeding resulting from the needle penetrations, and the general inflammatory response to the needle perforations together cause the prostate gland to swell initially and reach a maximum volume shortly after the completion of procedure followed by gradual resolution of the swelling.<sup>85,86</sup> Except for a few reports demonstrating a weak negative correlation of the procedure-induced percentage volume increase with the pre-implant prostate volume, published studies have not found any consistent correlation of either the amount of edema or its temporal resolution pattern with the known characteristics of a patient such as age, pre-implant gland volume, use of hormones, or with the details of the procedure such as radionuclide type, number of needles used, number of implanted sources, and total source strength.<sup>83,81-84</sup> In general, the degree of procedure-induced prostate edema and its rate of resolution varied significantly from patient to patient and remained unpredictable for individual patients at the completion of the procedure.

#### IV.2. QUANTITATIVE CHARACTERIZATION OF PROSTATE EDEMA

To facilitate the discussion, Fig. 9 illustrates an expected time course of procedure-induced prostate edema in permanent prostate brachytherapy. In Fig. 9,  $T_0$  and  $V_0$  denote, respectively, the time and prostate volume just before the surgical procedure,  $T_{max}$  denotes the time when the

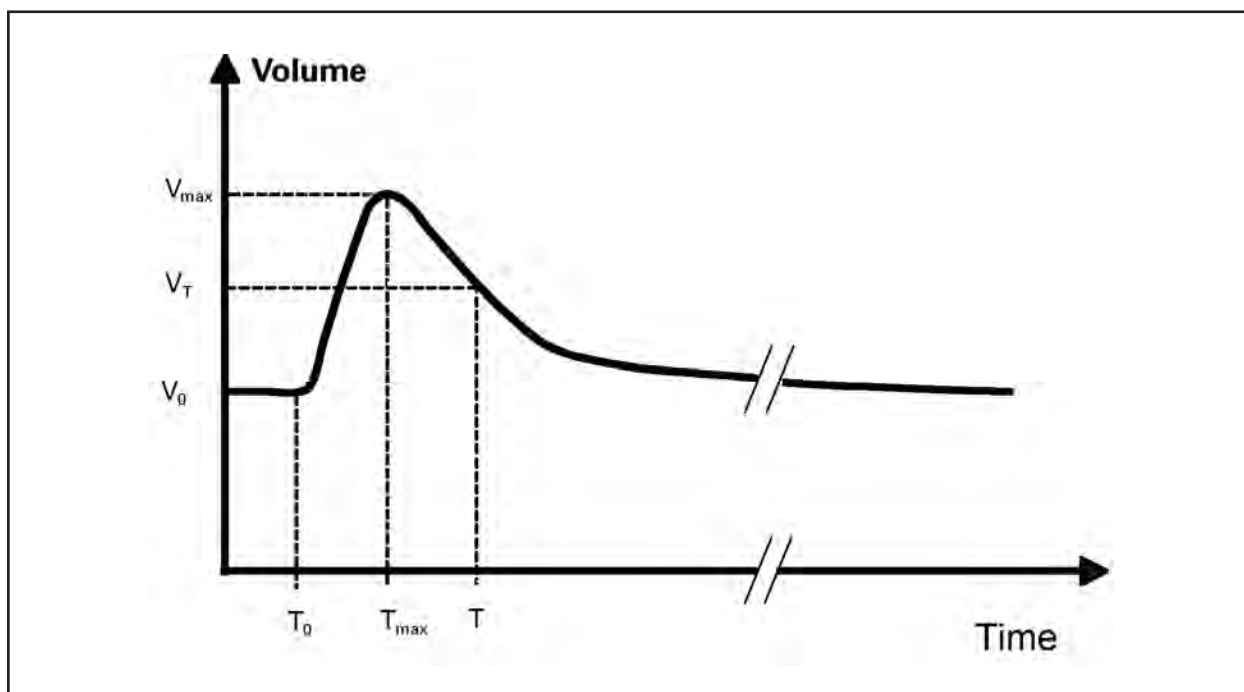


Fig. 9. Schematic illustration of the time course of prostate volume following source implantation.

prostate volume swells to a maximum volume,  $V_{\max}$ , and  $T$  denotes a user-selected time for post-implant imaging study or conventional dosimetry.

Prostate edema is typically characterized by an edema magnitude and a resolution half-life. The edema magnitude is usually defined by the pre- and post-implant prostate volume as:<sup>87</sup>

$$\Delta = V_T/V_0 \quad \text{or} \quad \Delta = 100\% \times (V_T/V_0 - 1). \quad (1)$$

Numerically,  $\Delta$  has often been reported as either a real number (i.e.,  $V_T/V_0$ ) or as a percent-volume-increase from the pre-implant volume (i.e.,  $100\% \times (V_T/V_0 - 1)$ ). The latter convention will be used in this report. The characterization of edema resolution for  $t > T_{\max}$  requires explicit knowledge on the functional form of the resolution. In a comprehensive study, it was demonstrated that the edema resolution could be described by a single exponential decaying function.<sup>83</sup> In line with that finding, a 1<sup>st</sup> resolution half-life (defined as the time it takes to resolve the maximum edema by 50%) has been used by many investigators. When edema resolution deviates from the exponential decay function one may need 2<sup>nd</sup> or 3<sup>rd</sup> resolution half-lives for a more comprehensive characterization. Table 4 summarizes the edema magnitude and the 1st resolution half-life reported by various studies.

#### IV.2.a. Edema Magnitude

It should be noted at the outset that the edema magnitudes reported in the literature were not always determined under the ideal condition for Eq. (1) because of the lack of exact knowledge of  $T_{\max}$  and the use of different imaging modalities in the determination of  $V_{\max}$  and  $V_0$ . When a selected time for imaging study deviates from the true  $T_{\max}$ , the edema magnitude would be underestimated by an amount that is dependent on the timing (see Fig. 9). When different imaging modalities are used for volume measurements, additional uncertainties are introduced because the amount of tissue visualized by different imaging modalities can be systematically different. The imaging time associated with various reported edema magnitudes ranged from immediately after the insertion of all guiding needles to immediately or several hours after the completion of source implantation to approximately 1 day or 3 days after the procedure.<sup>84,85; 82,83,88–90;55,72,81,91</sup> The mismatch of imaging modalities included TRUS for  $V_0$  with CT, MRI, or radiographic films for  $V_{\max}$ .<sup>72,81,82,89,91,92</sup> This lack of uniformity made it difficult to directly compare the edema magnitudes reported by different institutions. It also introduced additional artificial variations to the reported edema magnitudes that, if not fully appreciated, could lead to underestimation of the true magnitude of edema.

The average edema magnitude measured by TRUS at the completion of guiding needle insertion ranged from 10% (+1.2 to +32.5% for individual patients) in one cohort to 30% (+6 to +60% for individual patients) in another cohort of patients.<sup>84</sup> The mean edema magnitude measured by TRUS at the completion of source implantation had reported values of 20% and 18%.<sup>85</sup> The mean edema magnitude measured with pre- and post-implant CT at 2 to 4 hours after source implantation ranged from about 17% (–7% to +60%) to +30%, 52% (+33 to +96% for individual patients), and 53% at one day post-implant.<sup>88,90</sup>

When different imaging modalities were used (with TRUS image acquired 2 to 3 weeks before the procedure for  $V_0$  and CT for post-implant volume), the reported mean edema magnitude

**Table 4.** Representative reported characteristics of prostate edema.

Reference	# of Pts	Edema Magnitude		Edema Half-life (day)		Method		Comments	Source
		Mean	Range	Mean	Range	Imaging	Timing		
Narayana et al. (1997) <sup>55</sup>	10	1.53	-	-	-	CT	Pre, d1	$V_{CT}(d1)/V_{CT}(Pre)$	<sup>125</sup> I & <sup>103</sup> Pd
Moerland et al. (1997) <sup>72</sup>	21	1.30	1.1-1.5	-	-	AP films	d3, d30, d90	$V_F(d3)/V_F(d30)$ , little change from 1 to 3 months	<sup>125</sup> I
Prestidge et al. (1998) <sup>91</sup>	19	1.42 1.19	0.77-2.24	14%(d1 to d8), 10%(d8 to d30), 3%(d30 to d90), 2%(d90 to d180)	-	CT/US	d1, d8, d30, d90, d180	$V_{CT}(d1)/V_{US}(Pre)$ ; 11 ~ 24 h because $< V_{CT}/V_{US} > = 23\%$	<sup>125</sup> I & <sup>103</sup> Pd
Willin et al. (1998) <sup>88</sup>	11	1.17	0.93-1.60	Resolved between 2 to 6 months for all pts	-	CT	Pre, d0, d60, d180	$V_{CT}(d0)/V_{CT}(Pre)$ ; d0 = 2-4 h	<sup>125</sup> I
Waterman et al. (1998) <sup>83</sup>	10	1.52	1.33-1.96	9.3	4-25	CT	-d14, d0, d7, d21, d49, d105	V by mean seed radial distance $V_{n+1}/V_n = (<R_{>-n+1}/<R_{>-n})^3$	<sup>125</sup> I & <sup>103</sup> Pd
Merrick et al. (1998) <sup>89</sup>	10	1.21	1.16-1.32	10.6	8.6-14.3	Films	d0, d3, d14, d28	V by standard deviation of the seed positions	<sup>125</sup> I & <sup>103</sup> Pd
Radiozamani et al. (1999) <sup>81</sup>	50	1.70	1.36-2.04	-	-	CT/US	Pre, d1	$V_{CT}(d1)/V_{US}(Pre)$	<sup>125</sup> I & <sup>103</sup> Pd
Stocks et al. (2000) <sup>102</sup>	297	<0.8 (2%); 1.2-1.4 (18%); >1.4 (6%)	0.8-1.2 (74%); >1.4 (6%)	-	-	CT/US	Pre, ~d30	$V_{CT}(d30)/V_{US}(Pre)$ ; & believe $V_{CT}$ is comparable to $V_{US}$	<sup>125</sup> I
Speight et al. (2000) <sup>85</sup>	161	1.20	-	-	-	US	d0	$V_{US}(immediately\ post)/V_{US}$ (immediately before)	<sup>125</sup> I & <sup>103</sup> Pd
Dogan et al. (2002) <sup>90</sup>	25	1.30	-	-	-	CT	-d7, d0, d7, d28	$V_{CT}(d7)/V_{CT}(Pre) = 1.2$ , $V_{CT}(d28)/V_{CT}(Pre) = 1.1$	<sup>125</sup> I & <sup>103</sup> Pd
Waterman et al. (2002) <sup>99</sup>	50	1.53	1.33-1.73	-	-	CT	Pre, d0, (d21 - d134)	$V_{CT}(d0)/V_{CT}(Pre)$	<sup>125</sup> I
Yamada et al. (2003) <sup>84</sup>	50	1.30 (M) 1.18 (M)	1.06-1.60 (A) 1.09-1.41 (B)	-	-	US	D0	Intraoperative $V_{US}(post\ needle)/$ $V_{US}(before\ needle)$	<sup>125</sup> I & <sup>103</sup> Pd
Taussky et al. (2005) <sup>82</sup>	20	1.31 (M) 1.21 (M) 1.05 (M)	0.93-1.72 0.88-1.48 0.76-1.43	16 14.7 (M)	6.4-21.5	CT-MRI/ US	Pre, d0, d8, d30	$V_{MRI}(d0)/V_{US}(Pre)$ $V_{MRI}(d8)/V_{US}(Pre)$ $V_{MRI}(d30)/V_{US}(Pre)$	<sup>125</sup> I
Leclerc et al. (2006) <sup>92</sup>	66	1.58	1.20-2.20	30	3-170	Films US Model	-d14 (US), d0 (Film at 2-4h), ~d30 (CT: mean of d41 & STD of d8)	Used Waterman model; derived from <seed positions> on film and on planning US or post-implant CT	<sup>125</sup> I
<b>Average</b>	57	1.32	0.77-2.20	16	3-170	NA	NA	NA	<sup>125</sup> I & <sup>103</sup> Pd

**Abbreviations:** (M) = median; dn = day n; Pre = pre-implant;  $V_{CT}$  = CT volume;  $V_F$  = volume by film;  $V_{US}$  = ultrasound volume;  $V_{MRI}$  = MRI volume

varied from 42% (for postoperative CT acquired about 24 hours post-implantation) to 70% ( $\pm 34\%$ ) (with post-implant CT acquired on the next morning after the implant).<sup>81,91</sup> Because CT is known to overestimate the prostate volume, Prestidge et al.<sup>91</sup> concluded that the volume increase caused by edema in their study was only 19% at one day after implant (because their institutional experience had shown that prostate volume measured on CT was consistently larger than that from US image by 23%). This volume increase is much smaller than that reported by Waterman et al., and Narayana et al., when using CT for both postoperative day-1 and pre-implant CT volumes.<sup>91</sup>

The existing data do not establish a unique definitive  $T_{\max}$ . Continued volume increase from implant-day to 1 week post-implant (by about 5%) had been observed in some patients.<sup>83</sup> In general, the procedure-induced prostate edema can cause an average increase in prostate volume by about 30% immediately following source implantation and up to 50% within one day of source implantation. The average residual edema magnitude at 30 days post-implant can be on the order of 10%.<sup>83,89,90</sup> The existing studies have indicated consistently that the edema magnitude varied significantly from patient to patient with values ranging from a few percent to nearly twice the pre-implant volume.

#### IV.2.b. The 1<sup>st</sup> Half-life of Edema Resolution

There were only a few studies that can adequately address the quantitative edema resolution characteristics.<sup>82,83,89,91</sup> The report by Waterman et al., represents one of the most comprehensive and consistent study on post-implant edema resolution.<sup>83</sup> In their study, post-implant CT scans were obtained on the day of implant, and at approximately 1, 3, 7, and 15 weeks for 10 patients who did not receive *a priori* hormonal therapy. The change in prostate volume was determined from the mean inter-source distance (distance from the source to the geometric center of source distribution) calculated from each CT scan (in an effort to minimize subjective variations associated with contouring the prostate volume on CT images). They reported that the edema resolution fitted nicely to an exponentially decaying function for all 10 patients included in the study. The edema resolution half-life determined from the fit ranged from 4 to 25 days with an average of 9.3 days. Eight of the ten patients demonstrated edema with a half-life of less than 10 days. The edema remained at about 10% at 30 days post-implant. Neither the magnitude nor the half-life was found to correlate with the number of needles used, radionuclide used, the number of sources implanted, and the total source strength. Merrick et al., examined the edema change using source positions determined from orthogonal films acquired at 2 h, 3 d, 14 d, and 28 d post-implant.<sup>89</sup> The average edema half-life was estimated as 10.6 days (range 8.6–14.3 days). They found that the average volume decreased by 20.9% from day 0 to day 28. Prestidge et al., also reported a similar 24% average decrease of volume from day 1 to day 28.<sup>91</sup> Taussky et al., performed prospective sequential evaluation of prostate edema using CT-MRI image fusion for 20 patients and the estimated edema half-life had a mean value of 16 days (6.4 to 21.5 days).<sup>82</sup>

Qualitatively, the existing data suggest that the initial swelling of prostate occurs quickly and the maximum edema is attained on the order of one day after implant for most patients. The resolution of edema takes much longer than the initial swelling. The resolution is relatively quick for the first 2 weeks followed by a slow resolution that can last more than 1 month.<sup>81,83,89</sup> The estimated 1<sup>st</sup> resolution half-life varied widely among different patients with values ranging from

4 days up to 25 days. The mean half-life was about 10 days. A small fraction of patients may experience prolonged edema.<sup>93</sup>

### **IV.3. EFFECT OF PROSTATE EDEMA ON BRACHYTHERAPY DOSIMETRY**

#### **IV.3.a. Theoretical Expectations**

The procedure-induced prostate edema and its dynamic resolution force the treatment volume and the implanted source locations to vary with time. Conventional pre- and post-implant dosimetry, however, are based on static prostate volume and source locations determined at, typically, one user-selected time which does not take into account the dynamic variations caused by edema in the calculation of dosimetry indices. The influence of prostate edema on conventional implant dosimetry has been recognized and studied by many research groups since the late 1990s.<sup>55,72,81–92,94–102</sup>

In general, conventional pre-implant dosimetry based on pre-implant prostate volume is expected to overestimate the delivered dose because it ignores the edema-induced temporary increase in prostate volume and inter-source distances from the planned values before the procedure (assuming the pre-implant plan is reproduced exactly). The conventional post-implant dosimetry could either underestimate or overestimate the delivered dose depending on the timing of post-implant imaging study. If the prostate volume and source locations are measured shortly after the completion of the procedure (when the edema is large), the post-implant dosimetry is expected to underestimate the delivered dose. If the prostate volume and source locations were measured long after the completion of procedure (namely when the edema is mostly resolved), it would overestimate the delivered dose. In addition to the timing of dosimetry, the amount of under- or overestimation is also influenced by the magnitude of initial prostate swelling, the rate of its resolution, and the radioactive decay half-life of the implanted radionuclides.<sup>55,72,83,87–89,91,92,94–99</sup> For implants using the same radionuclide, the dosimetry error resulted from a conventional implant dosimetry can be very different from patient to patient because of the highly variable edema characteristics associated with individual patients. For a given patient, the magnitude of dosimetry error is generally larger for implants using radioactive sources with shorter decay half-life and/or lower effective photon energy.<sup>98</sup>

#### **IV.3.b. “Optimal” Timing of Post-Implant Dosimetry**

In principle, when the temporal variation of each implant’s edema is known the effects of edema can be fully incorporated into the dosimetry calculation within the TG-43 dose calculation formalism.<sup>103,104;95,97,98</sup> Because the edema-induced dosimetric errors resulting from conventional post-implant dosimetry change from underestimation to overestimation as a function of post-implant dosimetry time, conventional post-implant dosimetry performed at a judiciously selected time could also provide an accurate estimation of the delivered dose if the individual implant’s edema characteristics are known.<sup>97,98</sup> However, patient-specific edema characteristics can only be obtained, at present, by performing comprehensive post-implant imaging studies for each implant, which can be time consuming and inconvenient. In absence of this information, simulation studies have shown that a nominal optimum time exists for each radionuclide at which the errors resulting from conventional post-implant dosimetry are not zero but are clinically acceptable for all edema characteristics.<sup>96–98</sup> For edemas that follow exponential resolution, the nominal optimal time for performing post-implant dosimetry was found to be  $10 \pm 2$  days,  $16 \pm 2$  days,

and  $42 \pm 2$  days, respectively, for  $^{131}\text{Cs}$ ,  $^{103}\text{Pd}$ , and  $^{125}\text{I}$  implants.<sup>97,98</sup> The maximum error resulting from conventional implant dosimetry performed at these nominal optimal times would be less than 5% regardless of the edema characteristics.

### IV.3.c. Relationships between Dosimetry Performed at Different Post-Implant Times

These nominal optimal times for post-implant dosimetry all occur long after the completion of the source implantation. A major drawback of performing post-implant dosimetry at the nominal optimal time is that it does not readily provide active recourse during the procedure if the implant dosimetry was later found inadequate (although additional irradiation may be prescribed separately). The development of real-time dynamic dosimetry in the operating room (OR) is aimed to provide real-time implant modification such that a dosimetrically acceptable implant is always achieved at the completion of the procedure (see section VI). Many investigators have explored the possibility of using the implant dosimetry achieved at the completion of the procedure as the sole dosimetry documentation for the implant.<sup>99,105–108</sup> If this were possible, it would be convenient for the patients because the post-implant dosimetry at a later date could be eliminated. Because the average edema magnitude at the completion of implant procedure can reach up to 30%, conventional dosimetry performed in the OR at the completion of the procedure may be expected to underestimate the delivered dose. In other words, the dose delivered to the target and adjacent critical structures could be greater than what is assessed in the OR.

However, mixed results have been reported concerning the expected relationship between dosimetry performed on the implant day and that at a later time. Some studies have reported relationships between implant-day dosimetry and later dosimetry that are consistent with the theoretical expectations of edema, while others have found little difference between the dosimetry indices obtained at the two times.<sup>82,99,109;82,105–108</sup> For examples, Waterman et al., examined  $V_{100}$  and  $D_{90}$  based on the CT dosimetry performed on the implant-day and on day-46 ( $\pm 23$  days) for 50 consecutive patients treated with  $^{125}\text{I}$  implants.<sup>99</sup> The mean  $V_{100}$  and  $D_{90}$  increased from the values obtained at implant-day by  $5 \pm 6\%$  and  $15 \pm 17\%$ , respectively, consistent with expected edema resolution. The increase in  $V_{100}$  and  $D_{90}$  was found to be proportional to the edema magnitude and their values on the implant-day. However, the amount of increase varied widely among the patients; the standard deviation for the increase in  $D_{90}$  was  $\pm 24$  Gy. They concluded that predicting the  $V_{100}$  and  $D_{90}$  from the implant-day values would be a poor substitute for actual post-implant dosimetry performed on the later day. D'Souza et al., also observed that implant-day assessment underestimated the dosimetric coverage of the target, while 1-month dosimetry overestimated the true dose, which is consistent with the expected effects of edema.<sup>109</sup> Tausky et al., observed a smaller increase in  $V_{100}$  and  $D_{90}$  between implant-day and 30-day dosimetry.<sup>82</sup> The median  $V_{100}$  increased from 93.4 to 96.3% and median  $D_{90}$  increased from 105% to 111%. They noted that edema had much less influence on the dosimetry indices than previously assumed in high-quality implants. An implant-day  $V_{100}$  of  $>93\%$  is unlikely to increase  $>1\%$  after 30 days. Their implant was performed with a margin of 2 to 3 mm anteriorly and laterally, 5 mm in the cranial and caudal direction, and no margin at posterior rectal interface. They concluded that implant-day dosimetry provided a reasonably accurate evaluation of implant quality. Stone et al., have also reported smaller mean increase (3.4%) between the

1-month CT  $D_{90}$  and the implant-day TRUS  $D_{90}$  and suggested that their intraoperative dosimetry provided a close match to the actual delivered doses.<sup>105</sup> Potters et al., have reported a reduction in mean dosimetry indices from the real-time TRUS dosimetry to post-implant CT-dosimetry at 3 to 4 weeks for 164 patients who received either  $^{125}\text{I}$  or  $^{103}\text{Pd}$ .<sup>107</sup> The mean  $D_{90}$  and  $V_{100}$  on the implant-day was 109% and 96%, respectively, compared to 105% and 93% at 3 to 4 weeks later. They have acknowledged that tremendous subjectivity was associated with contouring the prostate on post-implant CT scan due to seed artifact, edema, and physician experience. For implants using stranded  $^{125}\text{I}$  seeds McLaughlin et al., have reported variations of implant-day and day-14 dosimetry that are not consistent with either edema magnitude or resolution half-life.<sup>110</sup> They highlighted that the averages were deceptive and that individual patient analysis showed that 96% of the patients had a change in  $D_{90}$  between day-0 and day-14. Forty percent of the patients with acceptable implants on day-0 had unacceptable implant on day-14. Fifty-seven percent of the patients that had unacceptable implants on day-0 had acceptable implants on day-14. They did not find any correlation to prostate swelling and attributed the results to the shifting of stranded seed relative to the prostate. Most studies, however, have consistently reported increased dose to rectum and urethra when comparing late post-implant dosimetry to that of implant-day.<sup>100,101,105,111,112</sup>

It should be cautioned that while mean dosimetry indices obtained at each time instance were typically used in discussing the effects of edema, all studies have reported large variations of dosimetry indices among individual patients. This is consistent with the tremendous variation of edema magnitude and half-life existing among different patients. In addition, other factors such as the size of the prostate, source migration, anisotropy in edema, and planning margin that may vary from patient to patient could also contribute to the variation in dosimetry indices. No study has provided enough information that would enable a systematic correction of the conventional dosimetry indices by the implant's edema or other factors. Nonetheless, edema was consistently found to be the strongest predictive factor of implant quality in correlations studies.<sup>90,102</sup>

#### IV.4. RECOMMENDATIONS ON TIMING OF IMAGING

Despite many reported studies and the theoretical considerations discussed earlier, there is currently no single post-implant dosimetry time that is followed consistently by every institution. The post-implant dosimetry time adopted by different clinics varied significantly, from immediately after the procedure to several hours or weeks after the procedure. Even within the same institution, a locally established dosimetry time was not always followed consistently for a variety of reasons.<sup>99,113</sup> For  $^{125}\text{I}$  implants, the traditional post-implant dosimetry time of about 1 month following the procedure was established without explicit consideration of edema and has been used by most clinics. It is very close to the calculated nominal optimal time that results in minimization of dosimetry error due to a lack of edema consideration in dose calculations.<sup>96,97</sup> This post-implant time was also used by some clinics for  $^{103}\text{Pd}$  implants before the effects of edema were actively investigated.<sup>105</sup> However, because of the differences in radioactive decay half-life, the nominal optimal times for  $^{103}\text{Pd}$  and the newly introduced  $^{131}\text{Cs}$  sources are significantly different from that for  $^{125}\text{I}$  implants.<sup>96-98</sup>

It is also important to note that the existing dose response reported by Stock et al., for  $^{125}\text{I}$  implants was based on the CT dosimetry ( $D_{90}$ ) performed at 1 month post-implant.<sup>114</sup> The

dose-response relationship for  $D_{90}$  reported by Potters et al., for  $^{125}\text{I}$  and  $^{103}\text{Pd}$  implants was also based on CT post-implant dosimetry performed at average 21 days (11 to 45 days) after the procedure.<sup>113</sup> Given our current understanding of prostate edema and its expected impact on dosimetry, there is a need to establish a consistent dosimetry time in order to minimize artificial fluctuations in the reported dosimetry indices. Such a dosimetry time should also be consistent with the established dose-response studies until a new dose response based on dosimetry quality indicators calculated at other times or with the full consideration of edema is established. In the meantime, new data that provide information relevant to prostate edema should also be reported to allow eventual correlation of the treatment response with the true dosimetry received by each implant.

In light of these considerations, the following data should be included in reporting prostate brachytherapy dosimetry.

1. Pre-implant prostate volume. Pre-implant prostate volume is known for almost all implants. It does not require additional effort unless a preferred imaging modality is specified.
2. Implant-day dosimetry. Implant-day dosimetry based on TRUS imaging and the actual or derived source locations is readily available for clinics currently performing real-time dynamic dosimetry. For those clinics that do not perform real-time dosimetry, dosimetry based on CT or MRI images acquired at 2 to 4 hours after the procedure is recommended. This has the clinical advantage of aiding future improvements by closing the learning curve early while memory of the details is still fresh. In the case of an obvious overdose to critical structures such as rectum, urethra, or erectile bodies, the physician can prepare a plan of prophylactic management of expected symptoms. The implant-day volume at the completion of the procedure is also relatively easy to obtain with TRUS.
3. Post-implant dosimetry at the nominal optimal dosimetry time for respective radionuclides. Because of the existing dose-response data, the post-implant dosimetry for  $^{125}\text{I}$  implants should be performed at 1 month ( $\pm 1$  week) after the procedure. For  $^{103}\text{Pd}$  and  $^{131}\text{Cs}$ , post-implant dosimetry should be performed at their respective nominal optimal times,  $16\pm 4$  days and  $10\pm 2$  days, respectively.

## **V. COMMON TREATMENT PLANNING APPROACHES FOR PROSTATE IMPLANTS**

The initial seed-placement approach when transperineal ultrasound-guided prostate implants began in Seattle in 1985 was to distribute a relatively large number of low-strength seeds evenly throughout the prostate.<sup>115</sup> The uniform seed-loading approach assumed the photon energy was sufficiently low that cumulative dose at large distance would be negligible. Even though the photons from radionuclides used in permanent prostate implants are attenuated with distance more rapidly than the inverse-square dependence indicates, the cumulative effects are not negligible when clinically relevant distances separate the sources. In any prostate volume filled with sources spaced at lattice points forming a 1 cm cubic grid, the central dose will be much higher

than the peripheral dose because of such cumulative effects. In the early Seattle implants, central prostate and urethral doses frequently exceeded 300% of the minimum prescribed peripheral dose. Within 2 years after the start of their program, unacceptably high urinary morbidity led them to abandon uniform loading in favor of a modified version. Nevertheless, the principles of their uniform-loading approach form the basis for most manually planned implants today.

At the opposite extreme from uniform loading is peripheral loading, which, as the name suggests, places sources only at the edge of the target volume. Although this approach is appropriate for small prostates or in patients with a large defect from a transurethral resection of the prostate where the epithelial surface of the defect must be spared, peripheral loading in typical prostate implants places the patient at risk of underdosing the prostate centrally in exchange for very high dose gradients close to the rectum. Wallner used this approach in his pioneering work at MSKCC that also helped define dose thresholds for high-grade morbidity.<sup>32</sup>

### V.1. MODIFIED UNIFORM AND MODIFIED PERIPHERAL LOADING

In response to the perceived shortcomings of uniform and peripheral loading, most manual treatment planning has evolved and converged to a hybrid known as either modified uniform or modified peripheral loading, depending on the user's starting reference. The hybrid may be described as taking the target volume and filling it according to uniform loading on a 1 cm lattice and then modifying the result. First, additional needles and seeds are placed on the lateral and anterior periphery of the target volume. Second, the seed density is reduced centrally by removing selected seeds. The number of seeds added peripherally and removed centrally depends on the chosen source strength and the radionuclide.

For a given seed distribution, it is always possible to find a source strength for any radionuclide and source model that will closely match several selected target dosimetric indices such as  $V_{100}$ , relative  $D_{90}$ , or urethral  $D_{10}$  obtained with a different source model and strength. However, the full relative DVHs where fractional volume is plotted against fractional prescribed dose cannot be matched between different radionuclides but can be closely approximated with different source models of the same radionuclide. An implant designed for one prescribed dose that is changed to a different prescribed dose can produce the same relative DVH using the same source model by changing the source strength according to:

$$\text{Source Strength}_{\text{Rx2}} = \frac{\text{Rx2}}{\text{Rx1}} \cdot \text{Source Strength}_{\text{Rx1}}. \quad (2)$$

Here, Rx is the prescribed dose and Source Strength refers to individual source strength and not the total strength of an implant.

### V.2. TARGET AND CRITICAL STRUCTURE DOSE INDICES

At the present time, there is little reason to spare any part of the prostate in dosimetric planning from the full prescribed dose, i.e., the planned  $V_{100}$  should be ~100%. In all pathological studies of surgically resected prostates, prostate cancer has been found to be multifocal in a majority of cases, although the second and higher foci are often microscopic.<sup>116</sup> For this reason there is virtually no enthusiasm among urologic surgeons to perform a type of male prostate lumpec-

tomy to reduce morbidity. In brachytherapy, the trend is to escalate the dose in areas shown to be positive for cancer either through mapping biopsies or imaging techniques such as MRI spectroscopy. Other prostate coverage and quality indices such as the planned  $D_{90}$  and  $V_{150}$  should be planned to lie in a narrow range, but the value of these parameters is dependent on the radionuclide and seed strength used as well as institutional preference. For beginning users, they should be considered variables adjusted in response to feedback from post-operative dosimetry.

There is considerable variability in the target dose indices chosen by an institution. Eight institutions participated in a study in which each was to design implants for the same prostate using their own criteria for monotherapy and boost therapy  $^{125}\text{I}$  and  $^{103}\text{Pd}$ .<sup>117</sup> Each of the four exercises produced an array of DVHs similar to those shown in Fig. 10 for  $^{125}\text{I}$  monotherapy. All implants were planned using modified uniform loading, but each institution used its own criteria for target dose indices, source strength, and PTV definition. Although postoperative dosimetry does not duplicate planning dosimetry, they are strongly correlated. The variation among these plans indicates that a patient would experience considerably different outcomes depending on the institution chosen to perform the brachytherapy implant.

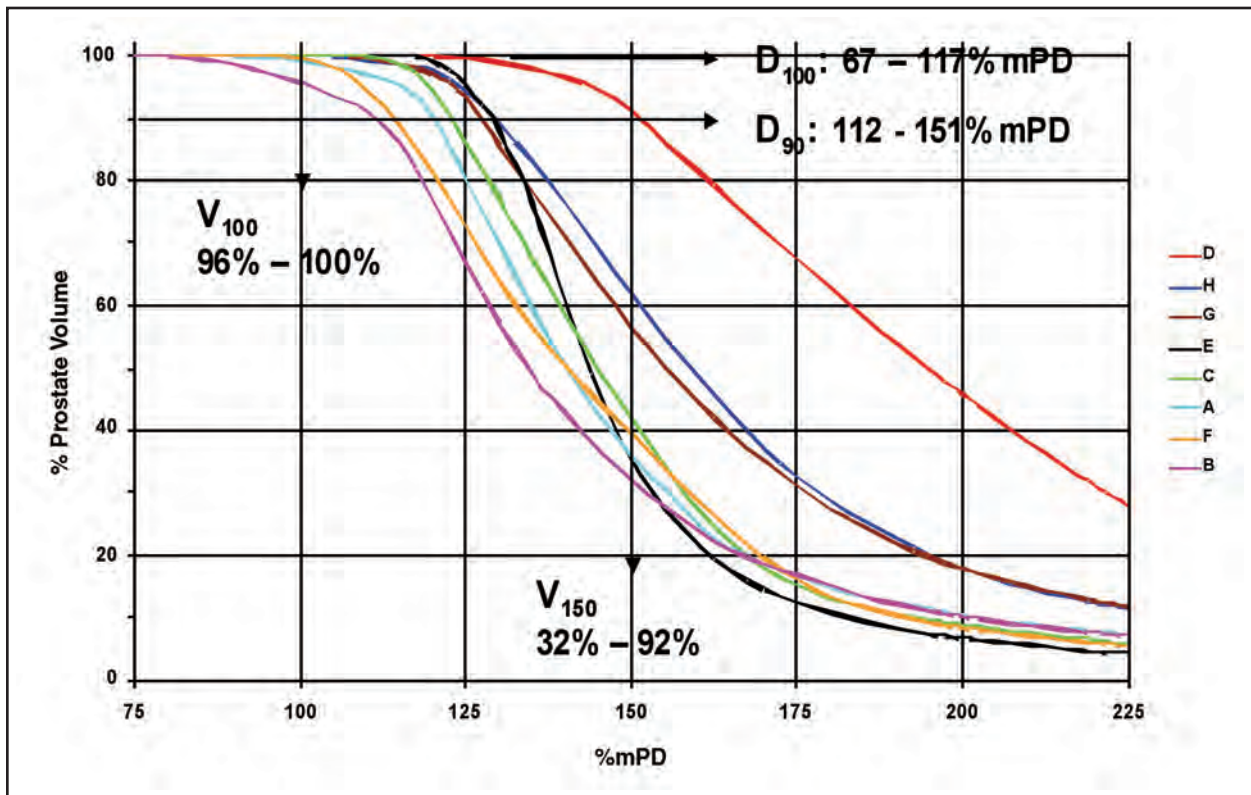


**Fig. 10.** Variability in planning the same prostate using  $^{125}\text{I}$  monotherapy among 8 institutions. Each institution used the same source model but chose the strength, planning target volume, and seed placement according to their institutional criteria. (Adapted from reference 117, *Brachytherapy*, vol 4, issue 4, G. S. Merrick, W. M. Butler, K. E. Wallner, J. C. Blasko, J. Michalski, J. Aronowitz, P. Grimm, B. J. Moran, P. W. McLaughlin, J. Usher, J. H. Lief, and Z. A. Allen., “Variability of prostate brachytherapy pre-implant dosimetry: a multi-institutional analysis,” © 2005 with permission from Elsevier. <http://www.sciencedirect.com/science/journal/15384721>.)

Regarding critical structures, none of the eight participating institutions explicitly contoured the rectum and bladder on the ultrasound volume studies, but all contoured the urethra. As with the prostate, there was considerable variation in urethral dosimetry, but only two groups allowed the urethral  $V_{150}$  to exceed 20% of the urethral volume. In all cases, however, the urethral  $V_{100}$  was 100%. For these institutions, urethral sparing means covering the urethral with the prescribed dose but limiting the volume receiving a high dose. This is in accord with a recent pathology study of whole mount prostates obtained as salvage prostatectomy after radiation therapy or brachytherapy failures.<sup>118</sup> Two-thirds of patients had cancer within 5 mm of the urethra (7% actually involving the urethra) and nearly half the patients had extra prostatic disease.

### V.3. TARGET VOLUME DEFINITION AND THE NECESSITY FOR MARGINS

In the planning exercise of Merrick et al., the number of extracapsular seeds placed as a percentage of the total ranged from 6% to 58% when the patient was defined as suitable for monotherapy.<sup>117</sup> Some planners expanded the prostate to an explicit PTV, most used an implicit dosimetric margin, and only one planner used no dosimetric margin around the prostate. Dosimetric margins are employed to encompass the likelihood of extracapsular extension of disease and the uncertainty of placing the needles and sources in the planned location.

In patients with a pretreatment PSA <10 ng/mL, approximately 50% manifest extracapsular disease at the time of radical prostatectomy.<sup>13</sup> Several studies on the distribution of extracapsular extension conclude that prostate margins of 5 mm will encompass 90% of disease extension.<sup>19,119,120</sup> Based on these studies, a margin of 3 mm is commonly used in planning prostate implants. Although it is unclear whether the nominal prescription dose or a lesser dose is necessary to sterilize extracapsular extension, one outcome study found that mean dosimetric margin was almost as good a predictor of freedom from biochemical failure as the widely used prostate  $D_{90}$ .<sup>121</sup> In patients treated with generous prostatic margins, clinical needle biopsy surrogates for extracapsular extension such as perineural invasion, Gleason pattern 4+3 versus 3+4, and percent positive biopsies were found to have negligible consequence on biochemical survival.<sup>122-124</sup>

### V.4. CHOICE OF RADIONUCLIDE

There is little evidence to support the choice of one radionuclide over the other. One radiobiological argument is that the shorter half-lives of  $^{103}\text{Pd}$  and  $^{131}\text{Cs}$  make them favored over  $^{125}\text{I}$  for faster growing, more aggressive tumors. This logic led many institutions to adopt  $^{125}\text{I}$  for low-risk, monotherapy patients and  $^{103}\text{Pd}$  or  $^{131}\text{Cs}$  for intermediate- and high-risk patients. On the other hand, there are many centers that use one radionuclide or the other for all patients and who report good results. In a randomized trial comparing  $^{125}\text{I}$  with  $^{103}\text{Pd}$  in low-risk patients, there was a slight trend in the preliminary results toward enhanced biochemical survival in the  $^{103}\text{Pd}$  arm.<sup>125</sup> PSA levels of patients implanted with  $^{103}\text{Pd}$  also fall to undetectable levels faster than those implanted with  $^{125}\text{I}$ .<sup>124</sup>

### V.5. APPROPRIATE SEED STRENGTHS

Increasing the seed strength will reduce the cost of an implant as long as manufacturers and hospitals bill by the number of seeds ordered and not by the total strength. However, the number of

seeds required is not a linear function of seed strength. The dosimetric impact of using increased seed strength with fewer seeds has been investigated by several research groups. Narayana and colleagues performed a randomized trial comparing high- versus low-strength  $^{125}\text{I}$  seeds and found that the high-strength implants were more robust and produced higher values of postoperative dosimetric parameters than the low-strength implants when comparing prostate  $D_{80}$  and  $V_{100,150,200}$ .<sup>126</sup> In the high-strength arm, rectal and urethral doses were not significantly higher, but the total volume covered by the prescription isodose was about 18% greater. Moerland and Batterman noted that this increased dose coverage may be a result of higher total activity that used the high-strength arm that were also responsible for the larger error tolerance and better outcome in the post-implant analysis compared with the low-strength implants.<sup>127</sup> In a planning study performed by Sloboda et al., higher-strength seeds were also found to provide better dose coverage and better urethral protection than lower-strength seeds for regularly spaced  $^{125}\text{I}$  sources within the PTV.<sup>128</sup> In a follow up study, they compared post-implant dose distributions for two groups of 20 consecutive patients treated to 145 Gy with 0.414 and 0.526 U  $^{125}\text{I}$  seeds. The dosimetric coverage, measured by  $D_{90}$ , was significantly better for the higher-strength seeds, with no apparent deleterious effects.<sup>129</sup> The robustness of permanent prostate implant dosimetry for various seed activities was also examined by Beaulieu et al., in the presence of seed misplacement and seed migration (seed loss).<sup>130</sup> They have shown that treatment plans were robust to misplacement and migration of  $^{125}\text{I}$  seeds over a wide range of seed activity up to about 0.7 mCi (0.89 U). These studies indicated that reducing the number of seeds by increasing individual seed strength to deliver the same prescribed dose as with lower-strength seeds seemed to be a viable approach (with proper attention to critical structure dose) and the resulting implants were no more susceptible to seed placement errors or even seed loss than the lower-strength implants. However, these results may be specific to their implantation techniques.

## V.6. CALCULATION ALGORITHM AND ITS EFFECT ON TARGET DOSE INDICES

Virtually all planned and postoperative dosimetry is calculated using a point source algorithm because of the difficulty to determine the orientation of permanent brachytherapy seeds via CT imaging. Improved imaging and source identification algorithms will allow routine identification of 3D seed orientations within implants, and will permit the routine use of line source dosimetry rather than historical point source models. Use of the 2D dosimetry formalism is recommended by the AAPM due to increased dose calculation accuracy, especially at the close distances relevant to prostate implants.<sup>104</sup> Most seed models have characteristic dosimetric anisotropy that reflects higher doses transverse to the long axis of the source compared to the ends of the source. Because implanted seeds, particularly those contained in stranding material, tend to align along the implant needle track, use of line source algorithms will increase the apparent dose in transverse planes and decrease the dose superiorly and inferiorly compared to point source calculations. Lindsay et al., showed that the effect was dependent on radionuclide and source anisotropy so that the effect with  $^{125}\text{I}$  was less than with  $^{103}\text{Pd}$  (due to the lower energy of the latter) and also less in sources with less anisotropy.<sup>131</sup> A more recent study comparing point source, line source randomized about the needle axis, and full Monte Carlo dosimetry calculations found similar radionuclide and source anisotropy effects and that the point source model underestimated the urethral and rectal dose relative to the line source calculation but that the line source model

slightly overestimated those doses relative to Monte Carlo by not accounting for interseed attenuation.<sup>132</sup> All of the historic dose response data, however, are based on point source calculations. An impending challenge is to translate these dose indices into their line source or Monte Carlo-based equivalents.

## **V.7. RECOMMENDATIONS FOR PLANNING AND DOSE REPORTING OF PROSTATE IMPLANTS**

Standardization of certain planning parameters would assist in understanding differences in outcomes and morbidity as well as differences in postoperative dosimetry. Users are encouraged to use the following definitions and procedures for planning and post-implant evaluations which were proposed by the PROBATE group of GEC ESTRO.<sup>69</sup> A brief summary of these PROBATE recommendations is presented below, and the reader is referred to the original document by Salembier et al., for details.<sup>69</sup>

We acknowledge that part of the recommendations in this section V.7 were based on this protocol.

### **1. Gross tumor volume (GTV):**

The gross tumor volume corresponds to the gross palpable, visible, or clinically demonstrable location and extent of the malignant growth. Given the TNM definition for prostate cancer, GTV can only be defined for tumor stages larger than T1c. Whenever possible the GTV should be contoured on the pre-implantation ultrasound-acquired images. Where necessary, correlation with endorectal coil magnetic resonance and spectroscopy should be used.

### **2. Clinical target volume (CTV):**

The clinical target volume is the volume that contains the GTV and includes subclinical malignant disease at a certain probability level. Delineation of the CTV is based on the probability of subclinical malignant cells present outside the GTV. It is well documented in surgical literature that prostate cancer is in the majority of cases a “whole gland” disease. Even in a very early stage, prostate cancer presents as a multi-focal disease—both lobes can contain microscopic disease. Given this specific behavior, at least the whole prostate gland has to be considered as “target” and included in the CTV. Extent of subclinical extraprostatic extension of early prostate cancer needs further study but is generally less than 3 mm in most studies. The clinical target volume for pre-implant dosimetry should be the prostate gland with a margin. For T1 – T2 prostate cancer the CTV corresponds to the visible contour of the prostate with a three-dimensional volume expansion of 3 mm. This three-dimensional expansion can be constrained to the anterior rectal wall (posterior direction) and the bladder neck (cranial direction).

### **3. Planning target volume (PTV):**

The PTV surrounds the CTV with a margin to compensate for the uncertainties in treatment delivery. The PTV is a geometric concept, introduced for treatment planning. A margin must be added to the CTV either to compensate for expected physiological movements and variations in size, shape, and position of the CTV during therapy (internal margin) or for uncertainties (inaccuracies and lack of reproducibility) in patient setup during irradiation, which may be random

or systematic. The CTV to PTV margin can be minimized in brachytherapy because there are no significant opportunities for setup error. Using online in vivo 3D dosimetry and fluoroscopy in addition to sonography to eliminate seed placement errors, there is no need for an expansion from the CTV to define the PTV, i.e.,  $PTV = CTV$ . However, this approach is debatable for permanent implants.

#### 4. Organs at risk (OAR):

Three different organs at risk can be defined in the pre-implantation setting for prostate treatment:

- a. *Prostatic urethra*: Common practice to obtain visualization of the urethra is to use a urinary catheter. This should be a small-gauge catheter, French gauge 10, to avoid distension of the urethra. The surface of the catheter can be used to define the urethral surface from the prostatic base to apex. However, in practice, the urethra is not a circular structure, and an alternative that might give a more accurate anatomical picture is to instill aerated gel into the urethra prior to obtaining the ultrasound images.
- b. *Rectum*: Using transrectal ultrasound (TRUS), the anterior rectal wall can be visualized but may introduce artifacts due to displacement and distension. Many brachytherapists simply outline the outer wall, and this should be regarded as the minimum requirement; others define outer and inner walls. In terms of the critical cells in the rectum for late damage, the latter is probably more correct.
- c. *Penile bulb and/or neurovascular bundles*: Currently this remains investigational.

#### 5. Prescription doses for prostate:

Prescription dose is the intended dose to the 100% isodose. Commonly used prescription doses for monotherapy are 145 and 125 Gy for  $^{125}\text{I}$  and  $^{103}\text{Pd}$ , respectively.<sup>133,134</sup> The values for  $^{131}\text{Cs}$  remain investigational; 100–125 Gy have been used or suggested by some.<sup>135–137</sup> It should be pointed out that these values are nominal values. The effectiveness of a nominal prescription dose for individual patients can vary depending on the radiobiological characteristics of the patient's cancer cells and on other factors such as the presence of procedure-induced edema. The dose prescribed to individual patients is primarily a clinical decision, and ideally should be established through clinical trials and confirmed by treatment outcome analysis. Recently, a group of experienced brachytherapists in the publication by Bice et al., recommended 115 Gy for  $^{131}\text{Cs}$  monotherapy implants and noted the increase in the original recommended prescription dose (from 100 Gy to 115 Gy) following revision of the dose-rate constant.<sup>138</sup>

#### 6. Planning criteria for target volumes and organs at risk:

For the CTV, the following conditions correlate with a good pre-implantation dosimetry:

- a. The  $V_{100}$  (the percentage of the CTV that receives at least the prescribed dose) must be at least 95% ( $V_{100} > 95\%$  of CTV). Therefore, the  $D_{90}$  (the dose that covers 90% volume of the CTV) will be larger than the prescription dose ( $D_{90} > 100\%$  of prescription dose).

- b. The  $V_{150}$  (the percentage of the CTV that receives at least 150% of the prescription dose), should be equal to or less than 50% ( $V_{150} \leq 50\%$  of CTV).

For the organs at risk, the following conditions correlate with acceptable levels of toxicity:

- a. *Rectum*: Primary parameter:  $D_{2cc} <$  reference prescription dose. Secondary parameter:  $D_{0.1cc} (D_{max}) <$  150% of reference prescription dose.
- b. *Prostatic urethra*: Primary parameter:  $D_{10} <$  150% of reference prescription dose. Secondary parameter:  $D_{30} <$  130% of reference prescription dose.
- c. *Penile bulb and neurovascular bundles*: Investigational at present, no parameters can be reliably defined.

## 7. Post-implant dose reporting:

The post-implant analysis should include the outline of the target volumes as described below for evaluation of the two- and three-dimensional dose distributions. In addition, it is recommended to construct the DVH for this target volume, and to document the dose levels that cover 100% and 90% of the target volume for post-implant evaluation, i.e.,  $D_{100}$  and  $D_{90}$ , and the fractional volume receiving 200%, 150%, 100%, and 90% of the prescribed dose, i.e.,  $V_{200}$ ,  $V_{150}$ ,  $V_{100}$ , and  $V_{90}$ . All implants should undergo post-implant evaluation including intraoperative implants. This should be based on imaging at optimum times after implantation, at which time effects of prostate edema are minimal. Optimal imaging should include MRI; but if not available, CT alone is adequate. Seed evaluation and localization is a critical step in post-implant dosimetry. There is a small risk of seed loss or seed migration. Depending on the implantation technique and on the type of seeds used (loose seeds versus stranded seeds), migration rates vary between 1% and 15% have been described anecdotally. If migration rates of 15% or more are observed, the implant technique should be changed to one associated with lower migration rates. For post-implant purposes, the exact number and position of seeds in the target area must be determined.

Post-implant it is almost always impossible to define a GTV on the radiological images due to interference from the seeds. Two different CTV definitions have been proposed by PROBATE:

- a. CTV-P = CTV for prostate, the post-implant contour of the prostatic gland defined by the capsule on radiological examination.
- b. CTV-PM = CTV for prostate plus margin, the post-implant contour of the prostatic gland defined by the capsule with a three-dimensional uniform expansion of 3 mm.

Post-implant, the only OAR that can be defined reliably both on CT and MRI is the rectum. For contouring purposes, using CT only the outer rectal wall can be reliably defined; using MR the outer and inner walls of the rectum over the whole region of interest can be indicated. The lower rectum is poorly defined on CT and best shown with MRI. Image-fusion techniques should therefore be of value. However, there is no consistent definition of the rectal volume to be outlined. Therefore, PROBATE recommended constructing the DVH for the volume, in  $\text{cm}^3$ , of the outer rectal wall.

Furthermore, Salembier et al.<sup>69</sup> recommended localizing the prostatic urethra and documenting the urethra dose in terms of the urethral  $V_{100}$ ,  $V_{150}$ ,  $D_{50}$ , and  $D_{10}$ . Urethra visualization

at the recommended imaging time, rather than immediately post-implantation, can involve additional catheterization and might not be possible or worth performing. It is hoped that a more convenient contrast-enhancing technique will become available in the near future. Correlation with or formal fusion of TRUS images with those obtained by CT or MR imaging may be the optimal non-invasive technique for localization of the urethra on the post-implant scan. Institutional policy should be described if urinary parameters are published.

Defining the penile bulb and neurovascular bundles is only possible with accuracy on MRI and may be performed if available.

As set by PROBATE, dose parameters in the post-implant setting are:

**Target volumes:**  $D_{90}$ ,  $V_{100}$ , and  $V_{150}$  are primary parameters and should always be reported for both CTV-P and CTV-PM. The secondary parameters,  $V_{200}$ ,  $V_{150}$ ,  $V_{90}$ ,  $D_{100}$ , and BED may also be reported although their value in relation to outcome is not proven and should be a focus for further research.

**Organs at risk:**  $D_{2cc}$  for the rectum and  $D_{10}$  for the urethra are the primary parameters. Secondary parameters,  $D_{0.1cc}$  and  $V_{100}$  for rectum and  $D_{0.1cc}$ ,  $D_{30}$ , and  $D_5$  for urethra, may also be reported. For organs at risk, volume parameters should be expressed in absolute values ( $\text{cm}^3$ ). No parameters can be given at present regarding penile bulb and neurovascular bundles. Further investigation and evaluation is needed.

This section V.7 has presented a comparison between the recommendations by the PROBATE group from GEC-ESTRO (Salembier et al.<sup>69</sup>) with the present recommendation. As shown in this section the differences between the two recommendations are related to selection of the CTV margin, the dose to rectal-wall volume versus dose to rectum volume, and the timing of the post-implant imaging procedure. Further research and analysis of patient data should be encouraged to clarify the clinical importance of these variations.

## VI. INTRAOPERATIVE PROSTATE PLANNING AND ITS IMPACT ON DOSE REPORTING

Recent advances in technology allow real-time treatment planning and dose calculations during the implantation procedure. This offers the opportunity to improve the quality of implants by appropriate modifications in the seed implants and replanning during the procedure itself. This technology of intraoperative treatment planning (ITP) raises unique challenges and opportunities for dose reporting in prostate implants. With treatment planning in the OR; the patient and TRUS probe are not moved during the time between the volume study and seed-insertion procedure. This procedure can be performed in three different forms:

- Intraoperative preplanning: Creation of a plan in the OR just before the implant procedure, with immediate execution of the plan.
- Interactive planning: Stepwise refinement of the treatment plan using computerized dose calculations derived from image-based needle-position feedback.

- Dynamic dose calculation: Constant updating of calculations of dose distribution using continuous deposited-seed-position feedback.

## VI.1. INTRAOPERATIVE PREPLANNING

Some institutions with generous inventory of seeds do not require the conventional preplanning visit (a few days or weeks prior to the implant) to obtain prostate volume and subsequent number and strength of seeds to order from a CT scan or ultrasound. TRUS is performed in the OR, and the images are imported in real-time into the treatment planning system (TPS). The target volume, rectum, and urethra are contoured on the TPS either manually or automatically, and a treatment plan is generated. The prostate is implanted according to the plan.

Wilkinson et al., have reported that, using the ABS dose evaluation indices, ITP-based implants were of better quality than those in patients treated with the conventional preplanned method.<sup>51,139</sup> When ITP was compared to the preplanned method, the median  $D_{90}$  increased from 120.5 Gy to 136.5 Gy, the  $V_{80}$  (volume of the prostate receiving 80% of the prescribed dose) increased from 90.4% to 95.6%, and the  $V_{100}$  increased from 76.2% to 84.9%.<sup>139</sup> These improvements were statistically significant. Similar results were confirmed by Gewanter et al.<sup>140</sup> However, it must be noted that these were prospective nonrandomized studies and are therefore subject to selection bias. In addition, studies comparing ITP to historic controls cannot distinguish between improvements due to ITP and those due to improved physician skill or to use of sources with larger total activity.

Intraoperative preplanning has some advantages over the conventional two-step preplanned method. It avoids the need for two separate TRUS procedures and for reproducing patient positioning, and setup is obviated. However, intraoperative preplanning does not account for intraoperative changes in prostate geometry or deviations of needle position from the preplan.<sup>141,142</sup>

## VI.2. INTERACTIVE PLANNING

In this approach, the process of seed ordering, image acquisition, target definition, and organ contouring is similar to the intraoperative preplanning method. An optimized treatment plan is then performed, the DVH is generated, and the plan is examined. If necessary, seeds can be added or deleted manually, and the new isodose distributions and DVH displays are regenerated. The needles are inserted as per plan. In interactive planning, it is critical that the dose calculation is updated based on estimated seed positions derived from actual (imaged) needle positions.<sup>143,144,145,146–148</sup> The needles are repositioned, or subsequent needle positions are altered in the plan, if there are adverse dosimetric consequences. The dose calculation is then updated based on actual needle location. The interval at which the dose distribution is recalculated is operator dependent.

Zelevsky et al., demonstrated consistent excellent dose coverage of the prostate using 1-month post-implant CT and ITP with a median of 96% for  $V_{100}$  and a median of 116% for  $D_{90}$ .<sup>149</sup> In a comparative dosimetric analysis of three implant techniques used at MSKCC, lower maximal urethral doses were observed significantly more frequently with the intraoperative computer-generated conformal plan in comparison to a CT preplan approach or an intraopera-

tive ultrasound manual optimized approach.<sup>146,149</sup> Using this ITP approach, intraoperative dose intensification has been accomplished by directing higher doses toward regions showing active disease on MR spectroscopy without exceeding dose constraints on the urethra and rectum.<sup>150</sup>

Lo et al., compared the dosimetry results generated intraoperatively to CT-based evaluation performed 1 month post-implant in 70 patients, (37 <sup>125</sup>I alone; 33 boost <sup>103</sup>Pd).<sup>151</sup> The mean  $D_{90}$  results intraoperatively compared to those seen post-implant were 178 Gy versus 188.5 Gy for <sup>125</sup>I implants and 98 Gy versus 98.5 Gy for boost <sup>103</sup>Pd implants, respectively.

Interactive planning represents an improvement over intraoperative preplanning, potentially allowing for a shortening of the learning curve for inexperienced brachytherapists, and the technical outcome of the procedure would be less operator dependent. However, in interactive planning the calculated dose distribution is based on implanted needle position, and hence interactive planning might not account for seed movement after deposition. This is most probably true and is the conclusion of a recent paper in which a comparison of the results from two different centers (one with experience and one without inexperience) using the same equipment was presented.<sup>152</sup>

### VI.3. DYNAMIC DOSE CALCULATION

In comparison to interactive planning, dynamic dose calculation requires the following additional components. The essential feature is that the deposited seed positions are captured in real-time, such as via an image-guided robotic brachytherapy device, and the optimization is based on deposited-seed location (rather than needle location). The dose distribution is updated dynamically based on actual positions as the seeds are deposited. The motion of the prostate during placement, as well as changes in prostate size and shape due to intraoperative edema, are accounted for. Post-implant evaluation is performed at time of surgery. Obviously, dynamic dose calculation entails a paradigm shift in dose prescription and specification in that an intended prescription dose is adaptively “painted” to a changing 3D target volume. This process of dose-painting can result in multiple alterations of a previously accepted isodose distribution and total implanted activity, until the end of the procedure when a satisfactory dose distribution is achieved.

At this time, dynamic dose calculation is not available for permanent prostate brachytherapy, because it is difficult to image individual seeds on TRUS. Dynamic dose calculation is feasible for high-dose-rate (HDR) prostate brachytherapy, because it requires imaging the needles, not the individual seeds, with TRUS. However, dynamic dose calculation has been used for HDR prostate brachytherapy, and some of its components could be adapted for permanent prostate dynamic dose calculation and may become available by the time this report is published.<sup>153,154</sup>

The technique of robotic assistance in prostate brachytherapy has attracted much research interest recently.<sup>155,156,157,158,159</sup> Several robotic-system designs have been proposed, including adaptation of an industrial robot, adaptation of a research robot, and robots specially designed for seed implantation.<sup>155,156</sup> It has been shown that the potentially larger implantation space made available by eliminating the restriction to a fixed-grid spacing can be used to advantage in dynamic-dose-calculation planning to counter deleterious effects of intraoperative edema if a periphery-to-center sequence of seed deposition by single needles is followed.<sup>160</sup> These robotic-assisted approaches open up many new issues regarding dose specification and delivery

of the prescribed dose in a dynamic setting. The AAPM Science Council has recently approved formation of the Robotic Brachytherapy working group to examine the role of robots for prostate implants.

#### **VI.4. RECOMMENDATIONS ON INTRAOPERATIVE PLANNING AND EVALUATION**

Intraoperative planning and dose evaluation offer the potential for enhancing the quality of implants and a more accurate determination of the dose distributions at the time of the implant. However, post-implant dosimetry (on the optimum day for imaging with respect to edema resolution) should be performed also in order to take into account the effects of edema and seed migration.

### **VII. SECTOR ANALYSIS OF POST-IMPLANT DOSIMETRY**

#### **VII.1. SECTOR ANALYSIS**

Any spatial information with regard to the dose distribution within the structure is lost in the creation of the DVH. From the DVH, one can see that there are high- and low-dose regions within the structure but not where they are. For brachytherapy, in which the dose can change dramatically over a few millimeters' distance, spatial dose information may be very useful: are the low-dose areas in the regions where cancer is expected, or are high-dose areas located where the higher dose levels might cause complications? There is a trade-off then between retaining spatial information of 3D dose distribution and having the DVH as an analytical tool.

In prostate brachytherapy this dilemma has been partly resolved by dividing the prostate into sectors, or quadrants. Bice et al., used this technique to compare compiled data from 58 patients performed by a single implant team operating at two different institutions: one that used loose seeds and spacers in needles and the other at which a Mick applicator was employed to implant the sources.<sup>161</sup> The authors divided the gland into 12 sectors, by first dividing the gland into thirds in the cranial-caudal direction—base, mid-gland, and apex. Then each third was further subdivided on each transverse slice into anterior, posterior, left, and right sectors. Each of the 12 sectors had its own DVH (Figs. 11, 12, and 13). The implant team discovered that their delivery with the Mick applicator did not provide the same degree of coverage as they were able to achieve with loose seeds in needles. They used sector analysis to pinpoint the weakness in coverage to the basal sectors, implying that seeds were being dragged away from the base as the applicator was withdrawn following deposition of the most basal sources. This problem is user dependent, and can also occur with preloaded needles.

A similar technique was employed by Spadinger et al.<sup>162</sup> By dividing the gland into four quadrants anterior-superior, posterior-superior, anterior-inferior, and posterior-inferior. The authors were able to determine from a study performed on 284 implants that for their series there was a tendency to underdose the anterior-superior quadrant with an average  $V_{100}$  of 78.5% as opposed to the other quadrants where the average  $V_{100}$  ranged from 92.6% to 98.7%. This was attributed to needle drag, needle splay, and contouring difficulties. Subsequently, the same group used this technique to analyze any differences in quality between stranded ( $n=81$ ) and loose



**Fig. 11.** This figure shows the prostate sectors from Bice, et al.<sup>161</sup> In the figure, transverse slices from base to apex are shown starting at the top left and moving down and to the right. The prostate, rectum, urethra, and source locations are depicted along with the prescription isodose line. Note the anterior sectors, 1, 5, and 9, are not completely covered with the prescription isodose.

seed ( $n=54$ ) implants.<sup>162</sup> They showed a slightly higher coverage, as indicated by  $D_{90}$  and  $V_{100}$ , for stranded technique in the inferior quadrants. The same inferior shift of the stranded sources and the subsequent high-dose regions,  $V_{150}$  and  $V_{200}$ , was noted in both the superior (not significant) and the inferior quadrants ( $p<0.001$ ).

According to published reports, sector analysis has been used exclusively to study implant techniques. The practitioners have examined how the dose to different sectors compared over a series of implants, either to analyze their implant methods or to compare between two delivery systems. It is likely sector analysis will become more important with regard to evaluating the dose distribution within individual implants. The introduction of saturation biopsies (typically using 30–80 cores; for example Merrick et al., used a median of 50 cores and found transperineal template-guided saturation biopsy to be a useful diagnostic technique for patients with prior negative TRUS biopsies<sup>163</sup>) and metabolic imaging have given brachytherapists the ability to localize disease within the prostate gland, providing an impetus to concentrate the dose on specific regions and expect different dosimetric outcomes in these areas.

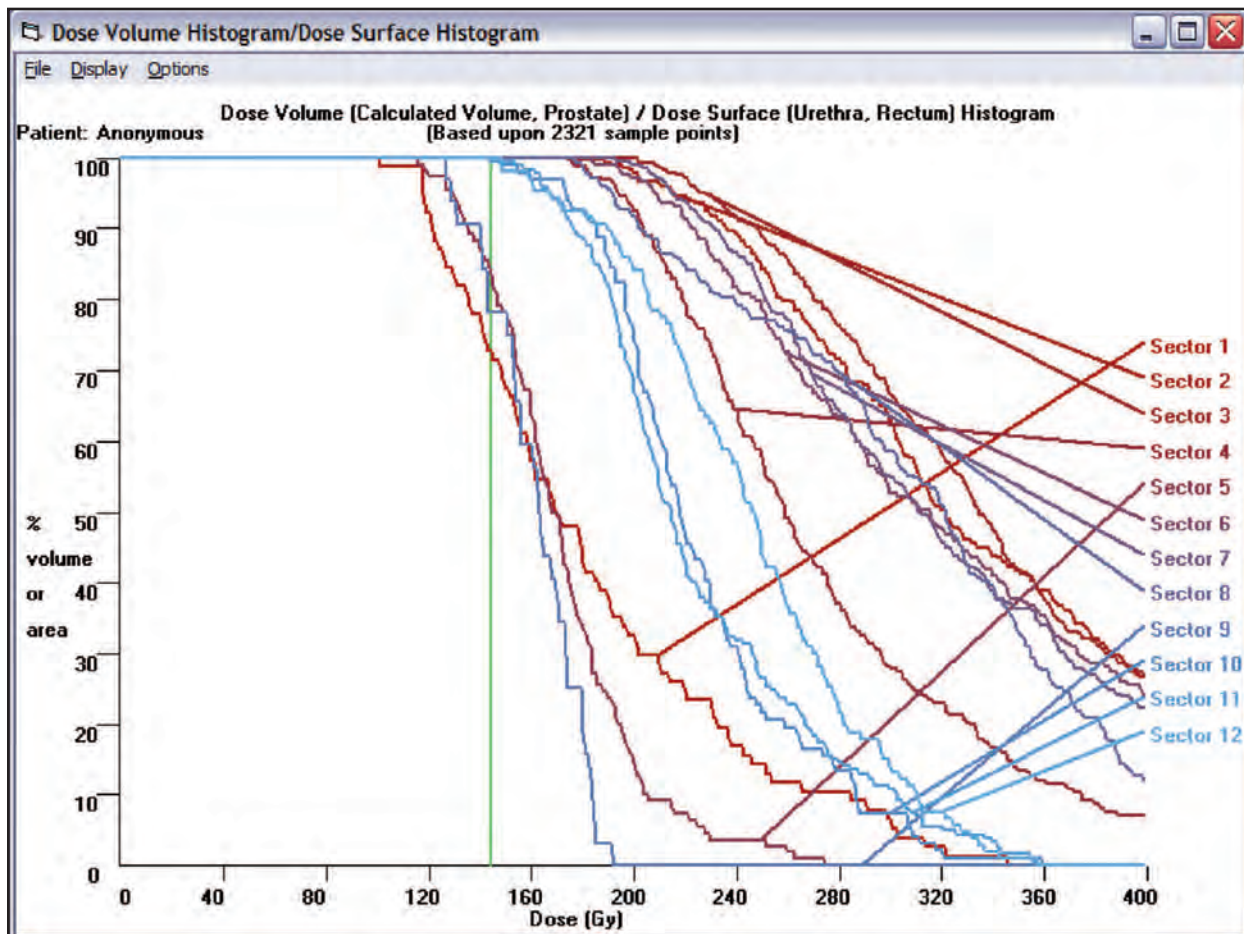


Fig. 12. DVH display for all 12 sectors. The prescription isodose value is shown as a vertical line at 145 Gy. Note sectors 1, 5, and 9 had some volume that received less than the prescription isodose.

## VII.2. RECOMMENDATIONS ON SECTOR ANALYSIS FOR PROSTATE IMPLANTS

In order to utilize fully the knowledge gained by recent pathology studies using biopsy data and advanced imaging techniques such as MR spectroscopy and single-photon emission computed tomography (SPECT),<sup>164,165</sup> it is important to start performing sector analysis of implant dose distributions in a research setting. It is recommended that TPS vendors start providing the tools for such analysis. Further, the community should move from arbitrary (geometrically) defined sectors to “true” anatomical sectors. This could be performed via atlas-matching of the contoured prostate volume or any other methods.

## VIII. BIOPHYSICAL MODELS USED FOR PROSTATE IMPLANTS

While not in popular use and not available in commercially available treatment-planning systems, it is of interest to the medical community to assess theoretical radiobiological effects for prostate implants. In permanent prostate brachytherapy, the tumor cells are subjected to contin-

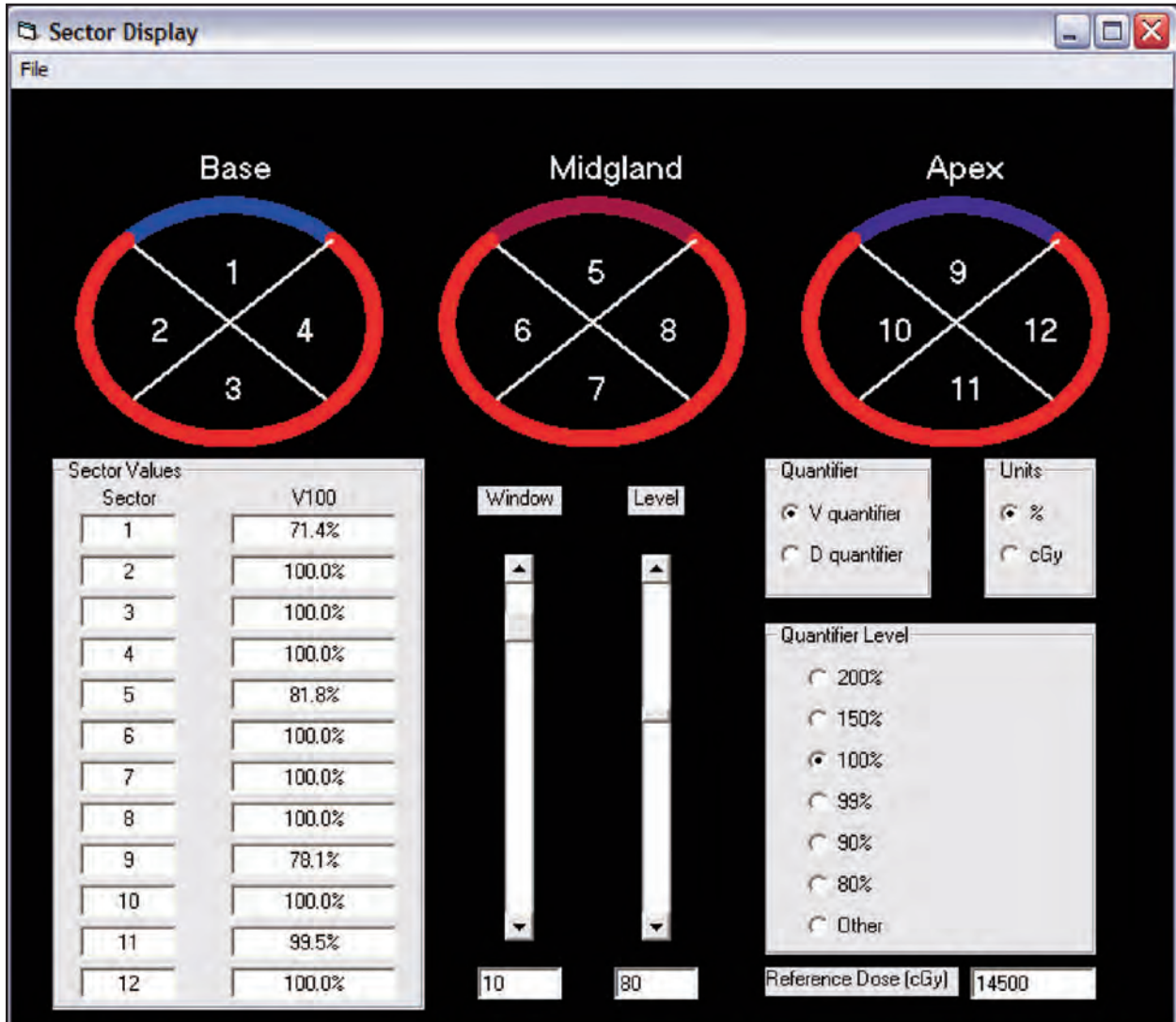


**Fig. 13.** Sector display. In order to simplify the sector results depicted in the graphical dose-volume histogram, this display shows the value of the  $V$  or  $D$  quantifiers for each sector as a color display, with settable window and level, blue being lower values, red higher values. Shown are values for  $V_{100}$  with window set at 10% and level set at 80%. Sectors with  $V_{100}$  at 90% or greater are shown as red and sectors with  $V_{100}$  less than 70% are shown as blue. Sectors with  $V_{100}$  between 70% and 90% are shown as a shade of purple, with bluish values at the lower end of the scale, reddish at the upper end.

uous irradiation of low-energy photons with instantaneous dose rates varying in both space and time. The spatial variation of dose rate is caused by both the sharp dose fall-off around the individual low-energy sources and the spatial relationship of the implanted sources. It is not uncommon to have dose rates differ by more than a factor of two within the prostate gland. The temporal variation of dose rate is caused primarily by the radioactive decay of the radionuclides and by the dynamic resolution of procedure-induced prostate edema. The prescribed initial dose rates vary from approximately 7 cGy/h for  $^{125}\text{I}$  sources to more than 21 cGy/h for  $^{103}\text{Pd}$  sources and more than 30 cGy/h for  $^{131}\text{Cs}$  sources. The duration needed to deliver, for example, 80% of

total dose varies from approximately 22 days for  $^{131}\text{Cs}$  implants to 140 days for  $^{125}\text{I}$  implants. With such diverse spatial and temporal variations, the dosimetric parameters such as  $D_{90}$ ,  $V_{100}$ ,  $V_{150}$ , and DVH discussed earlier in this report become insufficient to fully characterize the biological responses of different prostate implants because the cell repopulation and sub-lethal-damage repair can become significant during the course of dose delivery. There is a need to consider actively the interplay between the spatial-temporal patterns of dose delivery and the underlying cell kinetics in order to properly compare the permanent implants performed with different dose rates, spatial heterogeneities, and radionuclides or to compare an implant with other treatment modalities such as HDR brachytherapy and EBRT for prostate cancer.

Various models have been used in research settings to characterize the interplay of spatial-temporal patterns of dose delivery with the underlying cell kinetics. For permanent implants, an analytic expression of BED derived by Dale based on the linear-quadratic (LQ) cell-inactivation model has been used by many investigators in the examination of various issues related to prostate implant.<sup>166–168</sup> For example Ling et al., and others have used it to assess the effects of dose heterogeneity associated with prostate implants and the relative biological effectiveness (RBE) of different radionuclides.<sup>169–174</sup> Other investigators have used such a model to examine the relative effectiveness of low-dose-rate (LDR) and HDR irradiations, the radiobiological effects of mixing sources with different decay half-lives, the impact of tumor shrinkage during the implant, the effects of prostate edema, the probabilities of tumor control and long-term normal tissue complication, the possibility of dose escalation, and the biological effect of combining prostate brachytherapy with EBRT.<sup>175,176,177,178–180;46,181–183</sup> Recently, Stock et al., have also performed a dose response study for  $^{125}\text{I}$  implants using BED as the implant quality index.<sup>184</sup> Dale and Jones<sup>167</sup> have presented an excellent review on the application of this BED model in brachytherapy. In addition, other models such as equivalent uniform dose (EUD) and tumor control probability (TCP) have also been used in permanent implant evaluation.<sup>146,169,183,185,186</sup> In most of these works, TCP was determined by the Poisson probability of inactivating all tumor cells with the average surviving cells calculated according to Dale's BED. As shown in a study by Tucker et al., the Poisson model is known to underestimate the tumor cure rate when tumor-cell repopulation occurs during the treatment.<sup>187</sup> Zaider and Minerbo<sup>188</sup> have recently derived a more general TCP formalism capable of dealing with cell repopulation and applicable to different temporal patterns of dose delivery. A concern on the use of BED calculated at an "effective treatment time" in isoeffect comparison has also been raised recently in the literature.<sup>189</sup> Despite these new developments, the Dale formalism for BED is still used much more widely because of its mathematical tractability for inhomogeneous dose distributions. Nonetheless, medical physicists who are interested in or are engaged in using radiobiological indices should pay attention to these and future developments in radiobiological modeling.

Radiobiological modeling is intrinsically organ specific. For a given organ, factors that are important to the calculation of radiobiological indices include not only the physical dose or dose-rate distribution but also the properties of intrinsic dose response, tissue architecture of the irradiated organs, fractionation factors (e.g., the  $\alpha/\beta$  ratio in the LQ cell inactivation model), cell repopulation, and sub-lethal damage repair. Other factors that could affect the radiobiological responses such as the presence of hypoxic cells, cell cycle effects, and radiation-induced apoptosis should be considered as well for a complete radiobiological characterization.<sup>190;191,192;193–195</sup>

Considerable progress has been made in the last decade to incorporate these factors in the mathematical modeling of radiobiological responses.<sup>167</sup> At present, however, not all factors are well understood or quantitatively characterized. In addition, some of these factors are known to vary from patient to patient even for the same type of organ tissue. Indeed, the value of  $\alpha/\beta$  ratio for prostate cancer has been discussed and debated intensely in recent years. From this point of view, one should be cautioned that the indices recommended by AAPM in this report, are not meant to, and should not, be used as an absolute index for predicting the treatment outcome of individual patients. Nonetheless, the recommended indices represent, at present, the best available characterization of the interplay of physical dose with the underlying biological processes. When a given set of radiobiological parameters is used consistently, it can be a useful tool for assessing the treatment efficacies of different brachytherapy applications and for evaluating competing strategies of prostate implants. It is on this premise, the AAPM considers it important to discuss and report radiobiological evaluations for permanent prostate implant.

To facilitate the proper use of radiobiological indices and to increase the comparability of indices reported by different institutions, the AAPM believes that it is important to establish a consensus model and its associated parameters for the purpose of reporting biophysical indices. After reviewing the currently available radiobiological models and the associated parameter values for prostate cancer, it is recommended that the Dale BED model and a set of self-consistent parameter values to be used as the interim biophysical models for permanent prostate brachytherapy. EUD can be used as a secondary index. Recognizing the evolving nature of radiobiological modeling, this Task Group does not restrict the use of other models such as TCP or any new and improved models and/or parameters that become available in the future. When reporting these indices, it is recommended that adequate information about the model and the model parameters be included to facilitate easy relative comparison by others. It is well recognized that all models have limitations. Some models may be better than the others at describing or predicting a specific characteristic of the implant. *These recommendations do not imply that the selected models are superior to the others.* Also, the recommended parameter values should not be interpreted as *the* definitive radiobiological parameters for prostate cancer. These recommendations are intended primarily to help in establishing a level of consistency and comparability in the biophysical indices to be reported by different institutions for permanent prostate brachytherapy for relative comparisons.

### VIII.I. BED FOR SPATIALLY UNIFORM DOSE IRRADIATIONS

The BED is defined to provide a direct measure of the amount of cell kill resulted from a given irradiation<sup>166</sup>, i.e.:

$$\text{BED} = -\frac{1}{\alpha} \ln S \quad \text{or} \quad S = \exp[-\alpha \cdot \text{BED}], \quad (3)$$

where  $S$  and  $\alpha$  denote the surviving fraction and the intrinsic radiosensitivity of the irradiated cells, respectively.

### VIII.1.a. BED for Acute Irradiations

The linear-quadratic cell inactivation model is often used to calculate the cell survival from a given irradiation. For acute irradiations, where the cell repopulation and sublethal damage repair can be ignored during the irradiation, the LQ model gives the following well-known relationship between  $S$  and dose  $D$ ,

$$S = \exp[-\alpha D - \beta D^2], \quad (4)$$

where  $\alpha$  and  $\beta$  are coefficients that characterize the average yield of cell kills resulted from the one- and two-track actions, respectively.<sup>166</sup> The BED for such an irradiation, according to Eq. (3) is then given by

$$\text{BED} = D[1 + D/(\alpha/\beta)]. \quad (5)$$

### VIII.1.b. BED for Fractionated Irradiations

For a course of radiotherapy given in  $N$  fractionations with dose  $d$  per fraction, the LQ model predicts that

$$S = \exp\left[-\alpha Nd - \beta Nd^2 + \ln 2 \frac{(N-1)\gamma}{T_p}\right]. \quad (6)$$

The last term in the exponent accounts for the cell repopulation during the course of the treatment, modeled by a potential doubling time  $T_p$  (in days) for tumor cells. It assumes the repopulation is present at the start of the treatment and the treatment is given daily without interruption. The  $\gamma$  is the unit of the elapsed treatment time (in days) and equals 1 day. The intrafraction repair of sublethal damage was neglected in Eq. (6) as the time needed to deliver a typical fraction (e.g., 2 Gy) is usually short while the interfraction repair of sublethal damage was assumed complete within the 24-hour break between fractions.<sup>166</sup>

### VIII.1.c. BED for Prostate Implants Using a Single Type of Radionuclide

During the protracted dose delivery of permanent prostate brachytherapy, both cell repopulation and the repair of sublethal damage can become significant. Based on the LQ model, Dale has derived an analytic expression for BED for permanent implants with dose rate characterized by a single exponential decaying function.<sup>167,168</sup> In his derivation, the cell repopulation was also modeled by a cell potential doubling time similar to Eq. (6). The two-critical target model was used in modeling the repair of sub-lethal damage. In this model, a cell is considered to contain two critical targets susceptible to radiation damage. When only one of the critical targets is damaged by a radiation event, the damage is considered sub-lethal and is repairable. Cell inactivation occurs only when the damage to the other critical target occurs before the existing damage was fully repaired. It was assumed that the sub-lethal damage is repaired exponentially with time, i.e., if the sub-lethal damage was inflicted at time  $t_0$ , then the probability for it persisting

to time  $t$  is given by  $e^{-\mu(t-t_0)}$ . The repair capability is modeled by the time constant  $\mu$ . This model is fundamentally equivalent to the incomplete repair model of Thames for irradiations with constant dose rate.<sup>196</sup> Dale has obtained the following formula for the BED of permanent prostate implants,

$$\text{BED} = D(T_{\text{eff}}) \text{RE}(T_{\text{eff}}) - \ln 2 \frac{T_{\text{eff}}}{\alpha T_p}, \quad (7a)$$

where

$$\text{RE}(T_{\text{eff}}) = 1 + \left( \frac{\beta}{\alpha} \right) \frac{\dot{D}_0}{(\mu - \lambda)} \times \frac{1}{1 - e^{-\lambda T_{\text{eff}}}} \left\{ 1 - e^{-2\lambda T_{\text{eff}}} - \frac{2\lambda}{\mu + \lambda} \left( 1 - e^{-(\mu + \lambda)T_{\text{eff}}} \right) \right\}. \quad (7b)$$

In Eq. (7b),  $\dot{D}_0$  is the initial dose rate;  $\lambda$  is the decay constant of the radionuclide,  $\mu$  is the time constant for sub-lethal damage repair (inversely proportional to the repair half-time),  $T_{\text{eff}}$  is the effective treatment time for an implant, and  $D(T_{\text{eff}})$  is the total dose delivered by the implant within the time period of  $T_{\text{eff}}$ .

The existence of an effective treatment time arises from the two competing processes present in permanent implants, namely, the continuous cell repopulation and reduction of instantaneous dose rate. As the treatment time elapses, the rate of cell inactivation resulted from the instantaneous dose rate becomes exponentially smaller while the rate of cell repopulation remains the same. The  $T_{\text{eff}}$  is defined at which the rate of cell inactivation equals to the rate of cell repopulation for any hypothetically remaining cell, and is given by

$$T_{\text{eff}} = T_{\text{avg}} \ln \left[ \alpha \cdot D \cdot \frac{T_p}{T_{1/2}} \right], \quad (8)$$

where  $T_{1/2}$  is the half-life of the radionuclide,  $T_{\text{avg}} = 1.44T_{1/2}$ , and  $D$  is the total dose delivered to the full decay of the radionuclide. Beyond  $T_{\text{eff}}$ , a net cell kill is no longer attainable. While the definition of  $T_{\text{eff}}$  is physically intuitive, the need to use  $T_{\text{eff}}$  as *the* time point for BED calculation illustrates an inherent uncertainty in the application of this BED model to tumors that continuously repopulate in permanent implants. The BED value calculated at other time instances will be different from that calculated at  $T_{\text{eff}}$ . Even in relative comparisons of two implants, using BED calculated at  $T_{\text{eff}}$  versus using BED calculated at other time instances could lead quantitatively different results. Zaider and Hanin have recently pointed out that the use of Eq. (8) for proliferating tumors underestimates the isoeffective dose.<sup>189</sup> For temporary implants with source dwell time less than  $T_{\text{eff}}$ , the actual source dwell time should be used in Eq. (7) for calculating the BED.

The BED derived by Dale is characterized by four parameters that takes into account the effect of single-track lethality ( $\alpha$ ), inter-track quadratic interactions ( $\beta$ ), as well as the first order kinetics of sub-lethal damage repair ( $\mu$ ) and cell proliferation ( $T_p$ ) in permanent prostate brachytherapy. It also takes into account the exponential decay of the instantaneous dose rates.

The model shows that the effective cell-kill depends not only on the delivered dose but also on the temporal patterns of the dose delivery in presence of sub-lethal damage repair and cell repopulation. For implants with exponentially decaying radionuclides, the dose delivery pattern is determined by the radioactive decay half-life and the BED is a function of the radionuclides used. In general, BED is greater if the total delivered dose is larger. For the same prescribed dose, the model indicates that BED is always larger when the dose is delivered by radionuclides with shorter half-lives. The model has been used to compare different treatment techniques and other issues for which the absolute values of radiobiological parameters or model assumptions may not be critical. Note, however, that many radiobiological complexities are excluded by necessity, including non-exponential sub-lethal damage repair. In addition, as discussed earlier, concerns on the use of  $T_{eff}$  in BED calculation and its effect on isoeffect comparison has been raised recently in literature.<sup>189</sup>

#### VIII.I.d. BED for Implants Containing a Mixture of Radionuclides with Different Decay Half-lives

For implants containing multiple radionuclides with different radioactive decay half-lives, the temporal variation of dose rate at any tumor subvolume no longer follows a single exponential decaying function. Chen and Nath have shown that the expression of BED derived by Dale can be generalized to such an implant.<sup>177;168,197</sup> The resulting BED builds upon Eq. (7a) but with

$$D(T_{eff}) = \sum_{n=0}^{\infty} \frac{\dot{D}_n(0)}{\lambda_n} (1 - e^{-\lambda_n T_{eff}}) \quad (9a)$$

and

$$RE(T) = 1 + \left( \frac{\beta}{\alpha} \right) \frac{2}{D(T)} \sum_{i=0}^{\infty} \sum_{j=0}^{\infty} \frac{\dot{D}_i(0) \dot{D}_j(0)}{\mu - \lambda_i} \left\{ \frac{1}{\lambda_i + \lambda_j} (1 - e^{-(\lambda_i + \lambda_j)T}) - \frac{1}{\lambda_j + \mu} (1 - e^{-(\mu + \lambda_j)T}) \right\}. \quad (9b)$$

The summation in Eq. (9b) is with respect to the different types of radionuclide. For implants with a single type of radionuclide,  $i = j = 1$  and Eq. (9b) reduces to the original Dale equation.<sup>168,197</sup> Note, however, that Eq. (8) is a nontrivial result as it does *not* equate to the simple addition of the BED from each radionuclide type alone. Eq. (9) has been used by Chen and Nath for examining the relative benefits of performing permanent interstitial implants using a mixture of <sup>125</sup>I and <sup>103</sup>Pd radionuclides.<sup>177</sup> For such implants, the resulting BED was found to depend on the relative dose contributions by different types of radioactive sources used.

#### VIII.I.e. BED for Permanent Implants in Presence of Prostate Edema

In absence of edema, the implanted sources and the tumor volume are assumed to be stationary and the dose rate at a tumor subvolume  $P$  has a simple exponential dependence on time,

$$\dot{D}_p(t) = \dot{D}_p(0) e^{-\lambda_p t}, \quad (10)$$

where  $\dot{D}_p(0)$  is the total initial dose rate produced at  $P$  by all implanted sources.

In presence of edema, the dose rate is no longer governed by a simple exponential function of time because the distance between the sources and the tumor subvolume is now time dependent due to the prostate swelling and its protracted resolution. While direct numerical computation can be used to calculate the BED for such a situation, an analytical expression can also be obtained by parameterizing the dose fall-off from each source as an inverse power function.<sup>180</sup> Based on the edema resolution model reported by Waterman et al., Chen et al., have found that the dose rate at  $P$  can be modeled as<sup>83,97</sup>

$$\dot{D}_P(t) = \dot{D}_P(0) \frac{e^{-\lambda_l t}}{(1 + \Delta e^{-\lambda_E t})^{\tau/3}}, \quad (11)$$

where  $\dot{D}_P(0)$  is the initial dose rate produced at  $P$  by the implant before the onset of edema,  $\Delta$  is the edema magnitude,  $\lambda_E$  is the edema resolution time constant, and  $\tau$  is the exponent of the inverse power function that characterizes the dose fall-off around a given source. For an ideal point source with inverse-square dose fall-off, the exponent  $\tau$  is equal to 2. For the model 6711 <sup>125</sup>I seed and the model 200 <sup>103</sup>Pd seed,  $\tau$  was 2.35 and 2.85, respectively, based on the consensus TG-43 dataset. For the Model CS-1 <sup>131</sup>Cs seed,  $\tau$  was 2.20 based on the measured and Monte Carlo simulation data.<sup>198</sup> With Eq. (11), the dose rate can be expressed further as a sum of multiple exponential decaying functions by Taylor expansion such that

$$\dot{D}_P(t) = \sum_{n=0}^{\infty} \dot{D}_P^{(n)}(0) e^{-\lambda_n t}, \quad (12a)$$

with

$$\dot{D}_P^{(n)} = (-1)^n \prod_{j=0}^{n-1} (j + \tau/3) \frac{\Delta^j}{j!} \dot{D}_P(0), \quad (12b)$$

and

$$\lambda_n = \lambda_l + n\lambda_E. \quad (12c)$$

The Taylor expansion (well behaved mathematically for edemas with magnitude <100%) was purposely used as the BED of such an implant can now be calculated by using Eq. (9) derived by Chen and Nath for implants containing multiple sources of different half-lives.<sup>177</sup> It is interesting to note that Eq. (12) implies that the dose rate at  $P$  in the presence of edema is mathematically equivalent to an implant with multiple exponentially decaying “sources” whose initial dose rate and decay time constant are functions of the edema magnitude and half-life. Indeed, the  $n = 0$  source represents the dose contribution by the implant in the absence of edema and the rest of the “sources” ( $n \geq 1$ ) collectively give the correction due to edema. The BED for an implant without edema can also be calculated from Eq. (12) by setting the edema magnitude to zero. Eq. (12) in combination with Eq. (9) has been used in examining the impact of edema on cell survival for <sup>125</sup>I and <sup>103</sup>Pd implants<sup>179</sup> and for <sup>131</sup>Cs implants.<sup>199</sup>

## VIII.2. BED AND EQUIVALENT UNIFORM DOSE (EUD) FOR INHOMOGENEOUS DOSE DISTRIBUTIONS

### VIII.2.a. BED for Inhomogeneous Dose Distribution

The BED formulae discussed in section VIII.1 have assumed that the dose-rate distribution is spatially uniform, which is not true in a real implant. The dose-rate distribution inside a prostate implant is highly non-uniform. The BED for such an implant can be calculated by partitioning the tumor volume into small subvolumes so that the dose-rate distribution in each subvolume can be considered uniform.<sup>169,200</sup> The  $BED_i$  for a subvolume  $i$  with initial dose rate of  $\dot{D}_i(0)$  can then be calculated using the formulae discussed in section VIII.1. Mathematically, the BED for a clinical prostate implant can be calculated as

$$BED = -\frac{1}{\alpha} \ln \left( \sum_i v_i e^{-\alpha BED_i} \right), \quad (13)$$

where  $v_i$  is the fractional volume receiving the dose rate  $\dot{D}_i(0)$  with  $\sum_i v_i = 1$ .  $v_i$  is directly related to the differential dose (or initial dose rate) histogram of a permanent implant. The BED calculated with Eq. (13) takes into account not only the time-dependent dose-rate variation, cell repopulation, and sub-lethal damage repair during the dose delivery but also the spatial heterogeneity of dose-rate distribution in permanent prostate brachytherapy. Ling has used Eq. (13) in studying the effects of dose heterogeneity in permanent interstitial implants.<sup>169</sup>

The BED calculated according to Eq. (13) is preferentially weighted by low-dose-rates. To fully assess its significance, it may be beneficial to calculate the three-dimensional distribution of BED within a permanent prostate implant. The iso-BED distribution can be calculated by combining the BED formulae with the three-dimensional dose rate distributions.<sup>177,201</sup> With the iso-BED distributions, one can evaluate the biological significance of “hot” or “cold” dose-rate regions based on underlying anatomy. Similar considerations have also been used to construct radiobiologically relevant DVHs in EBRT.<sup>202–204</sup> It should be pointed out that the calculation of iso-BED distribution with Eq. (13) implicitly assumes that the tumor burden and their radiosensitivity is spatially uniform. Nonetheless, it would be straightforward to incorporate the spatial distribution of tumor burden and radiosensitivity into the calculation of BED or iso-BED distribution when such information is accurately known.

### VIII.2.b. EUD for Inhomogeneous Dose Distribution

Within the framework of biologically effective dose, the BED calculated according to Eq. (13) can be interpreted as corresponding to a permanent implant with an EUD as proposed initially by Niemierko for inhomogeneous distributions encountered in EBRT.<sup>185</sup> The EUD can be obtained by denoting  $D(T_{eff})$  in Eq. (7) as EUD and solving for EUD from the following equation based on Eq. (13) and Eq. (7),

$$EUD \times RE(EUD, T_{eff}) - \ln 2 \frac{T_{eff}}{\alpha T_p} = -\frac{1}{\alpha} \ln \left( \sum_i v_i e^{-\alpha \cdot BED_i} \right). \quad (14)$$

The EUD calculated in this fashion retains the temporal characteristics of dose delivery in permanent prostate brachytherapy. However, the solution is not readily expressible in analytic forms. Numerical methods are needed to find the solution.

In a more general approach, it is also possible to calculate an EUD from Eq. (13) that corresponds to any desired dose delivery technique based on the total cell kill. For examples, the BED or the corresponding cell kill resulting from a fractionated EBRT with uniform dose irradiations can be calculated and made equal to that given by Eq. (13) for a permanent prostate brachytherapy, namely,

$$\text{BED}_{\text{EBRT}} = -\frac{1}{\alpha} \ln \left( \sum_i v_i e^{-\alpha \cdot \text{BED}_i} \right). \quad (15)$$

Since BEDEBRT for fraction size  $d$  according to Eq. (6) is

$$\text{BED}_{\text{EBRT}} = D \left\{ 1 + \left( \frac{\beta}{\alpha} \right) d - \ln 2 \frac{\gamma}{\alpha T_p \cdot d} \right\} + \ln 2 \cdot \gamma / (\alpha T_p), \quad (16)$$

one can calculate an equivalent uniform total EBRT dose for fraction size  $d$  ( $\text{EUD}_d$ ) that would yield the same cell kill as permanent prostate brachytherapy as

$$\text{EUD}_d = \frac{-\ln \left( \sum_i v_i e^{-\alpha \cdot \text{BED}_i} \right) - \ln 2 \cdot \gamma / T_p}{\alpha + \beta d - \gamma \ln 2 / (d \cdot T_p)}. \quad (17)$$

It should be noted that, in deriving Eq. (17), one has assumed that the BED formulation has considered all the relevant factors for a true equivalence between the two different modalities. If this assumption holds, one can use Eq. (17) to calculate the EUD for a course of external beam with any fraction size, for example, of 2 Gy for the purpose of comparing the relative effectiveness of a permanent prostate brachytherapy with the traditional EBRT. The use of Eq. (17) would also make it easier for considering the overall effects of a combined modality using both permanent brachytherapy and EBRT for the same patient with prostate cancer if the underlying assumption is valid. As discussed in section VIII.2.a, the use of Eq. (17) implicitly assumes that the initial tumor burden and radiosensitivity are spatially uniform. Further, the RBE is assumed to be unity in the aforementioned analysis. On the other hand, several radiobiological studies using in vitro cell lines have shown that the RBE of continuous LDR irradiation using low-energy photons (typical in permanent prostate implants) can be significantly different from that of high-energy photons typically used in EBRT. The actual value of RBE is also affected by many factors such as the linear energy transfer (LET), the dose rate, and the biological properties of the irradiated tissue.<sup>205</sup> The reported LET-induced RBE for <sup>125</sup>I ( <sup>103</sup>Pd) ranged from 1.2 to 1.5 (1.6 to 1.9) compared to photons of <sup>60</sup>Co.<sup>206</sup> To determine the absolute equivalency between a LDR implant and an EBRT treatment, one needs to know the RBE specific to each irradiation condition (LET, dose rate) and the tumor cells being irradiated.

### VIII.3. TUMOR CONTROL PROBABILITY (TCP)

With BED, the radiation-induced cell kill is used as the surrogate of the biological response to a permanent prostate brachytherapy. The linkage between the amount of cell kill and a given clinical response, however, is not linear. It often depends on many other factors such as the architecture of the irradiated tissue or organ. Some investigators have calculated the probabilities of tumor control and normal tissue complications for permanent brachytherapy.

Traditionally, the calculation of TCP and normal tissue complication probability (NTCP) is based on empirical models constructed to fit an observed clinical dose-response.<sup>207,208</sup> For example, a logistic function that resembles the sigmoid-shape of many observed dose responses was used to model the TCP for uniform dose irradiations.

$$\text{TCP}(D) = \frac{1}{1 + (TCD_{50}/D)^k}. \quad (18)$$

The two model parameters,  $TCD_{50}$  and  $k$ , are to be fitted from the observed clinical data. The  $TCD_{50}$  gives the dose required to achieve a 50% probability of tumor control and  $k$  measures the slope of the dose-response curve.

One model that has often been used for TCP calculation is based on the assumption that the radiation-induced cell kill follows the Poisson statistics. In this model, the probability of cure (i.e., the probability of no tumor cell surviving) after a given irradiation is given by

$$\text{TCP} = \exp(-\langle N \rangle), \quad (19)$$

where  $\langle N \rangle$  represents the expectation value of the remaining tumor cells at the end of the treatment. Since BED is directly related to cell survival, one can explicitly evaluate Eq. (19) if the initial tumor burden or the total number of tumor cells ( $N_0$ ) prior to the start of the treatment is known, namely,

$$\text{TCP} = \exp[-N_0 \exp(-\alpha \cdot \text{BED})]. \quad (20)$$

Several investigators have used Eq. (20) to assess the TCP for external beam radiotherapy and for permanent prostate brachytherapy.<sup>183,186</sup> The calculated dose-response curve is usually much sharper than has been observed clinically. While the clinically observed dose response often represents the averaged effect among a population of patients, the TCP calculated according to Eq. (20) is often interpreted as representing individual patients.

It should be pointed out, however, that although the Poisson model was capable of describing the probability of tumor cure accurately when cell proliferation is not present during treatment, it usually underestimates the cure rate when tumor proliferation occurs during treatment.<sup>187</sup> Improved TCP models have been proposed recently.<sup>188,209</sup> In particular, a general analytic expression for TCP derived by Zaider and Minerbo<sup>188</sup>, which takes into account the tumor cell repopulation and is applicable for different temporal patterns of dose delivery, was found to give better fit to an experimental dose-response dataset than the binomial mode of Eq. (19)<sup>210</sup>. Despite of these new developments, the Poisson model (Eq. (20)) and the BED calculated at  $T_{eff}$

(Eqs. (7) and (13)) for permanent implants are still being used by many medical physicists, in part because the Poisson model and Eq. (13) are mathematically more tractable for inhomogeneous dose distributions and, perhaps more relevant, because of the lack of awareness to the new models. The Task Group encourages medical physicists who use TCP in permanent implant evaluation to become familiar with these new developments and to understand the assumptions and limitations of the existing models.

#### VIII.4. MODEL PARAMETERS FOR PROSTATE CANCER

To calculate BED, EUD, or TCP for permanent prostate implants, one needs to know the values of  $\alpha$ ,  $\alpha/\beta$ ,  $T_p$ ,  $T_{1/2}$  of sub-lethal damage repair, and  $N_0$  for prostate cancer cells. The numerical values of these parameters, especially the  $\alpha/\beta$  ratio, for prostate cancer have been subjected to intense discussions in the recent literature.<sup>211–229</sup> In 1999, Brenner et al. performed a radiobiological analysis of the treatment outcomes of prostate cancer between external beam radiotherapy and permanent brachytherapy and have reported that the  $\alpha/\beta$  ratio for prostate cancer appeared to be unusually low ( $\sim 1.5$  Gy) compared to that of typical tumors ( $> \sim 8$  Gy).<sup>211,226,230</sup> Following this report, a series of articles and debates has emerged which examined the differences in dose distribution, dose rate, relative biological effectiveness, tumor hypoxia, and other factors between EBRT and permanent brachytherapy and their effects on the estimated  $\alpha/\beta$  value. While the specific values of  $\alpha/\beta$  are still being debated, the emerging consensus is that the  $\alpha/\beta$  may indeed be low (in the range of 1 to 4 Gy) for prostate cancer.<sup>211,212,215,216,220,226</sup> However, there is no consensus on the specific values of the model parameters needed for the calculation of BED and TCP for prostate implants. Indeed, the value of each parameter is likely to be different from patient to patient. In the absence of a reliable technique to accurately determine patient-specific model parameters, the numerical values of a calculated BED or TCP cannot be used confidently as a predictor for the treatment outcomes of individual patients.

Nonetheless, a set of model parameters with nominal values representative of prostate cancer is needed to calculate the BED or TCP for permanent prostate implants. When a set of parameters is used consistently, the BED may become a useful index for comparing the relative merit of implants with different physical characteristics (e.g., differences in initial dose rate, radionuclide type, spatial source loading pattern, etc.). In addition, the BED or TCP calculated and reported by different institutions using the same model parameters would allow quantitative comparison of the implant techniques used by different institutions. For these purposes, the AAPM recommends a self-consistent set of parameters based on the reports by Wang et al.<sup>220,223,231</sup>. The nominal values are  $\alpha = 0.15 \text{ Gy}^{-1}$ ,  $\beta = 0.05 \text{ Gy}^{-2}$ ,  $\alpha/\beta = 3.0 \text{ Gy}$ ,  $T_p = 42$  days, repair half-life of 0.27 hour, and  $N_0 = 10^6$ . It should be emphasized that these recommended values should not be interpreted as the radiobiological parameters of any prostate cancers. See commentary by Fowler et al.<sup>221</sup>

Indeed, since the clinical dose responses reported in the literature usually represent the average dose responses from a population of patients treated in one or several institutions, the recommended nominal values at best only represent a population-averaged “patient” (associated with the clinical practice of particular institutions). However, no real patient is an “average” patient. The parameters for a given patient could be significantly different from the nominal value. In addition, many technical issues related to the collection and reporting of the dosimetry

and clinical response data can affect the values of the deduced model parameters. In fact, the nominal values estimated by different research groups for prostate cancer were quite different. Carlson et al. have recently conducted a systematic analysis of the in vitro experiments on prostate cancer cell lines using the LQ model and compared the estimated radiobiological parameters with the in vivo data reported in recent studies.<sup>232</sup> The  $\alpha$  estimated from the in vitro data ranged from 0.09 to 0.35 Gy<sup>-1</sup> and the  $\alpha/\beta$  ratio ranged from 1.09 to 6.29 Gy. They found that the differences in the radiosensitivity parameters determined from the data reported by different laboratories were as large as or larger than the differences in radiosensitivity parameters observed among the various prostate cell lines.<sup>232</sup> The estimated in vitro repair half-time ranged from 5.7 to 8.9 hours (with 95% confidence interval from 0.26 to 10.7 h) which appeared significantly larger than the estimates derived from clinical data.<sup>232</sup> The estimated  $T_p$  for prostate carcinoma also had a wide range from 10 to over 60 days.<sup>233</sup> Therefore, the uncertainties associated with the existing radiobiological parameters for prostate cancer are quite large. In a research setting, one should evaluate the validity and variability of the implications of radiobiological modeling by using the parameters sampled over their observed or expected uncertainty range.

### VIII.5. RECOMMENDATIONS FOR REPORTING RELATIVE RADIOBIOLOGICAL RESPONSE

1. When radiobiological indices are included in the reporting of permanent implant responses, AAPM recommends that adequate information on the radiobiological model and the model parameters should be included to facilitate easy intercomparison. Recognizing the evolving nature of radiobiological modeling, the BED (Eqs. (7) and (13)) calculated with a set of nominal model parameters (see below) is recommended as an interim primary radiobiological index for permanent prostate brachytherapy. Other models such as EUD, TCP, or future new/improved models may also be used in accordance with the above reporting guidelines.
2. For improved intercomparability, a set of model parameters with nominal values representative of prostate cancer is recommended for the calculation of BED and EUD for permanent prostate implants. The recommended values are  $\alpha = 0.15 \text{ Gy}^{-1}$ ,  $\beta = 0.05 \text{ Gy}^{-2}$ ,  $\alpha/\beta = 3.0 \text{ Gy}$ ,  $T_p = 42 \text{ days}$ , and repair half-life of 0.27 hour. It should be emphasized that these recommended values should not be interpreted as the radiobiological parameters of individual prostate cancer patients. Typical values of BED, EUD, and TCP (Poisson model) using these parameters are shown in Table 5, which can be used as a quality assurance check on algorithmic model implementation. It should be emphasized that these recommended values should not be interpreted as *the* radiobiological parameters of individual prostate cancer patients.
3. Ideally, all dosimetric quantities needed for calculating the radiobiological indices should be reported so that these indices can be recalculated when new or improved models become available. However, it is not possible, at the present, to include these data (for example, differential DVHs of individual patients) in conventional publications. It would be ideal to have a centralized data center so that the data of individual patients can be electronically pooled together and analyzed systematically.

**Table 5.** Examples of radiobiological indices for uniform dose distributions.

Indices	Radionuclide		
	<sup>125</sup> I	<sup>103</sup> Pd	<sup>131</sup> Cs
Dose (Gy)	145.0	125.0	120.0
BED (Gy)	101.7	112.7	115.7
TCP (%)	79.0	95.5	97.1
$T_{eff}$ (day)	236.2	94.1	61.0
<b>Calculated with:</b> $\alpha = 0.15 \text{ Gy}^{-1}$ , $\beta = 0.05 \text{ Gy}^{-2}$ , $\alpha/\beta = 3.0 \text{ Gy}$ , $T_p = 42 \text{ days}$ , repair half-life of 0.27 hour, and $N_0 = 10^6$			

4. The software vendors for brachytherapy are encouraged to incorporate calculations of radiobiological indices in their brachytherapy TPS to facilitate reporting and relative comparison of radiobiological responses. The radiobiological parameters should be implemented as user-modifiable input fields so that the impact of different radiobiological characteristics on the calculated radiobiological indices can be easily examined. The currently accepted parameter set could be used as the default values.

## IX. DISCUSSION

In this report, we focus on LDR permanent interstitial brachytherapy for treatment of prostate cancer. In contrast to this modality are temporary implants using HDR brachytherapy techniques, in which hollow needles are placed into the prostate gland and a single high-activity radioactive source (nominally 10 Ci <sup>192</sup>Ir) dwells in selected locations in each needle for approximately 5 to 15 minutes to deliver the prescribed dose. This procedure is repeated 2 to 3 times over several days. After all treatment is completed, the needles are removed. Because of the major differences in LDR and HDR techniques, the dose-reporting requirements are fundamentally different. In this report, we address only the issues related to LDR permanent brachytherapy of the prostate because of its wide applicability and unique clinical issues.

The present recommendations do not include tissue-heterogeneity corrections and interseed-shielding effects, primarily because the methods of their application have not been resolved at the present time. However, these issues need to be considered carefully once a practical model for their application is introduced. Dose calculations for transperineal implantation with <sup>125</sup>I or <sup>103</sup>Pd brachytherapy sources are typically performed assuming a point-source emitter in a homogeneous water phantom. The efficacy of this assumption has been investigated by several investigators using both experimental and Monte Carlo simulation techniques. For example, Chibani and colleagues have shown significant deviations for  $D_{90}$  due to calcifications.<sup>234</sup> Meigooni and Nath have found that the heterogeneity effect for different brachytherapy sources is a function of spatial location, tissue thickness, and photon energy.<sup>235</sup> However, DeMarco et al.<sup>236</sup> observed that

the effects of interseed attenuation in prostate implants with sources in the energy range of 20–36 keV are insignificant.

Presently, the dose at any point of a multi-seed implant is calculated by adding the doses from each seed, assuming that the presence of the other seeds does not affect the radiation field. However, in a typical prostate implant there are 40 to 100 seeds in close proximity to each other that can cause seed-to-seed interference. Using a thermoluminescent dosimetry (TLD) technique, Meigooni et al., showed a dose distortion of up to 10% in an assembly of 18  $^{125}\text{I}$  seeds.<sup>237</sup> Furthermore, using the Monte Carlo simulation technique, Burns and Raeside<sup>238</sup> showed up to 9.8% perturbation of the dose distribution around a single  $^{125}\text{I}$  seed (models 6702 and 6711) by the presence of 1 or 3 nonradioactive neighboring seeds. Recently, DeMarco et al.<sup>236</sup> used the Monte Carlo simulation method in a CT-based dosimetry calculation for  $^{125}\text{I}$  prostate implants, which simulated clinical applications. Contrary to previous findings, they concluded that the interseed effects were negligible in their implant patterns. In an independent investigation, Carrier et al.<sup>239,240</sup> examined the effect of dose perturbation in a multi-seed implant. They concluded based on an interseed attenuation study that computable dosimetric differences exist between plans with 0.38 U and 0.76 U sources, two initial activity levels often used in clinical practice. Because more sources are necessary for a plan with 0.38 U sources, a 2% increase in the attenuation level was calculated for two different prostate sizes. The tissue-composition effect has the same impact for all prostate sizes and seed densities when the prostate is approximated to a homogeneous organ. However, they proposed that a more realistic study taking into account local heterogeneities would be necessary to establish the consequences of this effect. In addition, seed design was also shown to strongly influence interseed attenuation.<sup>241</sup> These discrepancies are not yet resolved, and there is still a need for further investigation into Monte Carlo simulations and TLD measurements for multi-seed implants in heterogeneous media to clarify the role of interseed effects in patient dose delivery. Therefore, the recommendations in this report do not address the impact of heterogeneity on the final outcome, and these effects are excluded from the current recommendations.

## X. REFERENCES

- 1 B.R. Thomadsen, K. Ayyanger, L. Anderson, G. Luxton, W. Hanson, J.F. Wilson, “Brachytherapy Treatment Planning” in *Principles and Practice of Brachytherapy*. S. Nag (ed.). (Futura Publishing Co., Armonk, New York, 1997).
- 2 W.L. Smith, C. Lewis, G. Bauman, G. Rodrigues, D. D’Souza, R. Ash, D. Ho, V. Venkatesan, D. Downey, and A. Fenster. “Prostate volume contouring: a 3D analysis of segmentation using 3DTRUS, CT, and MR.” *Int J Radiat Oncol Biol Phys* 67:1238–1247 (2007).
- 3 W.M. Butler, R.R. Stewart, and G.S. Merrick. “A detailed radiobiological and dosimetric analysis of biochemical outcomes in a case-control study of permanent prostate brachytherapy patients.” *Med Phys* 36(3):776–787 (2009).
- 4 R. Nath, W.S. Bice, W.M. Butler, Z. Chen, A.S. Meigooni, V. Narayana, M.J. Rivard, and Y. Yu “AAPM recommendations on dose prescription and reporting methods for permanent interstitial brachytherapy for prostate cancer: Report of Task Group 137.” *Med Phys* 37:5310–5322 (2009).
- 5 ACS (American Cancer Society), ACS Cancer Facts and Figures 2007. (American Cancer Society, Atlanta, GA, 2007).

- 6 W.F. Whitmore, Jr. "Interstitial radiation therapy for carcinoma of the prostate." *Prostate* 1:157–168 (1980).
- 7 H.H. Holm, N. Juul, J.F. Pedersen, H. Hansen, and I. Stroyer. "Transperineal <sup>125</sup>iodine seed implantation in prostatic cancer guided by transrectal ultrasonography." *J Urol* 130:283–286 (1983).
- 8 J.C. Blasko, P.D. Grimm, and H. Ragde. "Brachytherapy and organ preservation in the management of carcinoma of the prostate." *Semin Radiat Oncol* 3:240–249 (1993).
- 9 J.E. Johansson, L. Holmberg, S. Johansson, R. Bergstrom, and H.O. Adami. "Fifteen-year survival in prostate cancer. A prospective, population-based study in Sweden." *JAMA* 277:467–471 (1997).
- 10 H. Ragde, J.C. Blasko, P.D. Grimm, G.M. Kenny, J.E. Sylvester, D.C. Hoak, K. Landin, and W. Cavanagh. "Interstitial iodine-125 radiation without adjuvant therapy in the treatment of clinically localized prostate carcinoma." *Cancer* 80:442–453 (1997).
- 11 F.L. Greene, D.L. Page, I.D. Fleming, A. Fritz, C.M. Balch, D.G. Haller, and M. Morrow. *AJCC Cancer Staging Manual* (6th ed.), p. 421 (Springer, New York, NY, 2002).
- 12 S.J. Frank, P.D. Grimm, J.E. Sylvester, G.S. Merrick, B.J. Davis, A. Zietman, B.J. Moran, D.C. Beyer, M. Roach 3<sup>rd</sup>, D.H. Clarke, R.G. Stock, W. R. Lee, J.M. Michalski, K.E. Wallner, M. Hurwitz, L. Potters, D.A. Kuban, B.R. Prestidge, R. Vera, S. Hathaway, and J.C. Blasko. "Interstitial implant alone or in combination with external beam radiation therapy for intermediate-risk prostate cancer: a survey of practice patterns in the United States." *Brachytherapy* 6:2–8 (2007).
- 13 A.W. Partin, L.A. Mangold, D.M. Lamm, P.C. Walsh, J.I. Epstein, and J.D. Pearson. "Contemporary update of prostate cancer staging nomograms (Partin tables) for the new millennium." *Urology* 58:843–848 (2001).
- 14 NCCN (National Comprehensive Cancer Network). NCCN Clinical Practice Guidelines in Oncology: Prostate Cancer V.1.2007 [http://www.nccn.org/professionals/physician\\_gls/PDF/prostate.pdf](http://www.nccn.org/professionals/physician_gls/PDF/prostate.pdf) V (2007).
- 15 K. Wallner, G. Merrick, L. True, T. Sherertz, S. Sutlief, W. Cavanagh, and W. Butler. "20 Gy versus 44 Gy supplemental beam radiation with Pd-103 prostate brachytherapy: preliminary biochemical outcomes from a prospective randomized multi-center trial." *Radiother Oncol* 75:307–310 (2005).
- 16 M.A. Elshaikh, J.C. Ulchaker, C.A. Reddy, K.W. Angermeier, E.A. Klein, N. Chehade, A. Altman, and J. P. Ciezki. "Prophylactic tamsulosin (Flomax) in patients undergoing prostate <sup>125</sup>I brachytherapy for prostate carcinoma: final report of a double-blind placebo-controlled randomized study." *Int J Radiat Oncol Biol Phys* 62:164–169 (2005).
- 17 P.F. Schellhammer, R. Moriarty, D. Bostwick, and D. Kuban. "Fifteen-year minimum follow-up of a prostate brachytherapy series: comparing the past with the present. [see comment]." *Urology* 56:436–439 (2000).
- 18 M.J. Zelefsky, D.A. Kuban, L.B. Levy, L. Potters, D.C. Beyer, J.C. Blasko, B.J. Moran, J.P. Ciezki, A.L. Zietman, T.M. Pisansky, M. Elshaikh, and E.M. Horwitz. "Multi-institutional analysis of long-term outcome for stages T1-T2 prostate cancer treated with permanent seed implantation." *Int J Radiat Oncol Biol Phys* 67:327–333 (2007).
- 19 K.K. Chao, N.S. Goldstein, D. Yan, C.E. Vargas, M.I. Ghilezan, H.J. Korman, K.M. Kernan, J.B. Hollander, J.A. Gonzalez, A.A. Martinez, F.A. Vicini, and L.L. Kestin. "Clinicopathologic analysis of extracapsular extension in prostate cancer: should the clinical target volume be expanded posterolaterally to account for microscopic extension?" *Int J Radiat Oncol Biol Phys* 65:999–1007 (2006).

- 20 M.J. Zelefsky and W.F. Whitmore, Jr. "Long-term results of retropubic permanent <sup>125</sup>iodine implantation of the prostate for clinically localized prostatic cancer." *J Urol* 158:23–29; discussion 29–30 (1997).
- 21 R. Nath, K. Roberts, M. Ng, R. Peschel, and Z. Chen. "Correlation of medical dosimetry quality indicators to the local tumor control in patients with prostate cancer treated with iodine-125 interstitial implants." *Med Phys* 25:2293–2307 (1998).
- 22 R.G. Stock, N.N. Stone, A. Tabert, C. Iannuzzi, and J.K. DeWyngaert. "A dose-response study for I-125 prostate implants." *Int J Radiat Oncol Biol Phys* 41:101–108 (1998).
- 23 L. Potters, Y. Cao, E. Calugaru, T. Torre, P. Fearn, and X.H. Wang. "A comprehensive review of CT-based dosimetry parameters and biochemical control in patients treated with permanent prostate brachytherapy." *Int J Radiat Oncol Biol Phys* 50:605–614 (2001).
- 24 M.J. Barry, F.J. Fowler, Jr., M.P. O'Leary, R.C. Bruskewitz, H.L. Holtgrewe, W.K. Mebust, and A.T. Cockett. "The American Urological Association symptom index for benign prostatic hyperplasia. The Measurement Committee of the American Urological Association." *J Urol* 148: 1549–1557; discussion 1564 (1992).
- 25 J. Desai, R.G. Stock, N.N. Stone, C. Iannuzzi, and J.K. DeWyngaert. "Acute urinary morbidity following I-125 interstitial implantation of the prostate gland." *Radiat Oncol Invest* 6:135–141 (1998).
- 26 R.G. Stock, N.N. Stone, M. Dahlal, and Y.C. Lo. "What is the optimal dose for <sup>125</sup>I prostate implants? A dose-response analysis of biochemical control, posttreatment prostate biopsies, and long-term urinary symptoms." *Brachytherapy* 1:83–89 (2002).
- 27 G.S. Merrick, W.M. Butler, B.G. Tollenaar, R.W. Galbreath, and J.H. Lief. "The dosimetry of prostate brachytherapy-induced urethral strictures." *Int J Radiat Oncol Biol Phys* 52:461–468 (2002).
- 28 K.M. Snyder, R.G. Stock, S.M. Hong, Y.C. Lo, and N.N. Stone. "Defining the risk of developing grade 2 proctitis following <sup>125</sup>I prostate brachytherapy using a rectal dose-volume histogram analysis." *Int J Radiat Oncol Biol Phys* 50:335–341 (2001).
- 29 M.A. Elshaikh, K. Angermeier, J.C. Ulchaker, E.A. Klein, M.A. Chidel, S. Mahoney, D. A. Wilkinson, C.A. Reddy, and J.P. Ciezki. "Effect of anatomic, procedural, and dosimetric variables on urinary retention after permanent iodine-125 prostate brachytherapy." *Urol* 61:152–155 (2003).
- 30 S. Jones, K. Wallner, G. Merrick, J. Corriveau, S. Sutlief, L. True, and W. Butler. "Clinical correlates of high intraprostatic brachytherapy dose volumes." *Int J Radiat Oncol Biol Phys* 53: 328–333 (2002).
- 31 G.S. Merrick, W.M. Butler, K.E. Wallner, R.W. Galbreath, B. Murray, D. Zeroski, and J. H. Lief. "Dysuria after permanent prostate brachytherapy." *Int J Radiat Oncol Biol Phys* 55:979–985 (2003).
- 32 K. Wallner, J. Roy, and L. Harrison. "Dosimetry guidelines to minimize urethral and rectal morbidity following transperineal I-125 prostate brachytherapy." *Int J Radiat Oncol Biol Phys* 32: 465–471 (1995).
- 33 A. Niehaus, G.S. Merrick, W.M. Butler, K.E. Wallner, Z.A. Allen, R.W. Galbreath, and E. Adamovich. "The influence of isotope and prostate volume on urinary morbidity after prostate brachytherapy." *Int J Radiat Oncol Biol Phys* 64:136–143 (2006).
- 34 G.S. Merrick, W.M. Butler, A.T. Dorsey, J.H. Lief, H.L. Walbert, and H.J. Blatt. "Rectal dosimetric analysis following prostate brachytherapy." *Int J Radiat Oncol Biol Phys* 43:1021–1027 (1999).

- 35 B.H. Han and K.E. Wallner. “Dosimetric and radiographic correlates to prostate brachytherapy-related rectal complications.” *Int J Cancer* 96:372–378 (2001).
- 36 G.S. Merrick, W.M. Butler, K. Wallner, R.W. Galbreath, R.L. Anderson, B.S. Kurko, and J.H. Lief. “Permanent prostate brachytherapy-induced morbidity in patients with grade II and III obesity.” *Urology* 60:104–108 (2002).
- 37 G.U. Rao, P.T. Kan, and R. Howells. “Interstitial volume implants with I-125 seeds.” *Int J Radiat Oncol Biol Phys* 7:431–438 (1981).
- 38 J.M. Crook, L. Potters, R.G. Stock, and M.J. Zelefsky. “Critical organ dosimetry in permanent seed prostate brachytherapy: defining the organs at risk.” *Brachytherapy* 4:186–194 (2005).
- 39 K. Elliott, K. Wallner, G. Merrick, and P. Herstein. “Medical malpractice of prostate brachytherapy.” *Brachytherapy* 3:231–236 (2004).
- 40 M.J. Zelefsky and J.F. Eid. “Elucidating the etiology of erectile dysfunction after definitive therapy for prostatic cancer.” *Int J Radiat Oncol Biol Phys* 40:129–133 (1998).
- 41 S.A. Mangar, M.R. Sydes, H.L. Tucker, J. Coffey, S.A. Sohaib, S. Gianolini, S. Webb, V.S. Khoo, and D.P. Dearnaley. “Evaluating the relationship between erectile dysfunction and dose received by the penile bulb: using data from a randomised controlled trial of conformal radiotherapy in prostate cancer (MRC RT01, ISRCTN47772397).” *Radiother Oncol* 80:355–362 (2006).
- 42 G.S. Merrick, W.M. Butler, K.E. Wallner, R.W. Galbreath, R.L. Anderson, B.S. Kurko, J.H. Lief, and Z.A. Allen. “Erectile function after prostate brachytherapy.” *Int J Radiat Oncol Biol Phys* 62:437–447 (2005).
- 43 V. Krishnaswamy. “Dose tables for <sup>125</sup>I seed implants.” *Radiology* 132:727–730 (1979).
- 44 F.M. Waterman and K.A. Strubler. “Absorbed dose determination for interstitial <sup>125</sup>I boost therapy.” *Med Phys* 10:155–158 (1983).
- 45 A. Wu, R.D. Zwicker, and E.S. Sternick. “Tumor dose specification of I-125 seed implants.” *Med Phys* 12:27–31 (1985).
- 46 Y. Yu. “A nondivergent specification of the mean treatment dose in interstitial brachytherapy.” *Med Phys* 23:905–909 (1996).
- 47 J.N. Roy, L.L. Anderson, K.E. Wallner, Z. Fuks, and C.C. Ling. “Tumor control probability for permanent implants in prostate.” *Radiother Oncol* 28:72–75 (1993).
- 48 J. Willins and K. Wallner. “CT-based dosimetry for transperineal I-125 prostate brachytherapy.” *Int J Radiat Oncol Biol Phys* 39:347–353 (1997).
- 49 Y. Yu, F.M. Waterman, N. Suntharalingam, and A. Schulsinger. “Limitations of the minimum peripheral dose as a parameter for dose specification in permanent <sup>125</sup>I prostate implants.” *Int J Radiat Oncol Biol Phys* 34:717–725 (1996).
- 50 D. Ash, A. Flynn, J. Battermann, T. de Reijke, P. Lavagnini, and L. Blank. “ESTRO/EAU/EORTC recommendations on permanent seed implantation for localized prostate cancer.” *Radiother Oncol* 57:315–321 (2000).
- 51 S. Nag, W. Bice, K. DeWynngaert, B. Prestidge, R. Stock, and Y. Yu. “The American Brachytherapy Society recommendations for permanent prostate brachytherapy postimplant dosimetric analysis.” *Int J Radiat Oncol Biol Phys* 46:221–230 (2000).
- 52 C.H. Bangma, A.Q. Niemer, D.E. Grobbee, and F.H. Schroder. “Transrectal ultrasonic volumetry of the prostate: in vivo comparison of different methods.” *Prostate* 28:107–110 (1996).
- 53 S. Tong, H.N. Cardinal, R.F. McLoughlin, D.B. Downey, and A. Fenster. “Intra- and inter-observer variability and reliability of prostate volume measurement via two-dimensional and three-dimensional ultrasound imaging.” *Ultrasound Med Biol* 24:673–681 (1998).

- 54 B.J. Davis, R.R. Kinnick, M. Fatemi, E.P. Lief, R.A. Robb, and J. F. Greenleaf. "Measurement of the ultrasound backscatter signal from three seed types as a function of incidence angle: application to permanent prostate brachytherapy." *Int J Radiat Oncol Biol Phys* 57:1174–1182 (2003).
- 55 V. Narayana, P.L. Roberson, A.T. Pu, H. Sandler, R.H. Winfield, and P.W. McLaughlin. "Impact of differences in ultrasound and computed tomography volumes on treatment planning of permanent prostate implants." *Int J Radiat Oncol Biol Phys* 37:1181–1185 (1997).
- 56 L. Gong, P.S. Cho, B.H. Han, K.E. Wallner, S.G. Sutlief, S.D. Pathak, D.R. Haynor, and Y. Kim. "Ultrasonography and fluoroscopic fusion for prostate brachytherapy dosimetry." *Int J Radiat Oncol Biol Phys* 54:1322–1330 (2002).
- 57 D.A. Todor, M. Zaider, G.N. Cohen, M. F. Worman, and M.J. Zelefsky. "Intraoperative dynamic dosimetry for prostate implants." *Phys Med Biol* 48:1153–1171 (2003).
- 58 M.M. Goodsitt, P.L. Carson, S. Witt, D.L. Hykes, and J.M. Kofler, Jr. "Real-time B-mode ultrasound quality control test procedures. Report of AAPM Ultrasound Task Group-1." *Med Phys* 25:1385–1406 (1998).
- 59 D. Pfeiffer, S. Sutlief, W. Feng, H.M. Pierce, and J. Kofler. "AAPM Task Group 128: Quality assurance tests for prostate brachytherapy ultrasound systems." *Med Phys* 35:5471–5489 (2008).
- 60 D.F. Dubois, B.R. Prestidge, L.A. Hotchkiss, J.J. Prete, and W.S. Bice, Jr. "Intraobserver and interobserver variability of MR imaging- and CT-derived prostate volumes after transperineal interstitial permanent prostate brachytherapy." *Radiology* 207:785–789 (1998).
- 61 W.R. Lee, M. Roach 3rd, J. Michalski, B. Moran, and D. Beyer. "Interobserver variability leads to significant differences in quantifiers of prostate implant adequacy." *Int J Radiat Oncol Biol Phys* 54:457–461 (2002).
- 62 J. Crook, M. Milosevic, P. Catton, I. Yeung, T. Haycocks, T. Tran, C. Catton, M. McLean, T. Panzarella, and M.A. Haider. "Interobserver variation in postimplant computed tomography contouring affects quality assessment of prostate brachytherapy." *Brachytherapy* 1:66–73 (2002).
- 63 B. Al-Qaisieh, D. Ash, D. M. Bottomley, and B.M. Carey. "Impact of prostate volume evaluation by different observers on CT-based post-implant dosimetry." *Radiother Oncol* 62:267–273 (2002).
- 64 M. Roach 3rd, P. Faillace-Akazawa, C. Malfatti, J. Holland, and H. Hricak. "Prostate volumes defined by magnetic resonance imaging and computerized tomographic scans for three-dimensional conformal radiotherapy." *Int J Radiat Oncol Biol Phys* 35:1011–1018 (1996).
- 65 P.W. McLaughlin, S. Troyer, S. Berri, V. Narayana, A. Meierowitz, P. L. Roberson, and J. Montie. "Functional anatomy of the prostate: implications for treatment planning." *Int J Radiat Oncol Biol Phys* 63:479–491 (2005).
- 66 B.H. Han, K. Wallner, G. Merrick, K. Badiozamani, and W. Butler. "The effect of interobserver differences in post-implant prostate CT image interpretation on dosimetric parameters." *Med Phys* 30:1096–1102 (2003).
- 67 P.W. McLaughlin, V. Narayana, T. Jackson, J.M. Crook, W.R. Lee, J. Michalski, B.R. Prestidge, and M.J. Zelefsky. "The impact of MRI training on improvement of CT based post implant dosimetry; A six physician study." *Int J Radiat Oncol Biol Phys* 63:S327 (2005).
- 68 V. Narayana, S. Troyer, V. Evans, R.J. Winfield, P.L. Roberson, and P.W. McLaughlin. "Randomized trial of high- and low-source strength <sup>125</sup>I prostate seed implants. [see comment]." *Int J Radiat Oncol Biol Phys* 61:44–51 (2005).
- 69 C. Salembier, P. Lavagnini, P. Nickers, P. Mangili, A. Rijnders, A. Polo, J. Venselaar, and P. Hoskin. "Tumour and target volumes in permanent prostate brachytherapy: a supplement to the ESTRO/EAU/EORTC recommendations on prostate brachytherapy." *Radiother Oncol* 83:3–10 (2007).

- 70 P.W. McLaughlin, V. Narayana, D.G. Drake, B.M. Miller, L. Marsh, J. Chan, R. Gonda, Jr., R.J. Winfield, and P.L. Roberson. "Comparison of MRI pulse sequences in defining prostate volume after permanent implantation." *Int J Radiat Oncol Biol Phys* 54:703–711 (2002).
- 71 P. McLaughlin, S. Berri, and V. Narayana. "Determination of rectal muscle, rectal mucosa and rectal wall dimensions: Dosimetric implications in prostate brachytherapy." *Brachytherapy* 6:105 (2007).
- 72 M.A. Moerland, H.K. Wijrdeman, R. Beersma, C.J. Bakker, and J.J. Battermann. "Evaluation of permanent I-125 prostate implants using radiography and magnetic resonance imaging." *Int J Radiat Oncol Biol Phys* 37:927–933 (1997).
- 73 D.F. Dubois, B.R. Prestidge, L.A. Hotchkiss, W.S. Bice, Jr., and J.J. Prete. "Source localization following permanent transperineal prostate interstitial brachytherapy using magnetic resonance imaging." *Int J Radiat Oncol Biol Phys* 39:1037–1041 (1997).
- 74 R.J. Amdur, D. Gladstone, K.A. Leopold, and R.D. Harris. "Prostate seed implant quality assessment using MR and CT image fusion." *Int J Radiat Oncol Biol Phys* 43:67–72 (1999).
- 75 P.L. Roberson, P.W. McLaughlin, V. Narayana, S. Troyer, G.V. Hixson, and M.L. Kessler. "Use and uncertainties of mutual information for computed tomography/magnetic resonance (CT/MR) registration post permanent implant of the prostate." *Med Phys* 32:473–482 (2005).
- 76 F.V. Coakley, H. Hricak, A.E. Wefer, J.L. Speight, J. Kurhanewicz, and M. Roach. "Brachytherapy for prostate cancer: endorectal MR imaging of local treatment-related changes." *Radiology* 219:817–821 (2001).
- 77 V. Narayana, P.W. McLaughlin, T. Jackson, and M. Zelefsky. "SU-FF-I-21: Can prostate CT contouring be improved?" *Med Phys* 32:1908 (2005).
- 78 C. Kirisits, F.A. Siebert, D. Baltas, M. De Brabandere, T. P. Hellebust, D. Berger, and J. Venselaar. "Accuracy of volume and DVH parameters determined with different brachytherapy treatment planning systems." *Radiother Oncol* 84:290–297 (2007).
- 79 F.A. Siebert, M. De Brabandere, C. Kirisits, G. Kovacs, and J. Venselaar. "Phantom investigations on CT seed imaging for interstitial brachytherapy." *Radiother Oncol* 85:316–323 (2007).
- 80 F.A. Siebert, P. Kohr, and G. Kovacs. "The design and testing of a solid phantom for the verification of a commercial 3D seed reconstruction algorithm." *Radiother Oncol* 74:169–175 (2005).
- 81 K.R. Badiozamani, K. Wallner, S. Sutlief, W. Ellis, J. Blasko, and K. Russell. "Anticipating prostatic volume changes due to prostate brachytherapy." *Radiat Oncol Invest* 7:360–364 (1999).
- 82 D. Taussky, L. Austen, A. Toi, I. Yeung, T. Williams, S. Pearson, M. McLean, G. Pond, and J. Crook. "Sequential evaluation of prostate edema after permanent seed prostate brachytherapy using CT-MRI fusion." *Int J Radiat Oncol Biol Phys* 62:974–980 (2005).
- 83 F.M. Waterman, N. Yue, B.W. Corn, and A.P. Dicker. "Edema associated with I-125 or Pd-103 prostate brachytherapy and its impact on post-implant dosimetry: an analysis based on serial CT acquisition." *Int J Radiat Oncol Biol Phys* 41:1069–1077 (1998).
- 84 Y. Yamada, L. Potters, M. Zaider, G. Cohen, E. Venkatraman, and M.J. Zelefsky. "Impact of intra-operative edema during transperineal permanent prostate brachytherapy on computer-optimized and preimplant planning techniques." *Am J Clin Oncol* 26:130–135 (2003).
- 85 J.L. Speight, K. Shinohara, B. Pickett, V.K. Weinberg, I.C. Hsu, and M. Roach 3<sup>rd</sup>. "Prostate volume change after radioactive seed implantation: possible benefit of improved dose volume histogram with perioperative steroid." *Int J Radiat Oncol Biol Phys* 48:1461–1467 (2000).
- 86 R. Whittington, G.A. Broderick, P. Arger, S.B. Malkowicz, R.D. Epperson, B. Arjomandy, and A. Kassae. "The effect of androgen deprivation on the early changes in prostate volume following transperineal ultrasound guided interstitial therapy for localized carcinoma of the prostate." *Int J Radiat Oncol Biol Phys* 44:1107–1110 (1999).

- 87 N. Yue, A.P. Dicker, R. Nath, and F.M. Waterman. "The impact of edema on planning  $^{125}\text{I}$  and  $^{103}\text{Pd}$  prostate implants." *Med Phys* 26:763–767 (1999).
- 88 J. Willins and K. Wallner. "Time-dependent changes in CT-based dosimetry of I-125 prostate brachytherapy." *Radiat Oncol Invest* 6:157–160 (1998).
- 89 G.S. Merrick, W.M. Butler, A.T. Dorsey, and H.L. Walbert. "Influence of timing on the dosimetric analysis of transperineal ultrasound-guided, prostatic conformal brachytherapy." *Radiat Oncol Invest* 6:182–190 (1998).
- 90 N. Dogan, N. Mohideen, G.P. Glasgow, K. Keys, and R.C. Flanigan. "Effect of prostatic edema on CT-based postimplant dosimetry." *Int J Radiat Oncol Biol Phys* 53:483–489 (2002).
- 91 B.R. Prestidge, W.S. Bice, E.J. Kiefer, and J.J. Prete. "Timing of computed tomography-based postimplant assessment following permanent transperineal prostate brachytherapy. [see comment]." *Int J Radiat Oncol Biol Phys* 40:1111–1115 (1998).
- 92 G. Leclerc, M.C. Lavalley, R. Roy, E. Vigneault, and L. Beaulieu. "Prostatic edema in  $^{125}\text{I}$  permanent prostate implants: dynamical dosimetry taking volume changes into account." *Med Phys* 33:574–583 (2006).
- 93 J. Crook, M. McLean, I. Yeung, T. Williams, and G. Lockwood. "MRI-CT fusion to assess post-brachytherapy prostate volume and the effects of prolonged edema on dosimetry following transperineal interstitial permanent prostate brachytherapy." *Brachytherapy* 3:55–60 (2004).
- 94 F.M. Waterman, N. Yue, S. Reisinger, A. Dicker, and B.W. Corn. "Effect of edema on the post-implant dosimetry of an I-125 prostate implant: a case study." *Int J Radiat Oncol Biol Phys* 38:335–339 (1997).
- 95 N. Yue, A.P. Dicker, B.W. Corn, R. Nath, and F.M. Waterman. "A dynamic model for the estimation of optimum timing of computed tomography scan for dose evaluation of  $^{125}\text{I}$  or  $^{103}\text{Pd}$  seed implant of prostate." *Int J Radiat Oncol Biol Phys* 43:447–454 (1999).
- 96 N. Yue, Z. Chen, R. Peschel, A.P. Dicker, F.M. Waterman, and R. Nath. "Optimum timing for image-based dose evaluation of  $^{125}\text{I}$  and  $^{103}\text{Pd}$  prostate seed implants." *Int J Radiat Oncol Biol Phys* 45:1063–1072 (1999).
- 97 Z. Chen, N. Yue, X. Wang, K. B. Roberts, R. Peschel, and R. Nath. "Dosimetric effects of edema in permanent prostate seed implants: a rigorous solution." *Int J Radiat Oncol Biol Phys* 47:1405–1419 (2000).
- 98 Z. Chen, J. Deng, K. Roberts, and R. Nath. "Potential impact of prostate edema on the dosimetry of permanent seed implants using the new  $^{131}\text{Cs}$  (model CS-1) seeds." *Med Phys* 33:968–975 (2006).
- 99 F.M. Waterman and A.P. Dicker. "Impact of postimplant edema on V(100) and D(90) in prostate brachytherapy: can implant quality be predicted on day 0?" *Int J Radiat Oncol Biol Phys* 53:610–621 (2002).
- 100 F.M. Waterman and A.P. Dicker. "Effect of post-implant edema on the rectal dose in prostate brachytherapy." *Int J Radiat Oncol Biol Phys* 45:571–576 (1999).
- 101 F.M. Waterman and A.P. Dicker. "The impact of postimplant edema on the urethral dose in prostate brachytherapy." *Int J Radiat Oncol Biol Phys* 47:661–664 (2000).
- 102 R.G. Stock, N.N. Stone, Y.C. Lo, N. Malhado, J. Kao, and J.K. DeWyngaert. "Postimplant dosimetry for  $^{125}\text{I}$  prostate implants: definitions and factors affecting outcome." *Int J Radiat Oncol Biol Phys* 48:899–906 (2000).
- 103 R. Nath, L.L. Anderson, G. Luxton, K.A. Weaver, J.F. Williamson, and A.S. Meigooni. "Dosimetry of interstitial brachytherapy sources: recommendations of the AAPM Radiation Therapy Committee Task Group No. 43. American Association of Physicists in Medicine. [see comment][erratum appears in *Med Phys* 23(9):1579 (1996)]." *Med Phys* 22:209–234 (1995).

- 104 M.J. Rivard, B.M. Coursey, L.A. DeWerd, W.F. Hanson, M.S. Huq, G.S. Ibbott, M.G. Mitch, R. Nath, and J.F. Williamson. "Update of AAPM Task Group No. 43 Report: A revised AAPM protocol for brachytherapy dose calculations. [see comment] [erratum appears in *Med Phys* 31(12):3532–3533 (2004)]." *Med Phys* 31:633–674 (2004).
- 105 N.N. Stone, S. Hong, Y.C. Lo, V. Howard, and R.G. Stock. "Comparison of intraoperative dosimetric implant representation with postimplant dosimetry in patients receiving prostate brachytherapy." *Brachytherapy* 2:17–25 (2003).
- 106 L. Potters, E. Calugaru, K.B. Thornton, T. Jackson, and D. Huang. "Toward a dynamic real-time intraoperative permanent prostate brachytherapy methodology." *Brachytherapy* 2:172–180 (2003).
- 107 L. Potters, E. Calugaru, A. Jassal, and J. Presser. "Is there a role for postimplant dosimetry after real-time dynamic permanent prostate brachytherapy?" *Int J Radiat Oncol Biol Phys* 65:1014–1019 (2006).
- 108 L. Chauveinc, T. Flam, S. Solignac, N. Thiounn, F. Firmin, B. Debre, J.C. Rosenwald, P. Philips, and J. M. Cosset. "Prostate cancer brachytherapy: Is real-time ultrasound-based dosimetry predictive of subsequent CT-based dose distribution calculation? A study of 450 patients by the Institut Curie/Hospital Cochin (Paris) Group." *Int J Radiat Oncol Biol Phys* 59:691–695 (2004).
- 109 W.D. D'Souza, H.K. Lee, M.B. Palmer, L.G. Smith, and A. Pollack. "Is intraoperative nomogram-based overplanning of prostate implants necessary?" *Int J Radiat Oncol Biol Phys* 56:462–467 (2003).
- 110 P. McLaughlin, V. Narayana, C. Pan, S. Berri, S. Troyer, J. Herman, V. Evans, and P. Roberson. "Comparison of day 0 and day 14 dosimetry for permanent prostate implants using stranded seeds." *Int J Radiat Oncol Biol Phys* 64:144–150 (2006).
- 111 D. Taussky, I. Yeung, T. Williams, S. Pearson, M. McLean, G. Pond, and J. Crook. "Rectal-wall dose dependence on postplan timing after permanent-seed prostate brachytherapy." *Int J Radiat Oncol Biol Phys* 65:358–363 (2006).
- 112 G. Gejerman, E. Mullokandov, A.J. Saini, V. Lanteri, J. Scheuch, J. Vitenson, J. Rosen, R. Garden, and I. Sawczuk. "The effects of edema on urethral dose following palladium-103 prostate brachytherapy." *Med Dosim* 27:221–225 (2002).
- 113 L. Potters, R. Purrazzella, S. Brustein, P. Fearn, S.A. Leibel, and M.W. Kattan. "A comprehensive and novel predictive modeling technique using detailed pathology factors in men with localized prostate carcinoma." *Cancer* 95:1451–1456 (2002).
- 114 R.G. Stock, N.N. Stone, A. Tabert, C. Iannuzzi, and J.K. DeWyngaert. "A dose-response study for I-125 prostate implants." *Int J Radiat Oncol Biol Phys* 41:101–108 (1998).
- 115 J.E. Sylvester. "The Seattle Prostate Institute Approach to Treatment Planning for Permanent Implants" in *Basic and Advanced Techniques in Prostate Brachytherapy*. A.P. Dicker, G.S. Merrick, F.M. Waterman, R.K. Valicenti, and L.G. Gomella (eds.). (Taylor and Francis, London, UK, 2005).
- 116 C.D. Scales, Jr., J.C. Presti, Jr., C.J. Kane, M.K. Terris, W.J. Aronson, C.L. Amling, and S.J. Freedland. "Predicting unilateral prostate cancer based on biopsy features: implications for focal ablative therapy-results from the SEARCH database." *J Urol* 178:1249–1252 (2007).
- 117 G.S. Merrick, W.M. Butler, K.E. Wallner, J.C. Blasko, J. Michalski, J. Aronowitz, P. Grimm, B.J. Moran, P.W. McLaughlin, J. Usher, J.H. Lief, and Z.A. Allen. "Variability of prostate brachytherapy pre-implant dosimetry: a multi-institutional analysis." *Brachytherapy* 4:241–251 (2005).
- 118 X. Huang, X. Zhang, B. Farahvash, and A. F. Olumi. "Novel targeted pro-apoptotic agents for the treatment of prostate cancer." *J Urol* 178:1846–1854 (2007).

- 119 B.J. Davis, T.M. Pisansky, T.M. Wilson, H.J. Rothenberg, A. Pacelli, D.W. Hillman, D.J. Sargent, and D.G. Bostwick. "The radial distance of extraprostatic extension of prostate carcinoma: implications for prostate brachytherapy." *Cancer* 85:2630–2637 (1999).
- 120 C. Sohayda, P.A. Kupelian, H.S. Levin, and E.A. Klein. "Extent of extracapsular extension in localized prostate cancer." *Urology* 55:382–386 (2000).
- 121 S. Choi, K.E. Wallner, G.S. Merrick, W. Cavanagh, and W.M. Butler. "Treatment margins predict biochemical outcomes after prostate brachytherapy." *Cancer J* 10:175–180 (2004).
- 122 G.S. Merrick, W.M. Butler, R.W. Galbreath, J.H. Lief, and E. Adamovich. "Perineural invasion is not predictive of biochemical outcome following prostate brachytherapy." *Cancer J* 7:404–412 (2001).
- 123 G.S. Merrick, W.M. Butler, R.W. Galbreath, J.H. Lief, and E. Adamovich. "Biochemical outcome for hormone-naïve patients with Gleason score 3+4 versus 4+3 prostate cancer undergoing permanent prostate brachytherapy." *Urology* 60:98–103 (2002).
- 124 G.S. Merrick, W.M. Butler, K.E. Wallner, R.W. Galbreath, Z. Allen, and E. Adamovich. "Temporal effect of neoadjuvant androgen deprivation therapy on PSA kinetics following permanent prostate brachytherapy with or without supplemental external beam radiation." *Brachytherapy* 3:141–146 (2004).
- 125 K. Wallner, G. Merrick, L. True, S. Sutlief, W. Cavanagh, and W. Butler. "<sup>125</sup>I versus <sup>103</sup>Pd for low-risk prostate cancer: preliminary PSA outcomes from a prospective randomized multicenter trial. [see comment]." *Int J Radiat Oncol Biol Phys* 57:1297–1303 (2003).
- 126 V. Narayana, S. Troyer, V. Evans, R.J. Winfield, P.L. Roberson, and P.W. McLaughlin. "Randomized trial of high- and low-source strength <sup>125</sup>I prostate seed implants." *Int J Radiat Oncol Biol Phys* 61:44–51 (2005).
- 127 M.A. Moerland and J.J. Battermann. "Randomized trial of high- and low-source strength <sup>125</sup>I prostate seed implants: In regard to Narayana et al. [Int J Radiat Oncol Biol Phys 61:44–51 (2005)]." *Int J Radiat Oncol Biol Phys* 62:941–942 (2005).
- 128 R.S. Sloboda, J.E. Pedersen, and R. Halperin. "Is there a preferred strength for regularly spaced <sup>125</sup>I seeds in inverse-planned prostate implants?" *Int J Radiat Oncol Biol Phys* 55:234–244 (2003).
- 129 R. S. Sloboda, J.E. Pedersen, J. Hanson, and R.M. Halperin. "Dosimetric consequences of increased seed strength for I-125 prostate implants. [see comment]." *Radiother Oncol* 68:295–297 (2003).
- 130 L. Beaulieu, L. Archambault, S. Aubin, E. Oral, R. Taschereau, and J. Pouliot. "The robustness of dose distributions to displacement and migration of <sup>125</sup>I permanent seed implants over a wide range of seed number, activity, and designs." *Int J Radiat Oncol Biol Phys* 58:1298–1308 (2004).
- 131 P. Lindsay, J. Battista, and J. Van Dyk. "The effect of seed anisotropy on brachytherapy dose distributions using <sup>125</sup>I and <sup>103</sup>Pd." *Med Phys* 28:336–345 (2001).
- 132 O. Chibani, J.F. Williamson, and D. Todor. "Dosimetric effects of seed anisotropy and interseed attenuation for <sup>103</sup>Pd and <sup>125</sup>I prostate implants." *Med Phys* 32:2557–2566 (2005).
- 133 J.F. Williamson, B.M. Coursey, L.A. DeWerd, W.F. Hanson, R. Nath, and G. Ibbott. "Guidance to users of Nycomed Amersham and North American Scientific, Inc., I-125 interstitial sources: dosimetry and calibration changes: recommendations of the American Association of Physicists in Medicine Radiation Therapy Committee Ad Hoc Subcommittee on Low-Energy Seed Dosimetry." *Med Phys* 26:570–573 (1999).

- 134 J.F. Williamson, B.M. Coursey, L.A. DeWerd, W.F. Hanson, R. Nath, M.J. Rivard, and G. Ibbott. "Recommendations of the American Association of Physicists in Medicine on  $^{103}\text{Pd}$  interstitial source calibration and dosimetry: implications for dose specification and prescription." *Med Phys* 27:634–642 (2000).
- 135 B.R. Prestidge, W.S. Bice, I. Jurkovic, E. Walker, S. Marianne, and A. Sadeghi. "Cesium-131 permanent prostate brachytherapy: an initial report." *Int J Radiat Oncol Biol Phys* 63(Suppl 1):S336–S337 (2005).
- 136 N. Yue, D.E. Heron, K. Komanduri, and M.S. Huq. "Prescription dose in permanent  $^{131}\text{Cs}$  seed prostate implants. [erratum appears in *Med Phys* 33(7):2655 (2006)]." *Med Phys* 32:2496–2502 (2005).
- 137 R. Byrnes, J. Musmacher, K. Satchwill, and L. Rumpf. "Dosimetric computation of cesium-131 and palladium-103 for permanent prostate brachytherapy." *Med Phys* 34:2440 (2007).
- 138 W.S. Bice, B.R. Prestidge, S.M. Kurtzman, S. Beriwal, B.J. Moran, R.R. Patel, and M.J. Rivard. "Recommendations for permanent prostate brachytherapy with  $^{131}\text{Cs}$ : a consensus report from the Cesium Advisory Group." *Brachytherapy* 7:290–296 (2008).
- 139 D.A. Wilkinson, E.J. Lee, J.P. Ciezki, D.S. Mohan, C. Zippe, K. Angermeier, J. Ulchaker, and E.A. Klein. "Dosimetric comparison of pre-planned and or-planned prostate seed brachytherapy." *Int J Radiat Oncol Biol Phys* 48:1241–1244 (2000).
- 140 R.M. Gewanter, C. Wu, J.L. Laguna, A.E. Katz, and R.D. Ennis. "Intraoperative preplanning for transperineal ultrasound-guided permanent prostate brachytherapy." *Int J Radiat Oncol Biol Phys* 48:377–380 (2000).
- 141 R.A. Cormack, H. Kooy, C.M. Tempny, and A.V. D'Amico. "A clinical method for real-time dosimetric guidance of transperineal  $^{125}\text{I}$  prostate implants using interventional magnetic resonance imaging." *Int J Radiat Oncol Biol Phys* 46:207–214 (2000).
- 142 R.A. Cormack, C.M. Tempny, and A.V. D'Amico. "Optimizing target coverage by dosimetric feedback during prostate brachytherapy." *Int J Radiat Oncol Biol Phys* 48:1245–1249 (2000).
- 143 Doggett. "Image registered real-time intraoperative treatment planning: Permanent seed brachytherapy." *Radiother Oncol* 55(Suppl 1):4; (Abstr.) 55:4 (2000).
- 144 M.J. Zelefsky, Y. Yamada, G. Cohen, E.S. Venkatraman, A.Y. Fung, E. Furhang, D. Silvern, and M. Zaider. "Postimplantation dosimetric analysis of permanent transperineal prostate implantation: improved dose distributions with an intraoperative computer-optimized conformal planning technique." *Int J Radiat Oncol Biol Phys* 48:601–608 (2000).
- 145 Y. Yu, J.B. Zhang, R.A. Brasacchio, P.G. Okunieff, D.J. Rubens, J.G. Strang, A. Soni, and E.M. Messing. "Automated treatment planning engine for prostate seed implant brachytherapy." *Int J Radiat Oncol Biol Phys* 43:647–652 (1999).
- 146 M. Zaider, M.J. Zelefsky, E.K. Lee, K.L. Zakian, H.I. Amols, J. Dyke, G. Cohen, Y. Hu, A.K. Endi, C. Chui, and J.A. Koutcher. "Treatment planning for prostate implants using magnetic-resonance spectroscopy imaging." *Int J Radiat Oncol Biol Phys* 47:1085–1096 (2000).
- 147 A.V. D'Amico, R. Cormack, C.M. Tempny, S. Kumar, G. Topulos, H.M. Kooy, and C.N. Coleman. "Real-time magnetic resonance image-guided interstitial brachytherapy in the treatment of select patients with clinically localized prostate cancer." *Int J Radiat Oncol Biol Phys* 42:507–515 (1998).
- 148 E.M. Messing, J.B. Zhang, D.J. Rubens, R.A. Brasacchio, J.G. Strang, A. Soni, M.C. Schell, P.G. Okunieff, and Y. Yu. "Intraoperative optimized inverse planning for prostate brachytherapy: early experience." *Int J Radiat Oncol Biol Phys* 44:801–808 (1999).

- 149 M.J. Zelefsky, G. Cohen, K.L. Zakian, J. Dyke, J.A. Koutcher, H. Hricak, L. Schwartz, and M. Zaider. "Intraoperative conformal optimization for transperineal prostate implantation using magnetic resonance spectroscopic imaging." *Cancer J* 6:249–255 (2000).
- 150 Y. Yu and M.C. Schell. "A genetic algorithm for the optimization of prostate implants." *Med Phys* 23:2085–2091 (1996).
- 151 Y.C. Lo, R.G. Stock, and S. Hong. "Prospective comparison of intraoperative real-time to post-implant dosimetry in patients receiving prostate brachytherapy." *Int J Radiat Oncol Biol Phys* 48:359 (2000).
- 152 J.F. Carrier, M. D'Amours, F. Verhaegen, B. Reniers, A.G. Martin, E. Vigneault, and L. Beaulieu. "Postimplant dosimetry using a Monte Carlo dose calculation engine: a new clinical standard." *Int J Radiat Oncol Biol Phys* 68:1190–1198 (2007).
- 153 G.K. Edmundson, D. Yan, and A.A. Martinez. "Intraoperative optimization of needle placement and dwell times for conformal prostate brachytherapy." *Int J Radiat Oncol Biol Phys* 33:1257–1263 (1995).
- 154 J. Stromberg, A. Martinez, J. Gonzalez, G. Edmundson, N. Ohanian, F. Vicini, J. Hollander, G. Gustafson, W. Spencer, D. Yan et al. "Ultrasound-guided high dose rate conformal brachytherapy boost in prostate cancer: treatment description and preliminary results of a phase I/II clinical trial." *Int J Radiat Oncol Biol Phys* 33:161–171 (1995).
- 155 Z. Wei, G. Wan, L. Gardi, G. Mills, D. Downey, and A. Fenster. "Robot-assisted 3D-TRUS guided prostate brachytherapy: system integration and validation." *Med Phys* 31:539–548 (2004).
- 156 G. Fichtinger, E.C. Burdette, A. Tanacs, A. Patriciu, D. Mazilu, L. L. Whitcomb, and D. Stoianovici. "Robotically assisted prostate brachytherapy with transrectal ultrasound guidance—Phantom experiments." *Brachytherapy* 5:14–26 (2006).
- 157 M. Meltsner, N. Ferrier, and B. Thomadsen. "Performance Evaluation of a Novel Brachytherapy Robot." [Abstract TH-B-224C-02]. *Med Phys* 33(6):2264 (2006).
- 158 C. Kennedy, I. Iordachita et al. "Robotically Assisted Needle Placement for Prostate Brachytherapy." [Abstract TH-B-224-C-03]. *Med Phys* 33(6):2264 (2006).
- 159 Y. Yu, T. Podder, Y. Zhang, W.S. Ng, V. Mistic, J. Sherman, L. Fu, D. Fuller, E. Messing, D. Rubens, J. Strang, and R. Brasacchio. "Robot-Assisted Prostate Brachytherapy" in Proceedings of Medical Image Computing and Computer-Assisted Intervention - MICCAI 2006. R. Larsen, M. Nielsen, J. Sporring (eds.). (Springer, LNCS41900041 4190, 41-49 (2006)).
- 160 V. Mistic, L. Fu, T.K. Podder, L. Liao, D.J. Rubens, R. Brasacchio, E.M. Messing, J.G. Strang, W.S. Ng, and Y. Yu. "Dynamic planning in single needle brachytherapy systems." *Int J CARS* 1:271–273 (2006).
- 161 W.S. Bice, Jr., B.R. Prestidge, and M.F. Sarosdy. "Sector analysis of prostate implants." *Med Phys* 28:2561–2567 (2001).
- 162 I. Spadinger, M. Hilt, M. Keyes, C. Smith, S. Sidhu, and W.J. Morris. "Prostate brachytherapy postimplant dosimetry: a comparison of suture-embedded and loose seed implants." *Brachytherapy* 5:165–173 (2006).
- 163 G.S. Merrick, S. Gutman, H. Andreini, W. Taubenslag, D.L. Lindert, R. Curtis, E. Adamovich, R. Anderson, Z. Allen, W. Butler, and K. Wallner. "Prostate cancer distribution in patients diagnosed by transperineal template-guided saturation biopsy." *Eur Urol* 52:715–723 (2007).
- 164 A.S. Barnes, S.J. Haker, R.V. Mulkern, M. So, A.V. D'Amico, and C.M. Tempny. "Magnetic resonance spectroscopy-guided transperineal prostate biopsy and brachytherapy for recurrent prostate cancer." *Urology* 66:1319 (2005).
- 165 R.J. Ellis and D.A. Kaminsky. "Fused radioimmunosintigraphy for treatment planning." *Rev Urol* 8 (Suppl 1):S11–S19 (2006).

- 166 J.F. Fowler. “The linear-quadratic formula and progress in fractionated radiotherapy.” *Br J Radiol* 62:679–694 (1989).
- 167 R.G. Dale and B. Jones. “The clinical radiobiology of brachytherapy.” *Br J Radiol* 71:465–483 (1998).
- 168 R.G. Dale. “The application of the linear-quadratic dose-effect equation to fractionated and protracted radiotherapy.” *Br J Radiol* 58:515–528 (1985).
- 169 C.C. Ling, J. Roy, N. Sahoo, K. Wallner, and L. Anderson. “Quantifying the effect of dose inhomogeneity in brachytherapy: application to permanent prostatic implant with  $^{125}\text{I}$  seeds.” *Int J Radiat Oncol Biol Phys* 28:971–978 (1994).
- 170 C.C. Ling. “Permanent implants using Au-198, Pd-103, and I-125: radiobiological considerations based on the linear quadratic model.” *Int J Radiat Oncol Biol Phys* 23:81–87 (1992).
- 171 G.R. Lazarescu and J.J. Battista. “Analysis of the radiobiology of ytterbium-169 and iodine-125 permanent brachytherapy implants.” *Phys Med Biol* 42:1727–1736 (1997).
- 172 A.P. Dicker, C.C. Lin, D.B. Leeper, and F.M. Waterman. “Isotope selection for permanent prostate implants? An evaluation of  $^{103}\text{Pd}$  versus  $^{125}\text{I}$  based on radiobiological effectiveness and dosimetry.” *Semin Urol Oncol* 18:152–159 (2000).
- 173 N. Yue, D.E. Heron, K. Komanduri, and M.S. Huq. “Prescription dose in permanent  $^{131}\text{Cs}$  seed prostate implants.” *Med Phys* 32:2496–2502 (2005).
- 174 C.I. Armpilia, R.G. Dale, I.P. Coles, B. Jones, and V. Antipas. “The determination of radiobiologically optimized half-lives for radionuclides used in permanent brachytherapy implants.” *Int J Radiat Oncol Biol Phys* 55:378–385 (2003).
- 175 A.B. Jani, C.M. Hand, A.E. Lujan, J.C. Roeske, G.P. Zagaja, S. Vijayakumar, and C.A. Pelizzari. “Biological effective dose for comparison and combination of external beam and low-dose rate interstitial brachytherapy prostate cancer treatment plans.” *Med Dosim* 29:42–48 (2004).
- 176 C.R. King. “LDR vs. HDR brachytherapy for localized prostate cancer: the view from radiobiological models.” *Brachytherapy* 1:219–226 (2002).
- 177 Z. Chen and R. Nath. “Biologically effective dose (BED) for interstitial seed implants containing a mixture of radionuclides with different half-lives.” *Int J Radiat Oncol Biol Phys* 55:825–834 (2003).
- 178 R.G. Dale, B. Jones, and I.P. Coles. “Effect of tumour shrinkage on the biological effectiveness of permanent brachytherapy implants.” *Br J Radiol* 67:639–645 (1994).
- 179 N. Yue, Z. Chen, and R. Nath. “Edema-induced increase in tumour cell survival for  $^{125}\text{I}$  and  $^{103}\text{Pd}$  prostate permanent seed implants—a bio-mathematical model.” *Phys Med Biol* 47:1185–1204 (2002).
- 180 M.P. Van Gellekom, M.A. Moerland, H.B. Kal, and J.J. Battermann. “Biologically effective dose for permanent prostate brachytherapy taking into account postimplant edema.” *Int J Radiat Oncol Biol Phys* 53:422–433 (2002).
- 181 R.J. Yaes. “Late normal tissue injury from permanent interstitial implants.” *Int J Radiat Oncol Biol Phys* 49:1163–1169 (2001).
- 182 R.E. Peschel, Z. Chen, K. Roberts, and R. Nath. “Long-term complications with prostate implants: iodine-125 vs. palladium-103.” *Radiat Oncol Invest* 7:278–288 (1999).
- 183 X.A. Li, J.Z. Wang, R.D. Stewart, and S.J. DiBiase. “Dose escalation in permanent brachytherapy for prostate cancer: dosimetric and biological considerations.” *Phys Med Biol* 48:2753–2765 (2003).
- 184 R.G. Stock, N.N. Stone, J.A. Cesaretti, and B.S. Rosenstein. “Biologically effective dose values for prostate brachytherapy: effects on PSA failure and posttreatment biopsy results.” *Int J Radiat Oncol Biol Phys* 64:527–533 (2006).

- 185 A. Niemierko. "Reporting and analyzing dose distributions: a concept of equivalent uniform dose." *Med Phys* 24:103–110 (1997).
- 186 A. Haworth, M. Ebert, D. Waterhouse, D. Joseph, and G. Duchesne. "Assessment of I-125 prostate implants by tumor bioeffect." *Int J Radiat Oncol Biol Phys* 59:1405–1413 (2004).
- 187 S.L. Tucker, H.D. Thames, and J.M. Taylor. "How well is the probability of tumor cure after fractionated irradiation described by Poisson statistics? [see comment]." *Radiat Res* 124:273–282 (1990).
- 188 M. Zaider and G.N. Minerbo. "Tumour control probability: a formulation applicable to any temporal protocol of dose delivery." *Phys Med Biol* 45:279–293 (2000).
- 189 M. Zaider and L. Hanin. "Biologically-equivalent dose and long-term survival time in radiation treatments." *Phys Med Biol* 52:6355–6362 (2007).
- 190 M.R. Horsman. "Hypoxia in Tumours: Its Relevance, Identification and Modification" in *Current Topics in Clinical Radiobiology of Tumours*. H.P. Beck-Bornholdt (ed.). pp. 99–112. (Springer-Verlag, Berlin, Germany, 1993).
- 191 E. Hall. *Radiobiology for the Radiologist*, 4th ed. (Lippincott, Philadelphia, PA, 1994).
- 192 S.J. Knox, W. Sutherland, and M.L. Goris. "Correlation of tumor sensitivity to low-dose-rate irradiation with G2/M-phase block and other radiobiological parameters." [Erratum appears in *Radiat Res* 136(3):439 (1993)]. *Radiat Res* 135:24–31 (1993).
- 193 C.C. Ling, C.-H. Chen, and Z. Fuks. "An equation for the dose response of radiation-induced apoptosis: possible incorporation with the LQ model. [see comment]." *Radiother Oncol* 33:17–22 (1994).
- 194 C.C. Ling, M. Guo, C.H. Chen, and T. Deloherey. "Radiation-induced apoptosis: effects of cell age and dose fractionation." *Cancer Res* 55:5207–5212 (1995).
- 195 D.R. Olsen. "Calculation of the biological effect of fractionated radiotherapy: the importance of radiation-induced apoptosis." *Br J Radiol* 68:1230–1236 (1995).
- 196 H.D. Thames. "An 'incomplete-repair' model for survival after fractionated and continuous irradiations." *Int J Radiat Biol Related Stud Phys Chem Med* 47:319–339 (1985).
- 197 R.G. Dale. "Radiobiological assessment of permanent implants using tumour repopulation factors in the linear-quadratic model." *Br J Radiol* 62:241–244 (1989).
- 198 M.K. Murphy, R.K. Piper, L.R. Greenwood, M.G. Mitch, P.J. Lamperti, S.M. Seltzer, M.J. Bales, and M.H. Phillips. "Evaluation of the new cesium-131 seed for use in low-energy x-ray brachytherapy." *Med Phys* 31:1529–1538 (2004).
- 199 Z. Chen, J. Deng, K. Roberts, and R. Nath. "On the need to compensate edema-induced dose reductions in pre-planned  $^{131}\text{Cs}$  prostate brachytherapy." *Int J Radiat Oncol Biol Phys* 70(1):303–310(2008).
- 200 R.G. Dale, I.P. Coles, C. Deehan, and J.A. O'Donoghue. "Calculation of integrated biological response in brachytherapy." *Int J Radiat Oncol Biol Phys* 38:633–642 (1997).
- 201 S.P. Lee, M.Y. Leu, J.B. Smathers, W.H. McBride, R.G. Parker, and H.R. Withers. "Biologically effective dose distribution based on the linear quadratic model and its clinical relevance." *Int J Radiat Oncol Biol Phys* 33:375–389 (1995).
- 202 T.E. Wheldon, C. Deehan, E.G. Wheldon, and A. Barrett. "The linear-quadratic transformation of dose-volume histograms in fractionated radiotherapy." *Radiother Oncol* 46:285–295 (1998).
- 203 L.B. Marks, G.W. Sherouse, M.T. Munley, G.C. Bentel, and D.P. Spencer. "Incorporation of functional status into dose-volume analysis." *Med Phys* 26:196–199 (1999).
- 204 Y. Lu, D.R. Spelbring, and G.T. Chen. "Functional dose-volume histograms for functionally heterogeneous normal organs." *Phys Med Biol* 42:345–356 (1997).

- 205 R. Nath, P. Bongiorno, Z. Chen, J. Gragnano, and S. Rockwell. “Relative biological effectiveness of  $^{103}\text{Pd}$  and  $^{125}\text{I}$  photons for continuous low-dose-rate irradiation of Chinese hamster cells.” *Radiat Res* 163:501–509 (2005).
- 206 C.C. Ling, W.X. Li, and L.L. Anderson. “The relative biological effectiveness of I-125 and Pd-103.” *Int J Radiat Oncol Biol Phys* 32:373–378 (1995).
- 207 M. Goitein and T.E. Schultheiss. “Strategies for treating possible tumor extension: some theoretical considerations.” *Int J Radiat Oncol Biol Phys* 11:1519–1528 (1985).
- 208 J.T. Lyman. “Complication probability as assessed from dose-volume histograms.” *Radiat Res* (Suppl 8):S13–S19 (1985).
- 209 S.L. Tucker and J.M. Taylor. “Improved models of tumour cure.” *Int J Radiat Biol* 70:539–553 (1996).
- 210 N.A. Stavreva, P.V. Stavrev, B. Warkentin, and B.G. Fallone. “Investigating the effect of cell repopulation on the tumor response to fractionated external radiotherapy.” *Med Phys* 30:735–742 (2003).
- 211 D.J. Brenner and E.J. Hall. “Fractionation and protraction for radiotherapy of prostate carcinoma. [see comment].” *Int J Radiat Oncol Biol Phys* 43:1095–1101 (1999).
- 212 G.M. Duchesne and L.J. Peters. “What is the alpha/beta ratio for prostate cancer? Rationale for hypofractionated high-dose-rate brachytherapy. [see comment].” *Int J Radiat Oncol Biol Phys* 44:747–748 (1999).
- 213 C.R. King and C.S. Mayo. “Is the prostate alpha/beta ratio of 1.5 from Brenner & Hall a modeling artifact.” *Int J Radiat Oncol Biol Phys* 47:536–539 (2000).
- 214 W.D. D’Souza and H.D. Thames. “Is the alpha/beta ratio for prostate cancer low? [see comment] [comment].” *Int J Radiat Oncol Biol Phys* 51:1–3 (2001).
- 215 J. Fowler, R. Chappell, and M. Ritter. “Is alpha/beta for prostate tumors really low? [see comment].” *Int J Radiat Oncol Biol Phys* 50:1021–1031 (2001).
- 216 C.R. King and J.F. Fowler. “A simple analytic derivation suggests that prostate cancer alpha/beta ratio is low. [see comment].” *Int J Radiat Oncol Biol Phys* 51:213–214 (2001).
- 217 D.J. Brenner, A.A. Martinez, G.K. Edmundson, C. Mitchell, H.D. Thames, and E.P. Armour. “Direct evidence that prostate tumors show high sensitivity to fractionation (low alpha/beta ratio), similar to late-responding normal tissue. [see comment].” *Int J Radiat Oncol Biol Phys* 52:6–13 (2002).
- 218 C.R. King and J.F. Fowler. “Yes, the alpha/beta ratio for prostate cancer is low or ‘methinks the lady doth protest too much...about a low alpha/beta that is’. [comment].” *Int J Radiat Oncol Biol Phys* 54:626–627; author reply 627–628 (2002).
- 219 W.R. Lee. “In regard to Brenner et al. Direct evidence that prostate tumors show high sensitivity to fractionation (low alpha/beta ratio) similar to late-responding normal tissue. [comment].” *Int J Radiat Oncol Biol Phys* 53:1392; author reply 1393 (2002).
- 220 J.Z. Wang, M. Guerrero, and X.A. Li. “How low is the alpha/beta ratio for prostate cancer? [see comment].” *Int J Radiat Oncol Biol Phys* 55:194–203 (2003).
- 221 J.F. Fowler, M.A. Ritter, J.D. Fenwick, and R.J. Chappell. “How low is the alpha/beta ratio for prostate cancer? In regard to Wang et al., *Int J Radiat Oncol Biol Phys* 2003;55:194–203. [comment].” *Int J Radiat Oncol Biol Phys* 57:593–595; author reply 595–596 (2003).
- 222 J.F. Fowler, M.A. Ritter, R.J. Chappell, and D.J. Brenner. “What hypofractionated protocols should be tested for prostate cancer?” *Int J Radiat Oncol Biol Phys* 56:1093–1104 (2003).
- 223 J.Z. Wang, X.A. Li, C.X. Yu, and S.J. DiBiase. “The low alpha/beta ratio for prostate cancer: what does the clinical outcome of HDR brachytherapy tell us?” *Int J Radiat Oncol Biol Phys* 57: 1101–1108 (2003).

- 224 H.B. Kal and M.P. Van Gellekom. “How low is the alpha/beta ratio for prostate cancer? [see comment].” *Int J Radiat Oncol Biol Phys* 57:1116–1121 (2003).
- 225 A.E. Nahum, B. Movsas, E.M. Horwitz, C.C. Stobbe, and J.D. Chapman. “Incorporating clinical measurements of hypoxia into tumor local control modeling of prostate cancer: implications for the alpha/beta ratio. [see comment].” *Int J Radiat Oncol Biol Phys* 57:391–401 (2003).
- 226 D.J. Brenner. “Hypofractionation for prostate cancer radiotherapy—what are the issues? [comment].” *Int J Radiat Oncol Biol Phys* 57:912–914 (2003).
- 227 C.G. Orton. “In regard to Nahum et al. (*Int J Radiat Oncol Biol Phys* 2003;57:391–401): Incorporating clinical measurements of hypoxia into tumor control modeling of prostate cancer: implications for the alpha/beta ratio. [comment].” *Int J Radiat Oncol Biol Phys* 58:1637; author reply 1637–1639 (2004).
- 228 S.M. Bentzen and M.A. Ritter. “The alpha/beta ratio for prostate cancer: what is it, really? [comment].” *Radiother Oncol* 76:1–3 (2005).
- 229 R. Valdagni, C. Italia, P. Montanaro, A. Lanceni, P. Lattuada, T. Magnani, C. Fiorino, and A. Nahum. “Is the alpha-beta ratio of prostate cancer really low? A prospective, non-randomized trial comparing standard and hyperfractionated conformal radiation therapy. [see comment].” *Radiother Oncol* 75:74–82 (2005).
- 230 H.D. Thames, S.M. Bentzen, I. Turesson, M. Overgaard, and W. Van den Bogaert. “Time-dose factors in radiotherapy: a review of the human data.” *Radiother Oncol* 19:219–235 (1990).
- 231 J.Z. Wang, N.A. Mayr, S. Nag, J. Montebello, N. Gupta, N. Samsami, and C. Kanellitsas. “Effect of edema, relative biological effectiveness, and dose heterogeneity on prostate brachytherapy.” *Med Phys* 33:1025–1032 (2006).
- 232 D.J. Carlson, R.D. Stewart, X.A. Li, K. Jennings, J.Z. Wang, and M. Guerrero. “Comparison of in vitro and in vivo alpha/beta ratios for prostate cancer.” *Phys Med Biol* 49:4477–4491 (2004).
- 233 K.M. Haustermans, I. Hofland, H. Van Poppel, R. Oyen, W. Van de Voorde, A.C. Begg, and J.F. Fowler. “Cell kinetic measurements in prostate cancer. [see comment].” *Int J Radiat Oncol Biol Phys* 37:1067–1070 (1997).
- 234 O. Chibani and J.F. Williamson. “MCPI: a sub-minute Monte Carlo dose calculation engine for prostate implants.” *Med Phys* 32:3688–3698 (2005).
- 235 A.S. Meigooni and R. Nath. “Tissue inhomogeneity correction for brachytherapy sources in a heterogeneous phantom with cylindrical symmetry.” *Med Phys* 19:401–407 (1992).
- 236 J.J. DeMarco, J.B. Smathers, C.M. Burnison, Q.K. Ncube, and T.D. Solberg. “CT-based dosimetry calculations for  $^{125}\text{I}$  prostate implants.” *Int J Radiat Oncol Biol Phys* 45:1347–1353 (1999).
- 237 A.S. Meigooni, J.A. Meli, and R. Nath. “Interseed effects on dose for  $^{125}\text{I}$  brachytherapy implants.” *Med Phys* 19:385–390 (1992).
- 238 G.S. Burns and D.E. Raeside. “The accuracy of single-seed dose superposition for I-125 implants.” *Med Phys* 16:627–631 (1989).
- 239 J.F. Carrier, L. Beaulieu, F. Therriault-Proulx, and R. Roy. “Impact of interseed attenuation and tissue composition for permanent prostate implants.” *Med Phys* 33:595–604 (2006).
- 240 J.F. Carrier, M. D’Amours, F. Verhaegen, B. Reniers, A. G. Martin, E. Vigneault, and L. Beaulieu. “Postimplant dosimetry using a Monte Carlo dose calculation engine: a new clinical standard.” *Int J Radiat Oncol Biol Phys* 68:1190–1198 (2007).
- 241 H. Afsharpour, M. D’Amours, B. Cote, J.F. Carrier, F. Verhaegen, and L. Beaulieu. “A Monte Carlo study on the effect of seed design on the interseed attenuation in permanent prostate implants.” *Med Phys* 35:3671–3681 (2008).
- 242 F.M. Waterman and A.P. Dicker. “Probability of late rectal morbidity in  $^{125}\text{I}$  prostate brachytherapy.” *Int J Radiat Oncol Biol Phys* 55:342–353 (2003).

- 243 S.J. DiBiase, K. Wallner, K. Tralins, and S. Sutlief. “Brachytherapy radiation doses to the neurovascular bundles.” *Int J Radiat Oncol Biol Phys* 46:1301–1307 (2000).
- 244 G.S. Merrick, W.M. Butler, A.T. Dorsey, J.H. Lief, and J.G. Donzella. “A comparison of radiation dose to the neurovascular bundles in men with and without prostate brachytherapy-induced erectile dysfunction.” *Int J Radiat Oncol Biol Phys* 48:1069–1074 (2000).
- 245 G.S. Merrick, W.M. Butler, R.W. Galbreath, R.L. Stipetich, L.J. Abel, and J.H. Lief. “Erectile function after permanent prostate brachytherapy.” *Int J Radiat Oncol Biol Phys* 52:893–902 (2002).
- 246 L. Potters, T. Torre, P.A. Fearn, S.A. Leibel, and M.W. Kattan. “Potency after permanent prostate brachytherapy for localized prostate cancer.” *Int J Radiat Oncol Biol Phys* 50:1235–1242 (2001).
- 247 R.A. Kiteley, W.R. Lee, A.F. deGuzman, M. Mirzaei, and D.L. McCullough. “Radiation dose to the neurovascular bundles or penile bulb does not predict erectile dysfunction after prostate brachytherapy.” *Brachytherapy* 1:90–94 (2002).
- 248 C.S. Hamilton, J.W. Denham, M. O’Brien, P. Ostwald, T. Kron, S. Wright, and W. Drr. “Underprediction of human skin erythema at low doses per fraction by the linear quadratic model. [see comment].” *Radiother Oncol* 40:23–30 (1996).
- 249 A.G. Macdonald, M. Keyes, A. Kruk, G. Duncan, V. Moravan, and W.J. Morris. “Predictive factors for erectile dysfunction in men with prostate cancer after brachytherapy: is dose to the penile bulb important?” *Int J Radiat Oncol Biol Phys* 63:155–163 (2005).

